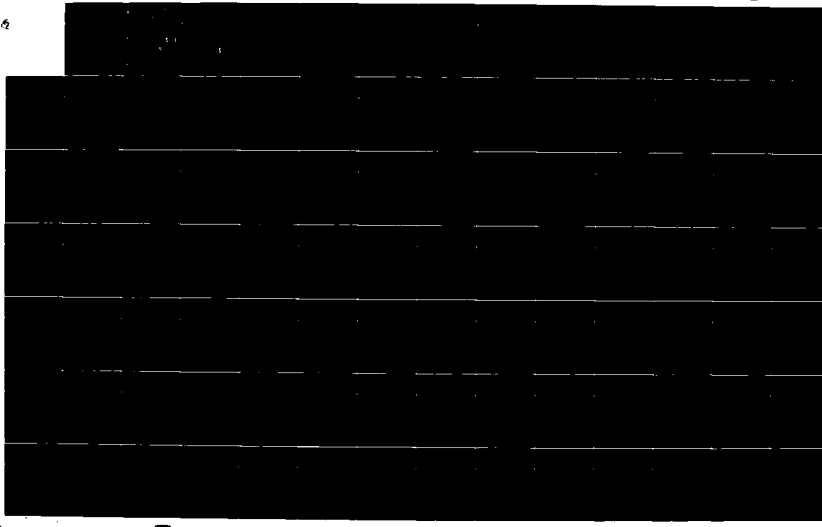
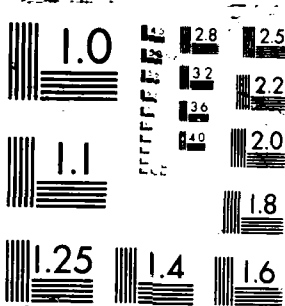


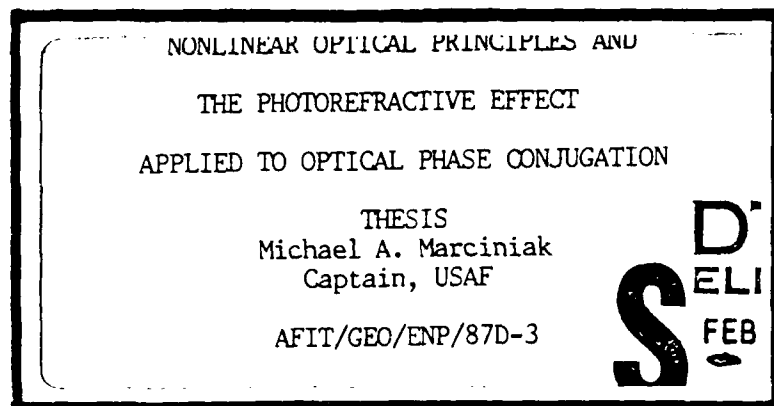
AD-A188 856 NONLINEAR OPTICAL PRINCIPLES AND THE PHOTOREFRACTIVE 1/2
EFFECT APPLIED TO OF. .(U) AIR FORCE INST OF TECH
WRIGHT-PATTERSON AFB OH SCHOOL OF ENGI.. M A MARCINIAK
UNCLASSIFIED DEC 87 AFII/GEO/EMP/87D-3 F/G 975 NL





1
DTIC FILE COPY

AD-A188 856



DISTRIBUTION STATEMENT A

Approved for public release
Distribution Unlimited

DEPARTMENT OF THE AIR FORCE
AIR UNIVERSITY
AIR FORCE INSTITUTE OF TECHNOLOGY

Wright-Patterson Air Force Base, Ohio

88 2 4 071

AFIT/GEO/ENP/87D-3

(1)

NONLINEAR OPTICAL PRINCIPLES AND
THE PHOTOREFRACTIVE EFFECT
APPLIED TO OPTICAL PHASE CONJUGATION

THESIS
Michael A. Marciak
Captain, USAF

AFIT/GEO/ENP/87D-3

DTIC
ELECTED
FEB 09 1988
S D
D

Approved for public release; distribution unlimited

AFIT/GEO/ENP/87D-3

NONLINEAR OPTICAL PRINCIPLES AND THE PHOTOREFRACTIVE
EFFECT APPLIED TO OPTICAL PHASE CONJUGATION

THESIS

Presented to the Faculty of the School of Engineering
of the Air Force Institute of Technology
Air University
In Partial Fulfillment of the
Requirements for the Degree of
Master of Science in Electrical Engineering



Michael A. Marciniak, B.S., B.S.F.E.

Captain, USAF

December 1987

Accession For	
NTIS	CRA&I <input checked="" type="checkbox"/>
DDIC	TAB <input type="checkbox"/>
Unpublished	<input type="checkbox"/>
Justification	
By	
Distribution	
Delivery Dates	
Requester's Name	
Date Received	
A-1	

Approved for public release; distribution unlimited

Preface

This tutorial is aimed at the nonlinear novice trying to get a handle on photorefractive processes. Often, the engineering or physics published article or text leaps from one point to the next with only a cleverly placed "it can be easily shown that..." -type expression as the connector. The author can hardly be blamed since these intermediate steps may seem redundant after being through them a good number of times. He is also, undoubtedly, working under a publisher's directive for economy of space.

The typical student, on the other hand, may not view this missing material as nonchalantly. Nevertheless, he often accepts the stated points on faith because the usual pressure of a time constraint prevents him from going through the tedium of a derivation. Valuable insights, implicit assumptions and boundaries of applicability remain hidden along with the true understanding of the concept and a "turn the crank" approach is accepted.

The purpose of this tutorial is to gather pertinent information from articles and texts into one place and fill in some of the blanks the original authors left behind. It is specifically designed to lay the foundation for another Master's thesis which would pick up where this tutorial leaves off and apply these theories to observed phenomena.

Of course, being a student, myself, I could not have put this paper together alone. First, I'd like to sincerely thank my advisor, Dr. Ted Luke, for lending me his expertise in the area and for his patience with me as I visited his office what seemed to be several times daily. I'd also like to thank Dr. Won Roh for valuable conversations on these topics. Finally, my unending gratitude goes to my wife, Melony, who was

an "AFIT widow" for most of this project then became the best typist I
could have hoped to find.

Michael A. Marciak

Table of Contents

	Page
Preface	ii
List of Figures	vi
List of Tables	viii
Abstract	ix
I. Introduction	1
II. Second and Third Order Nonlinear Optical Principles - Background to Optical Phase Conjugation	7
Second Order Nonlinear Principles	7
Third Order Nonlinear Principles	17
III. Optical Phase Conjugation by Degenerate Four Wave Mixing (A Third Order Nonlinear Process)	25
Third Order Polarization	25
The Wave Equation	27
Solutions for the Amplitudes of the Probe and Conjugate. .	29
Summary	31
IV. The Photorefractive Effect	32
Feinberg's Hopping Model	34
Kukhtarev Solid State Model	45
Summary	54
V. Steady State Two-Beam Coupling	58
Feinberg's Hopping Model	59
Two-Beam Coupling Assuming a Sinusoidal Index Grating Exists	64
Summary	67
VI. Diffraction Efficiency and Phase Conjugate Reflectivity	69
Feinberg's Hopping Model	70
Diffraction Efficiency Assuming a Sinusoidal Index Grating Exists	75
Phase Conjugate Reflectivity Assuming a Sinusoidal Index Grating Exists	76
Summary	81

	Page
VII. Applications of the Theory	82
Relationships Between Feinberg's $\Delta I_1/I_1$, n and R , and E_0 , Δ , k and ρW_0	82
Can the Direction of Energy Transfer in Steady State Two-Beam Coupling be Predicted?	90
Why is There Better Two-Beam Coupling and Diffraction Efficiency Crystallographic Orientations in BSO?	94
Summary	100
VIII. Conclusions and Recommendations	102
Conclusions	102
Recommendations for Further Research	106
Appendix A: The Index Ellipsoid	109
Appendix B: Recommendations for Further Research	114
Self-Pumped Phase Conjugate Mirrors (SPPCMs)	114
Transient Solutions to the Photorefractive Effect	115
How Much does Optical Activity Effect BSO Analyses?	116
Bibliography.	118
Vita.	120

List of Figures

Figure	Page
1. Illustration of Phase Conjugate Reflection.	1
2. PCM Application of Diffraction-Limited Focusing and Automatic Point-and-Track	2
3. PCM Application as a Mirror in a Laser Cavity	3
4. Geometry of Phase Conjugation by Four Wave Mixing	25
5. Intensities of Probe and Conjugate Waves as a Function of Position.	31
6. Illustration of the Photorefractive Effect.	33
7. Orientation of Interfering Beams and Photorefractive Crystal. .	38
8. Geometry for Formation of Index Grating	46
9. Orientation of Directional Cosines for Two-Beam Coupling. . . .	63
10. Geometry of Phase Conjugation in Photorefractive Crystals . . .	69
11. Orientation of Directional Cosines for Diffraction Efficiency and Phase Conjugate Reflectivity.	75
12. Two-Beam Coupling Gain versus Electric Field (BSO)	83
13. Diffractin Efficiency and Phase Conjugate Reflectivity versus Applied Field (BaTiO_3 and BSO)	84
14. Diffraction Efficiency versus Electric Field (BSO)	85
15. Diffraction Efficiency and Phase Conjugate Reflectivity versus Fringe Spacing (BSO)	86
16. Two-Beam Coupling Gain versus Grating Wave Vector (BaTiO_3) . .	87
17. Diffraction Efficiency versus Grating Wave Vector	88
18. Phase Conjugate Reflectivity versus Spatial Frequency	90
19. Directional Two-Beam Coupling in BaTiO_3	91
20. Illustration of the Photorefractive Effect with Direction of Phase Shift	92
21. Optimum Crystallographic Orientations in BSO.	94
22. PCS in BSO with No Applied Field.	95

Figure	Page
23. New PCSs in BSO with Applied Fields	97
24. Illumination of 110 Face of BSO	99
25. New PCSs in BSO with Illumination of 110 Face	99
26. Illustration of the Index Ellipsoid	109
27. Index Ellipsoid with Propagation Direction.	110
28. Self-Pumped Phase Conjugate Mirror.	114
29. Diffraction Efficiency and Two-Beam Coupling Gain versus Time (BSO)	116
30. Illustration of Optical Activity.	117

List of Tables

Table	Page
I. Third Order Nonlinear Susceptibilities	32
II. Linear Electro-Optic Coefficients	56

Abstract

This thesis presents a detailed interpretation of published theory of nonlinear optical phase conjugation by degenerate four wave mixing and by the photorefractive effect. Photorefractive phase conjugation is shown to be a low incident intensity alternative to degenerate four wave mixing (which requires high intensity incident light to achieve the nonlinear polarization of a medium).

The derivations of two models for the photorefractive effect, Feinberg's Hopping Model and Kukhtarev's Solid State Model, are presented. The significance of Kukhtarev's model is his development of criteria for which spatially sinusoidal incident light (interference fringes) produces a spatially sinusoidal electro-static field in the crystal - an assumption casually made in much photorefractive work. Both models culminate in expressions for the magnitude of the space-charge field and the spatial phase shift between the field and the incident interference pattern for small modulation conditions.

Feinberg's model is extended to develop expressions for two-beam coupling, diffraction efficiency and phase conjugate reflectivity. An alternative development for these expressions assumes the electro-static field exists in the crystal and modulates the crystal's refractive index by the linear electro-optic (Pockel's) effect.

The functional dependencies of Feinberg's expressions agree with (published) empirical data. However, specific crystallographic orientations exist for which the absolute magnitude of Feinberg's expressions or even the relative magnitudes between different orientations are inaccurate. Accurate relative magnitude expressions are

) made by assuming an electro-static field exists in the crystal and using
an index-ellipsoid approach to determine refractive indices.

NONLINEAR OPTICAL PRINCIPLES AND THE PHOTOREFRACTIVE EFFECT APPLIED TO
OPTICAL PHASE CONJUGATION

I. Introduction

Optical phase conjugation occurs when more than one coherent light beam is incident on a nonlinear material oriented properly. A new light beam is produced which is the phase conjugate of one of the incident beams, i.e., it propagates back in the direction of the incident light, and if the incident light is diverging, the phase conjugate will converge or vice versa. The phase conjugate, then, appears to be the time reversal of the incident beam. Because phase conjugation is often compared to reflection from a mirror, the nonlinear material producing this effect is referred to as a "phase conjugate mirror" or PCM (Figure 1) (1:157).

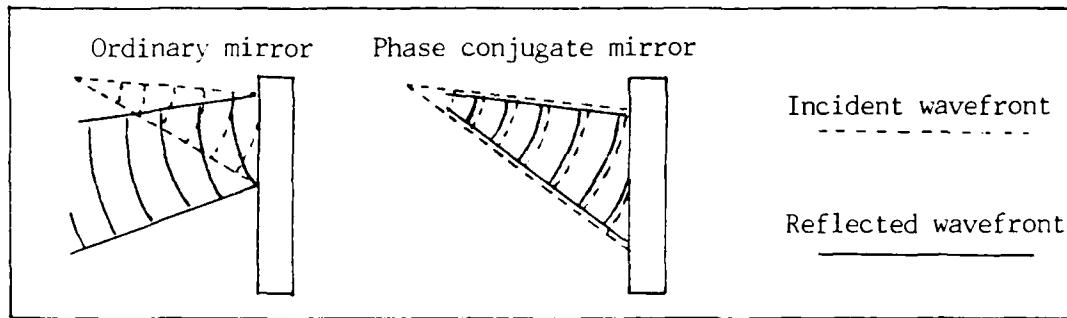


Figure 1. Illustration of phase conjugate reflection as compared to reflection from an ordinary mirror (1:157)

The practical usefulness of PCMs is evident in these few examples. First, since a PCM conjugates the phase of incident light, aberrations given to a wavefront as it passes through a medium will be removed if the wave back-propagates through that same medium. Because of this, glint from the illumination of a target may be amplified, reflected from

a PCM and passed back through the amplifier and aberrating medium to be focused (with much higher energy) to a diffraction-limited spot on the target. Because the direction of a phase conjugate wave is the reverse of the incident wave, this is an automatic point and track system (Figure 2) (1:175).

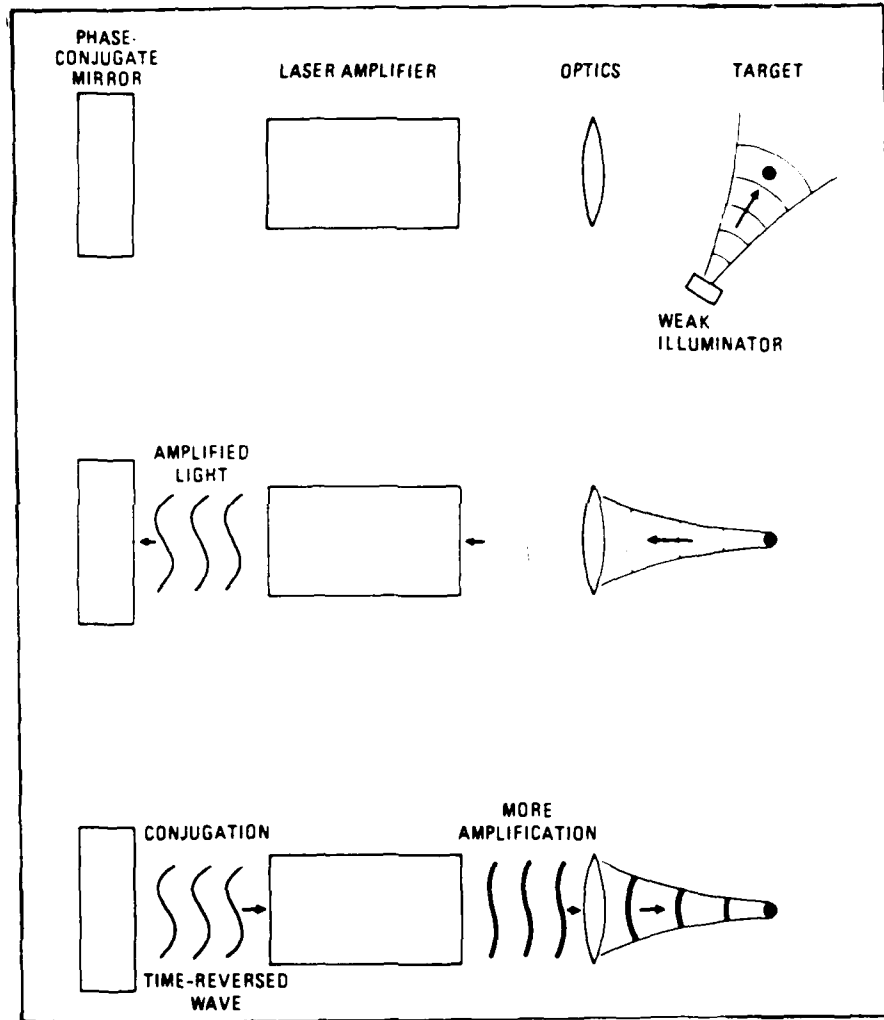


Figure 2. PCM application of diffraction-limited focusing and automatic point-and-track (1:175)

Another example is the use of a PCM in a laser cavity. Here, the phase conjugate's "time reversed" reflection removes the ordinary mirror

stability criteria of curvature and spacing, and allows only one more highly monochromatic mode. (Figure 3) (1:177-179).

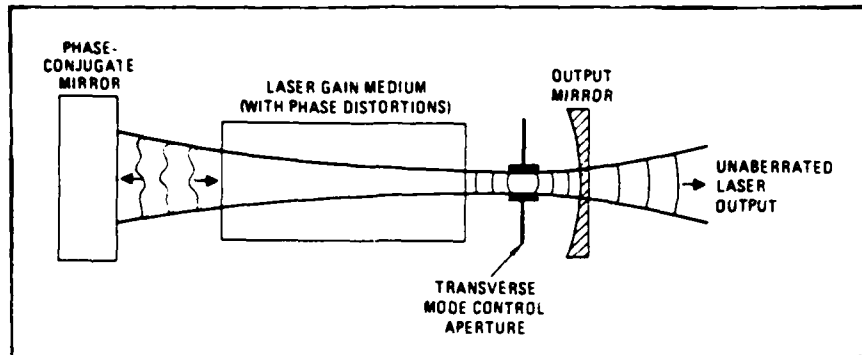


Figure 3. PCM application as one of the mirrors in a laser cavity (1:178)

The first PCMs were produced by degenerate four wave mixing (all waves are of the same frequency), a third order nonlinear process. The geometry for this effect consists of two counterpropagating, highly intense pump beams and a probe beam which are incident on and cause the polarization of a nonlinear material. There are several orders of polarization produced but the third order polarization wave is of interest because it stimulates an electro-magnetic wave which is the conjugate of the probe. Both the conjugate and probe beams then gain intensity by extracting energy from the pump beams.

The electric field which drives the third order polarization in this configuration is due to the superposition of the incident light waves. Since the third order optical susceptibility which "links" this E-field to the medium is very small in magnitude, very high intensity incident light is required to produce the phase conjugate effect.

A technique for producing phase conjugation with lower intensity incident light is through the use of photorefractive crystals. The interference of the (coherent) probe and one of the pump beams "writes"

a refractive index grating in the crystal. Then, the counterpropagating pump beam is diffracted off this grating and produces the conjugate of the probe.

The index grating is written through the photorefractive effect. A photorefractive crystal contains various sites in its lattice which accept and hold electrons with very low thermal probability of freedom. Under illumination, however, these charges are freed and the movement of either electrons or holes (depending on the crystal) occurs until the charge is retrapped in an area of the crystal which is not illuminated. In the case of interference fringes, then, interference maxima correspond to the location the charges left and minima to the locations where they are retrapped.

The separation of opposite charges, either electrons or holes (whichever is the carrier) and the ions left behind, causes an electro-static field to form. This field modulates the index of refraction of the crystal through the linear electro-optic (Pockel's) effect. Since the interference fringes are sinusoidal in intensity, the charge distribution, E-field and, thus, the index grating are all sinusoidal, as well.

For this type of effect, the E-field driving the nonlinearity of the crystal is the created space-charge field. The magnitude of this field is proportional to the modulation index of the interfering pump and probe beams. Since the modulation index is dependent on the relative intensities of these beams rather than the incident intensity of either of them, phase conjugation can be produced from lower intensity incident light.

In order to theoretically describe light incident on the index grating that is formed, a model describing the grating, itself, is first

necessary. Two models of the E-field forming the grating are Feinberg's Hopping Model and Kukhtarev's Solid State Model.

Feinberg's model is based on the idea that a charge may occupy any of a large number of sites in the photorefractive crystal and, under illumination, "hops" to any of its nearest neighbor sites. In this model, then, the probability of charge movement at any site is proportional to the probability that the site and its nearest neighbors are occupied and to the illumination at the site and at its nearest neighbors. The solution to the model for assumed spatially sinusoidal illumination yields spatial charge distribution (and, therefore, potential distribution and electro-static field distribution).

Kukhtarev's model is based on more standard solid state arguments such as charge generation rates and transport lengths. His solution (as well as Feinberg's) for the space-charge field, given sinusoidal illumination with small modulation index, is a sinusoidal field of the same spatial frequency as the illumination but which may be out of phase with it. This phase shift will be shown to be an important factor later.

It has been observed experimentally that when two beams write an index grating in a photorefractive crystal and propagate through the grating, one beam may experience a gain in intensity while the other experiences a corresponding loss. Two parallel theories describing this "two-beam coupling" are presented. One is developed from Feinberg's Hopping Model. The other assumes a sinusoidal index grating exists and can be described by the electro-static field through an "index ellipsoid"-type argument. Both conclude the key factor in two-beam coupling is the phase shift between the electro-static field and the incident interference fringes. Without such a phase shift, no energy transfer could occur.

Two-beam coupling can be considered a figure of merit for the photorefractive effect. Other such figures of merit are diffraction efficiency and phase conjugate reflectivity. Each of these figures of merit is important because they allow quantification of those aspects of the photorefractive effect which play a significant role in optical phase conjugation.

Diffraction efficiency is the amount of power in a wave diffracted at the Bragg angle off a grating compared to the amount of power in the wave incident on the grating. Phase conjugate reflectivity, in the photorefractive phase conjugation geometry described earlier, is the power in the conjugate wave diffracted off the grating compared to the power in the incident probe wave which had a part in writing the grating. Again, parallel theories from the extension of Feinberg's model and the sinusoidal grating assumption are presented. The mutual conclusion here is the magnitude of the (space-charge field and, therefore, the) index grating is proportional to the diffraction efficiency and also to the phase conjugate reflectivity.

II. Second and Third Order Nonlinear Optical Principles - Background to Optical Phase Conjugation

Two types of optical phase conjugation are presented in this paper - degenerate four wave mixing and photorefractive. The first, degenerate four wave mixing, occurs because the superposition of light waves in a nonlinear medium causes the nonlinear polarization of that medium. This polarization gives rise to an electro-magnetic wave as described by Maxwell's equations. In the proper configuration, this E-M wave can be the phase conjugate of one of the input waves.

This chapter presents a general development of the nonlinear processes mentioned above with the following chapter describing the special configuration for phase conjugation. Although four wave mixing is a third order nonlinear process, insight to nonlinear processes, in general, can be gained through the more simple case of the second order.

Second Order Nonlinear Principles

Second Order Nonlinear Polarization

When electric fields superimpose in a medium, the linear and nonlinear polarization of that medium may be written in the form:

$$P_i = \epsilon_0 \sum_j \chi_{ij} E_j + 2 \sum_j \sum_k d_{ijk} E_j E_k + \dots \quad (1)$$

where

P_i = i^{th} component of polarization ($i = x, y$ and z)

E_i = i^{th} component of the instantaneous field

χ_{ij} = Linear susceptibility

d_{ijk} = Second order nonlinear susceptibility

and the susceptibilities are invariant under shuffling of subscripts,

e.g. $\chi_{ij} = \chi_{ji}$ and $d_{ijk} = d_{ikj}$, etc. (2:504).

The linear polarization from equation (1) is:

$$P_i^L = \epsilon_0 \sum_j \chi_{ij} E_j \quad (2)$$

For example, the component of linear polarization in the x direction would be:

$$P_x^L = \epsilon_0 (\chi_{xx} E_x + \chi_{xy} E_y + \chi_{xz} E_z) \quad (3)$$

The second order polarization is:

$$P_i^{NL} = 2 \sum_j \sum_k d_{ijk} E_j E_k$$

for degenerate cases or, in general, for cases with E-fields of more than one frequency present, it is:

$$P_i^{NL}(t) = 2 \sum_j \sum_k \sum_l \sum_m d_{ijk} E_j^{\omega l}(t) E_k^{\omega m}(t) \quad (4)$$

For example, the x-component would take the form:

$$\begin{aligned} P_x^{NL}(t) = & 2 \{ d_{xxx} [E_x^{\omega 1}(t) + E_x^{\omega 2}(t) + \dots + E_x^{\omega n}(t)]^2 \\ & + 2 d_{xxy} [E_x^{\omega 1}(t) + E_x^{\omega 2}(t) + \dots + E_x^{\omega n}(t)] \\ & \quad [E_y^{\omega 1}(t) + E_y^{\omega 2}(t) + \dots + E_y^{\omega n}(t)] \\ & + 2 d_{xxz} [E_x^{\omega 1}(t) + E_x^{\omega 2}(t) + \dots + E_x^{\omega n}(t)] \\ & \quad [E_z^{\omega 1}(t) + E_z^{\omega 2}(t) + \dots + E_z^{\omega n}(t)] \\ & + d_{xyy} [E_y^{\omega 1}(t) + E_y^{\omega 2}(t) + \dots + E_y^{\omega n}(t)]^2 \\ & + 2 d_{xyz} [E_y^{\omega 1}(t) + E_y^{\omega 2}(t) + \dots + E_y^{\omega n}(t)] \\ & \quad [E_z^{\omega 1}(t) + E_z^{\omega 2}(t) + \dots + E_z^{\omega n}(t)] \\ & + d_{xzz} [E_z^{\omega 1}(t) + E_z^{\omega 2}(t) + \dots + E_z^{\omega n}(t)]^2 \} \quad (5) \end{aligned}$$

Expansion of the $E_j^{\omega l}(t) E_k^{\omega m}(t)$ terms gives:

$$\begin{aligned} E_j^{\omega l}(t) E_k^{\omega m}(t) &= (1/2) [A_j^{(\omega l)} \exp(i\omega_l t) + A_j^{(\omega l)*} \exp(-i\omega_l t)] \\ &\quad (1/2) [A_k^{(\omega m)} \exp(i\omega_m t) + A_k^{(\omega m)*} \exp(-i\omega_m t)] \\ &= (1/4) \{ [A_j^{(\omega l)} A_k^{(\omega m)} \exp[i(\omega_l + \omega_m)t] \\ &\quad + A_j^{(\omega l)*} A_k^{(\omega m)*} \exp[i(\omega_l - \omega_m)t]] \\ &\quad + [A_j^{(\omega l)*} A_k^{(\omega m)} \exp[-i(\omega_l - \omega_m)t] \\ &\quad + A_j^{(\omega l)*} A_k^{(\omega m)*} \exp[-i(\omega_l + \omega_m)t]] \} \quad (6) \end{aligned}$$

Thus, this combination produces frequency terms in the nonlinear polarization which are sum and difference frequencies of the driving

E-fields. The frequency terms in the previous example would be:

$$\begin{aligned} P_x^{NL}(t) &= P_x^{2\omega_1}(t) + P_x^{DC}(t) + P_x^{\omega_1 + \omega_2}(t) + P_x^{\omega_1 - \omega_2}(t) + \dots \\ &\quad + P_x^{\omega_1 + \omega_n}(t) + P_x^{\omega_1 - \omega_n}(t) + P_x^{2\omega_2}(t) + \dots \\ &\quad + P_x^{\omega_2 + \omega_n}(t) + P_x^{|\omega_2 - \omega_n|}(t) + \dots + P_x^{2\omega_n}(t) \end{aligned} \quad (7)$$

In general, the sum frequency terms are in the form:

$$\begin{aligned} P_i^{\omega_1 + \omega_2}(t) &= \exp[i(\omega_1 + \omega_2)t] \sum_j \sum_k d_{ijk} A_j^{(\omega_1)} A_k^{(\omega_2)} \\ &\quad + \exp[-i(\omega_1 + \omega_2)t] \sum_j \sum_k d_{ijk} A_j^{(\omega_1)*} A_k^{(\omega_2)*} \end{aligned} \quad (8)$$

where ω_1 and ω_2 are different frequencies. The form of the difference terms is:

$$\begin{aligned} P_i^{|\omega_1 - \omega_2|}(t) &= \exp[i(\omega_1 - \omega_2)t] \sum_j \sum_k d_{ijk} A_j^{(\omega_1)} A_k^{(\omega_2)*} \\ &\quad + \exp[-i(\omega_1 - \omega_2)t] \sum_j \sum_k d_{ijk} A_j^{(\omega_1)*} A_k^{(\omega_2)} \end{aligned} \quad (9)$$

Again, ω_1 and ω_2 are different. The general expression for the second harmonic case ($\omega_1 = \omega_2 = \omega$) is:

$$\begin{aligned} P_i^{2\omega}(t) &= (1/2) [\exp(i2\omega t) \sum_j \sum_k d_{ijk} A_j^{(\omega)} A_k^{(\omega)} \\ &\quad + \exp(-i2\omega t) \sum_j \sum_k d_{ijk} A_j^{(\omega)*} A_k^{(\omega)*}] \end{aligned} \quad (10)$$

The factor of 2 difference between expressions (8) and (10) follows directly from the expansion of equation (5) (2:506,507).

Tensor Form

The tensor form of the second harmonic nonlinear polarization is:

$$P^{(2\omega)} = \begin{pmatrix} P_x^{(2\omega)} \\ P_y^{(2\omega)} \\ P_z^{(2\omega)} \end{pmatrix} = \begin{pmatrix} d_{11} & d_{12} & d_{13} & d_{14} & d_{15} & d_{16} \\ d_{21} & d_{22} & d_{23} & d_{24} & d_{25} & d_{26} \\ d_{31} & d_{32} & d_{33} & d_{34} & d_{35} & d_{36} \end{pmatrix} \begin{pmatrix} A_x^{(\omega)2} \\ A_y^{(\omega)2} \\ A_z^{(\omega)2} \\ 2A_y^{(\omega)} A_z^{(\omega)} \\ 2A_x^{(\omega)} A_z^{(\omega)} \\ 2A_x^{(\omega)} A_y^{(\omega)} \end{pmatrix} \quad (11)$$

Since the second order susceptibilities, d_{ijk} , are invariant under shuffling of subscripts j and k , the form of the elements of the susceptibility tensor is $i = x = 1$, $y = 2$ or $z = 3$ and a contraction of

jk where $xx = 1$, $yy = 2$, $zz = 3$, $yz = zy = 4$, $xz = zx = 5$ and $xy = yx = 6$ (2:507). Certain elements of the second order nonlinear optical susceptibility tensor are always zero for specific crystal point groups. (Refer to Reference 2 (pages 508-511) for further details.)

Summary

An electro-magnetic wave may be defined by a traveling electric field oscillating at some frequency, ω . When a number of such E-fields superimpose in some medium, they may be mixed via the nonlinear susceptibility of the medium to produce a polarization of the medium. For second order polarization, no matter how many fields are present, simultaneously, the frequency components of the polarization can be defined by taking the fields two at a time. Such a component is then either the sum or difference of the frequencies of the two fields considered. The amplitude associated with each frequency component is given by the preceding equations and is dependent on the second order nonlinear optical susceptibilities, d_{ijk} .

Nonlinear Polarization in a Medium Gives Rise to an Electro-Magnetic Wave

The nonlinear polarization produced by the interaction of light waves through the nonlinear susceptibility of a medium will be shown through Maxwell's equations, to be the stimulus which generates a new light wave.

The Wave Equation

The first of Maxwell's equations to be used is

$$\nabla \times H = J + \partial D / \partial t \quad (12)$$

where

H = Magnetic field vector

J = Electric current density

$$= \sigma \mathbf{E}$$

σ = Conductivity

E = Electric field vector

D = Electric displacement vector

$$= \epsilon_0 \mathbf{E} + \mathbf{P}$$

ϵ_0 = Permittivity of free space

P = Electric polarization

$$= \epsilon_0 \chi_L \mathbf{E} + \mathbf{P}_{NL}$$

χ_L = Linear susceptibility

\mathbf{P}_{NL} = Nonlinear polarization

then:

$$\nabla \times \mathbf{H} = \sigma \mathbf{E} + \epsilon \partial \mathbf{E} / \partial t + \partial \mathbf{P}_{NL} / \partial t \quad (13)$$

where

ϵ = Dielectric tensor

$$= \epsilon_0 (1 + \chi_L)$$

The second Maxwell's equation used is:

$$\nabla \times \mathbf{E} = -\partial / \partial t (\mu_0 \mathbf{H}) \quad (14)$$

where

μ_0 = Permeability of free space

If the curl of both sides of equation (14) is taken:

$$\nabla \times \nabla \times \mathbf{E} = -\partial / \partial t (\mu_0 \nabla \times \mathbf{H})$$

using the vector identity:

$$\nabla \times \nabla \times \mathbf{E} = \nabla \cdot \nabla \cdot \mathbf{E} - \nabla^2 \mathbf{E}$$

with the assumption that the E-fields are perpendicular to their propagation (**k**) vectors (3:8) so:

$$\nabla \cdot \nabla = 0$$

and equation (14), equation (13) becomes:

$$\nabla^2 \mathbf{E} = \mu_0 \sigma \partial \mathbf{E} / \partial t + \mu_0 \epsilon \partial^2 \mathbf{E} / \partial t^2 + \mu_0 \partial^2 \mathbf{P}_{NL} / \partial t^2 \quad (15)$$

If the i^{th} component ($i = x, y, \text{ or } z$) of \mathbf{E} at frequency, ω_3 , is written as:

$$E_i^{\omega_3}(\mathbf{r}, t) = (1/2) [A_i^{\omega_3}(\mathbf{r}) \exp[i(\omega_3 t - \mathbf{k}_3 \cdot \mathbf{r})] + A_i^{\omega_3*}(\mathbf{r}) \exp[-i(\omega_3 t - \mathbf{k}_3 \cdot \mathbf{r})]] \quad (16)$$

then:

$$\begin{aligned} \partial^2 E_i^{\omega_3}(\mathbf{r}, t) / \partial x^2 &= (1/2) \{ [\partial^2 A_i^{\omega_3}(\mathbf{r}) / \partial x^2] \exp[i(\omega_3 t - \mathbf{k}_3 \cdot \mathbf{r})] \\ &\quad + 2 [\partial A_i^{\omega_3}(\mathbf{r}) / \partial x] (-ik_{3x}) \exp[i(\omega_3 t - \mathbf{k}_3 \cdot \mathbf{r})] \\ &\quad + A_i^{\omega_3}(\mathbf{r}) (-k_{3x}^2) \exp[i\omega_3 t - \mathbf{k}_3 \cdot \mathbf{r})] \\ &\quad + [\partial^2 A_i^{\omega_3*}(\mathbf{r}) / \partial x^2] \exp[-i(\omega_3 t - \mathbf{k}_3 \cdot \mathbf{r})] \\ &\quad + 2 [\partial A_i^{\omega_3*}(\mathbf{r}) / \partial x] (ik_{3x}) \exp[-i(\omega_3 t - \mathbf{k}_3 \cdot \mathbf{r})] \\ &\quad + A_i^{\omega_3*}(\mathbf{r}) (-k_{3x}^2) \exp[-i(\omega_3 t - \mathbf{k}_3 \cdot \mathbf{r})] \} \end{aligned} \quad (17)$$

with similar expressions for $\partial^2 / \partial y^2$ and $\partial^2 / \partial z^2$.

When the complex envelope varies little over one optical period, a "Slowly Varying Envelope Approximation" (SVEA) can be made:

$$\partial^2 A_i^{\omega_3}(\mathbf{r}) / \partial x^2 \ll \partial A_i^{\omega_3}(\mathbf{r}) / \partial x \quad (18)$$

likewise for $\partial^2 / \partial y^2$ and $\partial^2 / \partial z^2$. This approximation is necessary to make the math manageable as the development continues.

The Laplacian of $E_i^{\omega_3}(\mathbf{r}, t)$ now becomes:

$$\begin{aligned} \nabla^2 E_i^{\omega_3}(\mathbf{r}, t) &= \{-i[k_{3x} \partial A_i^{\omega_3}(\mathbf{r}) / \partial x + k_{3y} \partial A_i^{\omega_3}(\mathbf{r}) / \partial y \\ &\quad + k_{3z} \partial A_i^{\omega_3}(\mathbf{r}) / \partial z] \\ &\quad - (1/2)|\mathbf{k}_3|^2 A_i^{\omega_3}(\mathbf{r})\} \exp[i(\omega_3 t - \mathbf{k}_3 \cdot \mathbf{r})] \\ &\quad + \{i[k_{3x} \partial A_i^{\omega_3*}(\mathbf{r}) / \partial x + k_{3y} \partial A_i^{\omega_3*}(\mathbf{r}) / \partial y \\ &\quad + k_{3z} \partial A_i^{\omega_3*}(\mathbf{r}) / \partial z] \\ &\quad - (1/2)|\mathbf{k}_3|^2 A_i^{\omega_3*}(\mathbf{r})\} \exp[-i(\omega_3 t - \mathbf{k}_3 \cdot \mathbf{r})] \end{aligned} \quad (19)$$

The first and second time derivatives of $E_i^{\omega_3}(\mathbf{r}, t)$ are in the forms:

$$\partial E_i^{\omega_3}(\mathbf{r}, t) / \partial t = i\omega_3 E_i^{\omega_3}(\mathbf{r}, t)$$

and:

$$\partial^2 E_i^{\omega_3}(\mathbf{r}, t) / \partial t^2 = -\omega_3^2 E_i^{\omega_3}(\mathbf{r}, t) \quad (20)$$

The wave equation now becomes:

$$\begin{aligned}
 & \{-i[k_{3x} \partial A_i^{\omega_3}(\mathbf{r}) / \partial x + k_{3y} \partial A_i^{\omega_3}(\mathbf{r}) / \partial y + k_{3z} \partial A_i^{\omega_3}(\mathbf{r}) / \partial z] \\
 & - (1/2) |\mathbf{k}_3|^2 A_i^{\omega_3}(\mathbf{r})\} \exp[i(\omega_3 t - \mathbf{k}_3 \cdot \mathbf{r})] \\
 & + \{i[k_{3x} \partial A_i^{\omega_3*}(\mathbf{r}) / \partial x + k_{3y} \partial A_i^{\omega_3*}(\mathbf{r}) / \partial y + k_{3z} \partial A_i^{\omega_3*}(\mathbf{r}) / \partial z] \\
 & - (1/2) |\mathbf{k}_3|^2 A_i^{\omega_3*}(\mathbf{r})\} \exp[-i(\omega_3 t - \mathbf{k}_3 \cdot \mathbf{r})] \\
 & = (i \mu_0 \sigma \omega_3 / 2) \{A_i^{\omega_3}(\mathbf{r}) \exp[i(\omega_3 t - \mathbf{k}_3 \cdot \mathbf{r})] \\
 & - A_i^{\omega_3*}(\mathbf{r}) \exp[-i(\omega_3 t - \mathbf{k}_3 \cdot \mathbf{r})]\} \\
 & - (\mu_0 \epsilon \omega_3^2 / 2) \{A_i^{\omega_3}(\mathbf{r}) \exp[i(\omega_3 t - \mathbf{k}_3 \cdot \mathbf{r})] \\
 & + A_i^{\omega_3*}(\mathbf{r}) \exp[-i(\omega_3 t - \mathbf{k}_3 \cdot \mathbf{r})]\} \\
 & + \mu_0 \partial^2 P_i^{\omega_3}(\mathbf{r}, t) / \partial t^2 \quad (21)
 \end{aligned}$$

Difference Frequency Components

Consider the component of nonlinear polarization which is the difference of two interacting light frequencies. With the "conservation of energy" condition, $\omega_3 = \omega_1 - \omega_2$, the nonlinear polarization term takes the form:

$$\begin{aligned}
 P_i^{\omega_3} &= \omega_1 - \omega_2(\mathbf{r}, t) \\
 &= \exp[i((\omega_1 - \omega_2)t - (\mathbf{k}_1 - \mathbf{k}_2) \cdot \mathbf{r})] \sum_j \sum_k d_{ijk} A_j^{\omega_1}(\mathbf{r}) A_k^{\omega_2*}(\mathbf{r}) \\
 &\quad + \exp[-i((\omega_1 - \omega_2)t - (\mathbf{k}_1 - \mathbf{k}_2) \cdot \mathbf{r})] \sum_j \sum_k d_{ijk} A_j^{\omega_1*}(\mathbf{r}) A_k^{\omega_2}(\mathbf{r})
 \end{aligned}$$

$$\partial^2 P_i^{\omega_3} = \omega_1 - \omega_2(\mathbf{r}, t) / \partial t^2 = -(\omega_1 - \omega_2)^2 P_i^{\omega_3} = \omega_1 - \omega_2(\mathbf{r}, t) \quad (22)$$

Equating terms synchronous with $\exp(i\omega_3 t)$ from either side of the wave equation (21):

$$\begin{aligned}
 & \{-i[k_{3x} \partial A_i^{\omega_3}(\mathbf{r}) / \partial x + k_{3y} \partial A_i^{\omega_3}(\mathbf{r}) / \partial y + k_{3z} \partial A_i^{\omega_3}(\mathbf{r}) / \partial z] \\
 & - (1/2) |\mathbf{k}_3|^2 A_i^{\omega_3}(\mathbf{r})\} \exp[-i(\mathbf{k}_3 \cdot \mathbf{r})] \\
 & = (i \mu_0 \sigma \omega_3 / 2) A_i^{\omega_3}(\mathbf{r}) \exp[-i(\mathbf{k}_3 \cdot \mathbf{r})] \\
 & - (\mu_0 \epsilon \omega_3^2 / 2) A_i^{\omega_3}(\mathbf{r}) \exp[-i(\mathbf{k}_3 \cdot \mathbf{r})] \\
 & - \omega_3^2 \mu_0 \sum_j \sum_k d_{ijk} A_j^{\omega_1}(\mathbf{r}) A_k^{\omega_2*}(\mathbf{r}) \exp[-i(\mathbf{k}_1 - \mathbf{k}_2) \cdot \mathbf{r}] \quad (23)
 \end{aligned}$$

Since $|\mathbf{k}_3|^2 = \omega_3^2 \mu_0 \epsilon$, then:

$$\begin{aligned}
& k_{3x} \frac{\partial A_i}{\partial x} \omega^3(\mathbf{r}) + k_{3y} \frac{\partial A_i}{\partial y} \omega^3(\mathbf{r}) + k_{3z} \frac{\partial A_i}{\partial z} \omega^3(\mathbf{r}) \\
& = (-\mu_0 \sigma \omega_3 / 2) A_i \omega^3(\mathbf{r}) \\
& \quad - i \omega_3^2 \mu_0 \sum_j \sum_k d_{ijk} A_j \omega^1(\mathbf{r}) A_k \omega^2(\mathbf{r}) \exp[-i(\mathbf{k}_1 - \mathbf{k}_2 - \mathbf{k}_3) \cdot \mathbf{r}] \quad (24)
\end{aligned}$$

Similarly, equating terms synchronous with $\exp(-i\omega_3 t)$ gives:

$$\begin{aligned}
& k_{3x} \frac{\partial A_i}{\partial x} \omega^{3*}(\mathbf{r}) + k_{3y} \frac{\partial A_i}{\partial y} \omega^{3*}(\mathbf{r}) + k_{3z} \frac{\partial A_i}{\partial z} \omega^{3*}(\mathbf{r}) \\
& = (-\mu_0 \sigma \omega_3 / 2) A_i \omega^{3*}(\mathbf{r}) \\
& \quad + i \mu_0 \omega_3^2 \sum_j \sum_k d_{ijk} A_j \omega^{1*}(\mathbf{r}) A_k \omega^2(\mathbf{r}) \exp[i(\mathbf{k}_1 - \mathbf{k}_2 - \mathbf{k}_3) \cdot \mathbf{r}] \quad (25)
\end{aligned}$$

Sum Frequency Components

Consider the nonlinear polarization component which is the sum of two interacting frequencies where these frequencies are different, $\omega_1 \neq \omega_2$. The conservation of energy condition is $\omega_3 = \omega_1 + \omega_2$ and the polarization is in the form:

$$\begin{aligned}
P_i \omega^3 &= \omega^1 + \omega^2(\mathbf{r}, t) \\
&= \exp[i((\omega_1 + \omega_2)t - (\mathbf{k}_1 + \mathbf{k}_2) \cdot \mathbf{r})] \sum_j \sum_k d_{ijk} A_j \omega^1(\mathbf{r}) A_k \omega^2(\mathbf{r}) \\
&\quad + \exp\{-i((\omega_1 + \omega_2)t - (\mathbf{k}_1 + \mathbf{k}_2) \cdot \mathbf{r})\} \sum_j \sum_k d_{ijk} A_j \omega^{1*}(\mathbf{r}) A_k \omega^{2*}(\mathbf{r}) \\
\partial_t^2 P_i \omega^3 &= \omega^1 + \omega^2(\mathbf{r}, t) / \partial t^2 = -(\omega_1 + \omega_2)^2 P_i \omega^3 = \omega^1 + \omega^2(\mathbf{r}, t) \quad (26)
\end{aligned}$$

Equating synchronous terms from either side of equation (21) yields, for $\exp(i\omega_3 t)$:

$$\begin{aligned}
& k_{3x} \frac{\partial A_i}{\partial x} \omega^3(\mathbf{r}) + k_{3y} \frac{\partial A_i}{\partial y} \omega^3(\mathbf{r}) + k_{3z} \frac{\partial A_i}{\partial z} \omega^2(\mathbf{r}) \\
& = (-\mu_0 \sigma \omega_3 / 2) A_i \omega^3(\mathbf{r}) \\
& \quad - i \omega_3^2 \mu_0 \sum_j \sum_k d_{ijk} A_j \omega^1(\mathbf{r}) A_k \omega^2(\mathbf{r}) \exp[-i(\mathbf{k}_1 + \mathbf{k}_2 - \mathbf{k}_3) \cdot \mathbf{r}] \quad (27)
\end{aligned}$$

and for $\exp(-i\omega_3 t)$:

$$\begin{aligned}
& k_{3x} \frac{\partial A_i}{\partial x} \omega^{3*}(\mathbf{r}) + k_{3y} \frac{\partial A_i}{\partial y} \omega^{3*}(\mathbf{r}) + k_{3z} \frac{\partial A_i}{\partial z} \omega^{3*}(\mathbf{r}) \\
& = (-\mu_0 \sigma \omega_3 / 2) A_i \omega^{3*}(\mathbf{r}) \\
& \quad + i \mu_0 \omega_3^2 \sum_j \sum_k d_{ijk} A_j \omega^{1*}(\mathbf{r}) A_k \omega^{2*}(\mathbf{r}) \exp[i(\mathbf{k}_1 + \mathbf{k}_2 - \mathbf{k}_3) \cdot \mathbf{r}] \quad (28)
\end{aligned}$$

Second Harmonic Case

Finally, consider the component of nonlinear polarization which is

the sum of two interacting frequencies and these frequencies are the same. The conservation of energy condition is $\omega_3 = 2\omega$ and the form of the nonlinear polarization is:

$$P_i^{\omega_3} = 2\omega(\mathbf{r}, t) = (1/2)\{[\exp[i(2\omega t - 2\mathbf{k} \cdot \mathbf{r})]\sum_j \sum_k d_{ijk} A_j \omega(\mathbf{r}) A_k \omega(\mathbf{r}) + \exp[-i(2\omega t - 2\mathbf{k} \cdot \mathbf{r})]\sum_j \sum_k d_{ijk} A_j \omega^*(\mathbf{r}) A_k \omega^*(\mathbf{r})]\}$$

$$\partial^2 P_i^{\omega_3} / \partial t^2 = 2\omega^2 P_i^{\omega_3} = 2\omega(\mathbf{r}, t) \quad (29)$$

Again, equating synchronous terms yields, for $\exp(i2\omega t)$:

$$\begin{aligned} k_{3x} \partial A_i \frac{2\omega(\mathbf{r})}{\partial x} + k_{3y} \partial A_i \frac{2\omega(\mathbf{r})}{\partial y} + k_{3z} \partial A_i \frac{2\omega(\mathbf{r})}{\partial z} \\ = -\mu_0 \sigma \omega A_i \frac{2\omega(\mathbf{r})}{\partial t} \\ - i 2\omega^2 \mu_0 \sum_j \sum_k d_{ijk} A_j \omega(\mathbf{r}) A_k \omega(\mathbf{r}) \exp[-i(2\mathbf{k} - \mathbf{k}_3) \cdot \mathbf{r}] \end{aligned} \quad (30)$$

and for $\exp(-i2\omega t)$:

$$\begin{aligned} k_{3x} \partial A_i \frac{2\omega^*(\mathbf{r})}{\partial x} + k_{3y} \partial A_i \frac{2\omega^*(\mathbf{r})}{\partial y} + k_{3z} \partial A_i \frac{2\omega^*(\mathbf{r})}{\partial z} \\ = -\mu_0 \sigma \omega A_i \frac{2\omega^*(\mathbf{r})}{\partial t} \\ + i 2\omega^2 \mu_0 \sum_j \sum_k d_{ijk} A_j \omega^*(\mathbf{r}) A_k \omega^*(\mathbf{r}) \exp[i(2\mathbf{k} - \mathbf{k}_3) \cdot \mathbf{r}] \end{aligned} \quad (31)$$

Summary

The nonlinear polarization wave produced by the mixing of electric fields in a nonlinear medium gives rise to another E-field (and thus a new light wave). The amplitude of this field can be described by solution to Maxwell's wave equation and, under conservation of energy, the frequency of the response is the same as the frequency of the stimulus. Therefore, the frequency of this new light wave is the same as the frequency of the polarization.

Phase Matching's Role in the Selection of the Wave of Highest Energy Transfer (A Nondepleted Input Example)

The amplitude of the light wave produced via the nonlinear polarization of a medium was derived in the previous section. The propagation vector of this wave will now be derived.

Consider the sum-frequency conservation of energy condition,

$\omega_3 = \omega_1 + \omega_2$. The amplitude relationships are given by equations (27) and (28).

First assumption: the medium is assumed to be transparent at ω_3 , then $\sigma = 0$ and equation (27) reduces to:

$$\begin{aligned} k_{3x} \partial A_i^{\omega_3}(\mathbf{r}) / \partial x + k_{3y} \partial A_i^{\omega_3}(\mathbf{r}) / \partial y + k_{3z} \partial A_i^{\omega_3}(\mathbf{r}) / \partial z \\ = -i \omega_3^2 \mu_0 \sum_j \sum_k d_{ijk} A_j^{\omega_1}(\mathbf{r}) A_k^{\omega_2}(\mathbf{r}) \exp(-i\Delta\mathbf{k} \cdot \mathbf{r}) \end{aligned} \quad (32)$$

where $\Delta\mathbf{k} = \mathbf{k}_1 + \mathbf{k}_2 - \mathbf{k}_3$ and with similar expressions for equation (28).

Second assumption: The depletion of the mixing beams (those at ω_1 and ω_2) is assumed negligible:

$$\partial A_j^{\omega_1}(\mathbf{r}) / \partial x = \partial A_k^{\omega_2}(\mathbf{r}) / \partial x = 0 \quad (33)$$

with similar expressions for x , y and the conjugates. Then:

$$\begin{aligned} A_j^{\omega_1}(\mathbf{r}) &= A_j^{\omega_1*} \\ A_j^{\omega_1*}(\mathbf{r}) &= A_j^{\omega_1*} \\ A_k^{\omega_2}(\mathbf{r}) &= A_k^{\omega_2} \\ A_k^{\omega_2*}(\mathbf{r}) &= A_k^{\omega_2*} \end{aligned} \quad (34)$$

Equation (59) now becomes:

$$\begin{aligned} k_{3x} \partial A_i^{\omega_3}(\mathbf{r}) / \partial x + k_{3y} \partial A_i^{\omega_3}(\mathbf{r}) / \partial y + k_{3z} \partial A_i^{\omega_3}(\mathbf{r}) / \partial z \\ = -i \omega_3^2 \mu_0 \sum_j \sum_k d_{ijk} A_j^{\omega_1} A_k^{\omega_2} \exp(-i\Delta\mathbf{k} \cdot \mathbf{r}) \end{aligned} \quad (35)$$

with a similar expression for the conjugate.

If the solution to equation (35) is assumed to be in the form:

$$A_i^{\omega_3}(\mathbf{r}) = K \exp(-i\Delta\mathbf{k} \cdot \mathbf{r}) + C \quad (36)$$

then:

$$\partial A_i^{\omega_3}(\mathbf{r}) / \partial x = -iK \Delta k_x \exp(-i\Delta\mathbf{k} \cdot \mathbf{r}) \quad (37)$$

with similar expressions for y and z .

Equation (35) becomes:

$$-iK (\Delta\mathbf{k} \cdot \mathbf{k}_3) \exp(-i\Delta\mathbf{k} \cdot \mathbf{r}) = -i \omega_3^2 \mu_0 \sum_j \sum_k d_{ijk} A_j^{\omega_1} A_k^{\omega_2} \exp(-i\Delta\mathbf{k} \cdot \mathbf{r}) \quad (38)$$

so the constant, K , is in the form:

$$K = \frac{\omega_3^2 \mu_0 \sum_j \sum_k d_{ijk} A_j^{\omega 1} A_k^{\omega 2}}{\Delta \mathbf{k} \cdot \mathbf{k}_3} \quad (39)$$

If there is no interaction length within the medium, no nonlinear polarization is produced to drive a new E-M field. Therefore, the amplitude of the new wave is zero. Thus, the boundary condition:

$$\begin{aligned} A_i^{\omega 3}(0,0,0) &= 0 = K + C \\ C &= -K \end{aligned} \quad (40)$$

The solution to equation (35) is:

$$A_i^{\omega 3}(\mathbf{r}) = K[\exp(-i \Delta \mathbf{k} \cdot \mathbf{r}) - 1] \quad (41)$$

By similar development, the conjugate solution is:

$$A_i^{\omega 3*}(\mathbf{r}) = K^* [\exp(i \Delta \mathbf{k} \cdot \mathbf{r}) - 1] \quad (42)$$

where

$$K^* = \frac{\omega_3^2 \mu_0 \sum_j \sum_k d_{ijk} A_j^{\omega 1*} A_k^{\omega 2*}}{\Delta \mathbf{k} \cdot \mathbf{k}_3} \quad (43)$$

From Poynting's theorem (2:13), the i^{th} mode power/unit area at ω_3 , at some interaction length, $k_3 L$ (in the direction of the wave, \mathbf{k}_3), is given by:

$$\begin{aligned} P_i^{\omega 3}/\text{area} &= (1/2)(\epsilon/\mu_0)^{1/2} A_i^{\omega 3}(k_{3x}L, k_{3y}L, k_{3z}L) \\ &\quad A_i^{\omega 3*}(k_{3x}L, k_{3y}L, k_{3z}L) \\ &= (1/2)(\epsilon/\mu_0)^{1/2} K \left[\frac{\exp(-i \Delta \mathbf{k} \cdot \mathbf{k}_3 L/2) - \exp(i \Delta \mathbf{k} \cdot \mathbf{k}_3 L/2)}{\exp(-i \Delta \mathbf{k} \cdot \mathbf{k}_3 L/2)} \right] \\ &\quad K^* \left[\frac{\exp(i \Delta \mathbf{k} \cdot \mathbf{k}_3 L/2) - \exp(-i \Delta \mathbf{k} \cdot \mathbf{k}_3 L/2)}{\exp(-i \Delta \mathbf{k} \cdot \mathbf{k}_3 L/2)} \right] \\ &= (L^2/2) (\epsilon/\mu_0)^{1/2} \omega_3^4 \mu_0^2 \left(\sum_j \sum_k d_{ijk} A_j^{\omega 1} A_k^{\omega 2} \right) \\ &\quad \left(\sum_j \sum_k d_{ijk} A_j^{\omega 1*} A_k^{\omega 2*} \right) [\sin^2(\Delta \mathbf{k} \cdot \mathbf{k}_3 L/2) / (\Delta \mathbf{k} \cdot \mathbf{k}_3 L/2)^2] \quad (44) \end{aligned}$$

The power in the produced wave (at ω_3) is maximized when the argument of the $(\sin x)/x$ term in equation (44) approaches zero. This implies $\Delta \mathbf{k} \cdot \mathbf{k}_3 = 0$ and, therefore, that:

$$\Delta \mathbf{k} = 0 \quad (45)$$

This is the "conservation of momentum" condition.

Similar arguments can be made for the frequency-difference and second harmonic cases with similar results: $\Delta \mathbf{k} = 0$ for significant power transfer.

Summary

The light wave produced from the second order polarization is of a frequency which results from the mixing (either sum or difference) of two input optical frequencies. There may be an infinite number of input frequencies available (either by the overlapping of a large number of beams or the generation of additional frequencies via the mixing process) but a specific frequency, ω_3 , is selected by meeting the conservation of energy requirement ($\omega_3 = \omega_1 + \omega_2$, $\omega_3 = \omega_1 - \omega_2$) and the conservation of momentum requirement ($\Delta \mathbf{k} = 0$) so the only significant energy transfer occurs to the newly created beam at ω_3 and \mathbf{k}_3 .

Third Order Nonlinear Principles

The concepts of nonlinear polarization, Maxwell's equations and phase matching in the second order will now be extended to the third order. Phase conjugation by degenerate four wave mixing is then a special case of these third order concepts.

Third Order Nonlinear Polarization

Again, when E-fields superimpose in a nonlinear medium, the polarization of that medium may be written as in equation (1):

$$P_i = \epsilon_0 \sum_j \chi_{ij} E_j + 2 \sum_j \sum_k d_{ijk} E_j E_k \\ + 4 \sum_j \sum_k \sum_l \chi_{ijkl} E_j E_k E_l + \dots$$

The third order nonlinear polarization for the degenerate case is:

$$P_i^{NL} = 4 \sum_j \sum_k \sum_l \chi_{ijkl} E_j E_k E_l \quad (46)$$

or for cases when more than one frequency E-fields are present:

$$P_i^{NL} = 4 \sum_j \sum_k \sum_l \sum_m \sum_p \sum_q \chi_{ijkl} E_j^{\omega_m} E_k^{\omega_p} E_l^{\omega_q} \quad (47)$$

Expansion of the $E_j^{\omega_m} E_k^{\omega_p} E_l^{\omega_q}$ term gives:

$$\begin{aligned} E_j^{\omega_m}(t) E_k^{\omega_p}(t) E_l^{\omega_q}(t) = & (1/8) \{ A_j^{\omega_m} A_k^{\omega_p} A_l^{\omega_q} \exp[i(\omega_m + \omega_p + \omega_q)t] \\ & + A_j^{\omega_m} A_k^{\omega_p} A_l^{\omega_q*} \exp[i(\omega_m + \omega_p - \omega_q)t] \\ & + A_j^{\omega_m} A_k^{\omega_p*} A_l^{\omega_q} \exp[i(\omega_m - \omega_p + \omega_q)t] \\ & + A_j^{\omega_m} A_k^{\omega_p*} A_l^{\omega_q*} \exp[i(\omega_m - \omega_p - \omega_q)t] \\ & + A_j^{\omega_m*} A_k^{\omega_p} A_l^{\omega_q} \exp[-i(\omega_m + \omega_p - \omega_q)t] \\ & + A_j^{\omega_m*} A_k^{\omega_p*} A_l^{\omega_q} \exp[-i(\omega_m + \omega_p - \omega_q)t] \\ & + A_j^{\omega_m*} A_k^{\omega_p*} A_l^{\omega_q*} \exp[-i(\omega_m - \omega_p + \omega_q)t] \\ & + A_j^{\omega_m*} A_k^{\omega_p*} A_l^{\omega_q*} \exp[-i(\omega_m + \omega_p + \omega_q)t] \} \end{aligned} \quad (48)$$

Thus, the frequency components of the third order nonlinear polarization are:

$$P_i^{NL}(t) = \sum_m \sum_p \sum_q P_i^{\omega_m + \omega_p + \omega_q}(t) + P_i^{|\omega_m + \omega_p - \omega_q|}(t) \quad (49)$$

The expansion of the first component yields:

$$\begin{aligned} P_i^{\omega_m + \omega_p + \omega_q}(t) = & K \sum_j \sum_k \sum_l \chi_{ijkl} [A_j^{\omega_m} A_k^{\omega_p} A_l^{\omega_q} \exp[i(\omega_m + \omega_p + \omega_q)t] \\ & + A_j^{\omega_m*} A_k^{\omega_p*} A_l^{\omega_q*} \exp[-i(\omega_m + \omega_p + \omega_q)t]] \end{aligned} \quad (50)$$

where

$$\begin{aligned} K &= 3 \quad \text{if } \omega_m, \omega_p \text{ and } \omega_q \text{ are different} \\ &= 3/2 \quad \text{if two of } \omega_m, \omega_p, \text{ or } \omega_q \text{ are same, one different} \\ &= 1/2 \quad \text{if } \omega_m, \omega_p, \text{ and } \omega_q \text{ are all the same} \end{aligned}$$

the values of K result from an expansion of equation (47) similar to that for the sum-frequency and second harmonic cases in the previous chapter. The amplitudes are:

$$\begin{aligned} P_i^{(\omega_m + \omega_p + \omega_q)} &= 2K \sum_j \sum_k \sum_l \chi_{ijkl} A_j^{\omega_m} A_k^{\omega_p} A_l^{\omega_q} \\ P_i^{(\omega_m + \omega_p + \omega_q)*} &= 2K \sum_j \sum_k \sum_l \chi_{ijkl} A_j^{\omega_m*} A_k^{\omega_p*} A_l^{\omega_q*} \end{aligned} \quad (51)$$

The other components yield:

$$\begin{aligned}
P_i^{\omega_m + \omega_p - \omega_q} (t) &= K \sum_j \sum_k \sum_l \chi_{ijkl} [A_j^{\omega_m} A_k^{\omega_p} A_l^{\omega_q} \exp[i(\omega_m + \omega_p - \omega_q)t] \\
&\quad + A_j^{\omega_m*} A_k^{\omega_p*} A_l^{\omega_q} \exp[-i(\omega_m + \omega_p - \omega_q)t]]
\end{aligned} \tag{52}$$

where the amplitudes are:

$$\begin{aligned}
P_i^{|\omega_m + \omega_p - \omega_q|} &= 2K \sum_j \sum_k \sum_l \chi_{ijkl} A_j^{\omega_m} A_k^{\omega_p} A_l^{\omega_q} \\
P_i^{|\omega_m + \omega_p - \omega_q|*} &= 2K \sum_j \sum_k \sum_l \chi_{ijkl} A_j^{\omega_m*} A_k^{\omega_p*} A_l^{\omega_q}
\end{aligned} \tag{53}$$

Just as with the second order nonlinear polarization, any number of electric fields may superimpose in a medium and their frequencies may be mixed via the nonlinear susceptibility of the medium. For third order nonlinear polarization, however, the fields are considered three at a time to produce a polarization frequency component which is some combination of sums and differences of those three frequencies. The amplitude of such a component is given by the preceding equations and dependent on the third nonlinear susceptibility, χ_{ijkl} .

The Wave Equation

Just as in the second order case, the nonlinear polarization will be a stimulus for which the response is an electromagnetic wave. The wave equation developed from Maxwell's equations, equation (21), is in the following form:

$$\begin{aligned}
&[-i[k_{3x} \partial A_i^{\omega_3}(\mathbf{r})/\partial x + k_{3y} \partial A_i^{\omega_3}(\mathbf{r})/\partial y + k_{3z} \partial A_i^{\omega_3}(\mathbf{r})/\partial z] \\
&\quad - (1/2)|\mathbf{k}_3|^2 A_i^{\omega_3}(\mathbf{r})] \exp[i(\omega_3 t - \mathbf{k}_3 \cdot \mathbf{r})] \\
&+ \{i[k_{3x} \partial A_i^{\omega_3*}(\mathbf{r})/\partial x + k_{3y} \partial A_i^{\omega_3*}(\mathbf{r})/\partial y + k_{3z} \partial A_i^{\omega_3*}(\mathbf{r})/\partial z] \\
&\quad - (1/2)|\mathbf{k}_3|^2 A_i^{\omega_3*}(\mathbf{r})\} \exp[-i(\omega_3 t - \mathbf{k}_3 \cdot \mathbf{r})] \\
&= (i \mu_0 \sigma \omega_3^2 / 2) \{A_i^{\omega_3}(\mathbf{r}) \exp[i(\omega_3 t - \mathbf{k}_3 \cdot \mathbf{r})] - A_i^{\omega_3*}(\mathbf{r}) \exp[-i(\omega_3 t - \mathbf{k}_3 \cdot \mathbf{r})]\} \\
&\quad - (\mu_0 \epsilon \omega_3^2 / 2) \{A_i^{\omega_3}(\mathbf{r}) \exp[i(\omega_3 t - \mathbf{k}_3 \cdot \mathbf{r})] + A_i^{\omega_3*}(\mathbf{r}) \exp[-i(\omega_3 t - \mathbf{k}_3 \cdot \mathbf{r})]\} \\
&\quad + \mu_0 \partial^2 P_i^{\omega_3}(\mathbf{r}, t) / \partial t^2
\end{aligned}$$

The third order nonlinear polarization with conservation of energy

condition, $\omega_3 = \omega_1 + \omega_2 - \omega_4$, is:

$$\begin{aligned} p_i^{\omega_3} = \omega_1 + \omega_2 - \omega_4(\mathbf{r}, t) &= 3 \sum_j \sum_k \sum_l \chi_{ijkl} [A_j^{\omega_1}(\mathbf{r}) A_k^{\omega_2}(\mathbf{r}) A_l^{\omega_4*}(\mathbf{r}) \\ &\quad \exp\{i[(\omega_1 + \omega_2 - \omega_4)t - (\mathbf{k}_1 + \mathbf{k}_2 - \mathbf{k}_4) \cdot \mathbf{r}]\}] \\ &\quad + A_j^{\omega_1*}(\mathbf{r}) A_k^{\omega_2*}(\mathbf{r}) A_l^{\omega_4}(\mathbf{r}) \\ &\quad \exp\{-i[(\omega_1 + \omega_2 - \omega_4)t - (\mathbf{k}_1 + \mathbf{k}_2 - \mathbf{k}_4) \cdot \mathbf{r}]\} \end{aligned} \quad (54)$$

then:

$$\begin{aligned} \partial^2 p_i^{\omega_3} / \partial t^2 &= \omega_1 + \omega_2 - \omega_4(\mathbf{r}, t) \\ &= -(\omega_1 + \omega_2 - \omega_4)^2 p_i^{\omega_3} = \omega_1 + \omega_2 - \omega_4(\mathbf{r}, t) \end{aligned} \quad (55)$$

Equating terms synchronous with $\exp(i\omega_3 t)$ from either side of the wave equation gives:

$$\begin{aligned} &\{-i[k_{3x} \partial A_i^{\omega_3}(\mathbf{r}) / \partial x + k_{3y} \partial A_i^{\omega_3}(\mathbf{r}) / \partial y + k_{3z} \partial A_i^{\omega_3}(\mathbf{r}) / \partial z] \\ &\quad - (1/2)|\mathbf{k}_3|^2 A_i^{\omega_3}(\mathbf{r})\} \exp(-i\mathbf{k}_3 \cdot \mathbf{r}) \\ &= (i \mu_0 \sigma \omega_3 / 2 - \mu_0 \epsilon \omega_3^2 / 2) A_i^{\omega_3}(\mathbf{r}) \exp(-i\mathbf{k}_3 \cdot \mathbf{r}) \\ &\quad - 3 \mu_0 \omega_3^2 \sum_j \sum_k \sum_l \chi_{ijkl} A_j^{\omega_1}(\mathbf{r}) A_k^{\omega_2}(\mathbf{r}) A_l^{\omega_4*}(\mathbf{r}) \\ &\quad \exp[-i(\mathbf{k}_1 + \mathbf{k}_2 - \mathbf{k}_4) \cdot \mathbf{r}] \end{aligned} \quad (56)$$

Since $|\mathbf{k}_3|^2 = \omega_3^2 \mu_0 \epsilon$, then:

$$\begin{aligned} k_{3x} \partial A_i^{\omega_3}(\mathbf{r}) / \partial x + k_{3y} \partial A_i^{\omega_3}(\mathbf{r}) / \partial y + k_{3z} \partial A_i^{\omega_3}(\mathbf{r}) / \partial z \\ = (-\mu_0 \sigma \omega_3 / 2) A_i^{\omega_3}(\mathbf{r}) \\ - i 3 \mu_0 \omega_3^2 \sum_j \sum_k \sum_l \chi_{ijkl} A_j^{\omega_1}(\mathbf{r}) A_k^{\omega_2}(\mathbf{r}) A_l^{\omega_4*}(\mathbf{r}) \\ \exp[-i(\mathbf{k}_1 + \mathbf{k}_2 - \mathbf{k}_4 - \mathbf{k}_3) \cdot \mathbf{r}] \end{aligned} \quad (57)$$

Similarly equating terms synchronous with $\exp(-i\omega_3 t)$ gives:

$$\begin{aligned} k_{3x} \partial A_i^{\omega_3*}(\mathbf{r}) / \partial x + k_{3y} \partial A_i^{\omega_3*}(\mathbf{r}) / \partial y + k_{3z} \partial A_i^{\omega_3*}(\mathbf{r}) / \partial z \\ = (-\mu_0 \sigma \omega_3 / 2) A_i^{\omega_3*}(\mathbf{r}) \\ + i 3 \mu_0 \omega_3^2 \sum_j \sum_k \sum_l \chi_{ijkl} A_j^{\omega_1*}(\mathbf{r}) A_k^{\omega_2*}(\mathbf{r}) A_l^{\omega_4}(\mathbf{r}) \\ \exp[i(\mathbf{k}_1 + \mathbf{k}_2 - \mathbf{k}_4 - \mathbf{k}_3) \cdot \mathbf{r}] \end{aligned} \quad (58)$$

Similar developments can be made for other sum and difference

frequency combinations.

Summary

Just as in the second order, the third order nonlinear polarization wave produced by the mixing of electric fields in a nonlinear medium gives rise to a new E-field (and, thus, a new light wave). The amplitude of this new field can be determined using the wave equation and, under conservation of energy conditions, the frequency of the light wave is the same as that of the polarization wave.

Phase Matching

Again, just as in the second order development, a condition for high energy transfer from the input waves to the produced wave will be developed. The conservation of energy condition, $\omega_3 = \omega_1 + \omega_2 - \omega_4$, will again be considered. Equations (57) and (58) give the amplitude relationships.

The two assumptions made in the second order development are again made: the medium is transparent at ω_3 , therefore, $\sigma=0$; and the input beams are not significantly depleted by the mixing process so:

$$\partial A_j^{\omega_1}(\mathbf{r})/\partial x = \partial A_k^{\omega_2}(\mathbf{r})/\partial x = \partial A_l^{\omega_4}(\mathbf{r})/\partial x = 0 \quad (59)$$

with similar expressions for y, z and the conjugates. Then:

$$\begin{aligned} A_j^{\omega_1}(\mathbf{r}) &= A_j^{\omega_1} & A_j^{\omega_1*}(\mathbf{r}) &= A_j^{\omega_1*} \\ A_k^{\omega_2}(\mathbf{r}) &= A_k^{\omega_2} & A_k^{\omega_2*}(\mathbf{r}) &= A_k^{\omega_2*} \\ A_l^{\omega_4}(\mathbf{r}) &= A_l^{\omega_4} & A_l^{\omega_4*}(\mathbf{r}) &= A_l^{\omega_4*} \end{aligned} \quad (60)$$

Equation (57) becomes

$$\begin{aligned} k_{3x} \partial A_i^{\omega_3}(\mathbf{r})/\partial x + k_{3y} \partial A_i^{\omega_3}(\mathbf{r})/\partial y + k_{3z} \partial A_i^{\omega_3}(\mathbf{r})/\partial z \\ = -i \mu_0 \sum_j \sum_k \sum_l \chi_{ijkl} A_j^{\omega_1} A_k^{\omega_2} A_l^{\omega_4*} \exp(-i\Delta\mathbf{k}\cdot\mathbf{r}) \end{aligned} \quad (61)$$

where $\Delta\mathbf{k} = \mathbf{k}_1 + \mathbf{k}_2 - \mathbf{k}_4 - \mathbf{k}_3$. The solution to equation (61) is assumed to be in the form:

$$A_i^{\omega_3}(\mathbf{r}) = K \exp(-i \Delta \mathbf{k} \cdot \mathbf{r}) + C$$

then:

$$\partial A_i^{\omega_3}(\mathbf{r}) / \partial x = -i \Delta k_x K \exp(-i \Delta \mathbf{k} \cdot \mathbf{r})$$

with similar expressions for y and z. Equation (61) becomes:

$$-i K (\Delta \mathbf{k} \cdot \mathbf{k}_3) \exp(-i \Delta \mathbf{k} \cdot \mathbf{r}) = -i 3 \mu_0 \omega_3^2 \sum_j \sum_k \sum_l x_{ijkl} A_j^{\omega_1} A_k^{\omega_2} A_l^{\omega_4*} \exp(-i \Delta \mathbf{k} \cdot \mathbf{r}) \quad (62)$$

so the constant, K, is in the form:

$$K = \frac{3\mu_0 \omega_3^2 \sum_j \sum_k \sum_l x_{ijkl} A_j^{\omega_1} A_k^{\omega_2} A_l^{\omega_4*}}{\Delta \mathbf{k} \cdot \mathbf{k}_3} \quad (63)$$

Again, as in the second order, if there is no interaction length within the medium, no nonlinear polarization occurs and no new wave can be produced:

$$A_i^{\omega_3}(0,0,0) = 0 = K + C$$

$$C = -K$$

The solution to equation (61) is:

$$A_i^{\omega_3}(\mathbf{r}) = K[\exp(-i \Delta \mathbf{k} \cdot \mathbf{r}) - 1] \quad (64)$$

By similar development, the conjugate solution is:

$$A_i^{\omega_3*}(\mathbf{r}) = K^* [\exp(i \Delta \mathbf{k} \cdot \mathbf{r}) - 1] \quad (65)$$

where

$$K^* = \frac{3 \mu_0 \omega_1^2 \sum_j \sum_k \sum_l x_{ijkl} A_j^{\omega_1*} A_k^{\omega_2*} A_l^{\omega_4}}{\Delta \mathbf{k} \cdot \mathbf{k}_3} \quad (66)$$

Again, from Poynting's Theorem (2:13), the i^{th} mode power/unit area at ω_3 , at some interaction length, $k_3 L$ (in the direction of the wave, \mathbf{k}_3), is given by:

$$\begin{aligned}
P_i^{\omega_3}/\text{area} &= (1/2)(\epsilon/\mu_0)^{1/2} A_i^{\omega_3}(k_{3x}L, k_{3y}L, k_{3z}L) \\
&\quad A_i^{\omega_3*}(k_{3x}L, k_{3y}L, k_{3z}L) \\
&= (L^2/2) (\epsilon/\mu_0)^{1/2} \mu_0^2 \omega_3^2 \\
&\quad (\sum_j \sum_k \sum_l \chi_{ijkl} A_j^{\omega_1} A_k^{\omega_2} A_l^{\omega_4*}) \\
&\quad (\sum_j \sum_k \sum_l \chi_{ijkl} A_j^{\omega_1*} A_k^{\omega_2*} A_l^{\omega_4}) \\
&\quad [\sin^2(\Delta\mathbf{k} \cdot \mathbf{k}_3 L/2) / (\Delta\mathbf{k} \cdot \mathbf{k}_3 L/2)^2] \tag{67}
\end{aligned}$$

Again, the power in the response wave (at ω_3) is maximized when the argument of the $(\sin x)/x$ term approaches zero. This implies $\Delta\mathbf{k} \cdot \mathbf{k}_3 = 0$ and, therefore, the conservation of momentum condition, $\Delta\mathbf{k} = 0$.

Similar developments may be made for other sum and difference input frequencies with similar results.

Summary

As in the second order case, the light wave produced via the third order nonlinear polarization is of a frequency which is the result of mixing three input frequencies (in some sum or difference combination) meeting the conservation of energy condition. The direction of propagation of this wave, \mathbf{k}_3 is determined by meeting the conservation of momentum condition, $\Delta\mathbf{k} = 0$, so that energy transferred to this newly created beam is significant.

III. Optical Phase Conjugation by Degenerate Four Wave Mixing (A Third Order Nonlinear Process)

In the previous chapter, the third order concepts of nonlinear polarization, Maxwell's wave equation and phase matching were developed. A special case of these third order concepts, optical phase conjugation by degenerate four wave mixing, will now be described.

Figure 4 shows the geometry to be considered. E_1 and E_2 are counterpropagating, non-depleted pump beams. E_p is the probe beam and E_c is the conjugate of the probe. It is shown that in order to meet phase match conditions, the conjugate and the probe must also counterpropagate. Expressions for the amplitudes of the conjugate and probe, which extract energy from the pumps, are also derived.

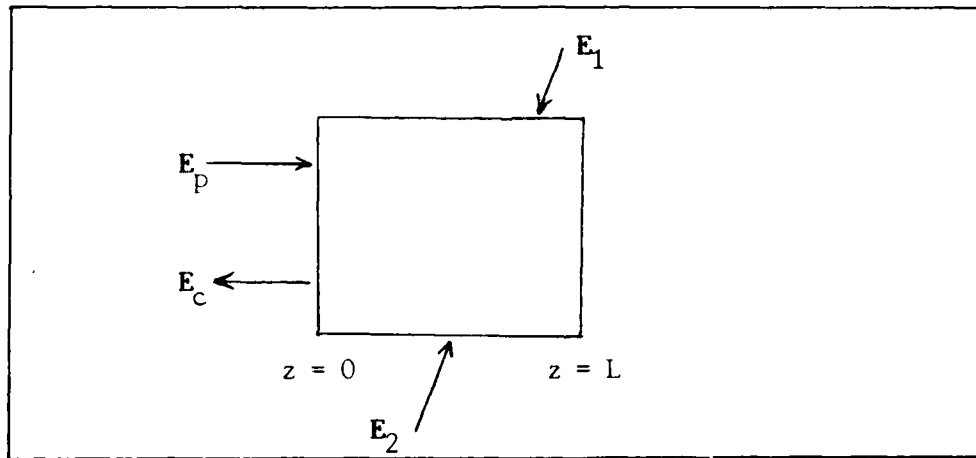


Figure 4. Geometry of phase conjugation by four wave mixing (3:29).

Third Order Polarization

The polarization of the nonlinear medium due to the superposition of the four electric fields is given by equation (1):

$$P_i = \epsilon_0 \sum_j X_{ij} E_j + 2 \sum_{jk} \sum d_{ijk} E_j E_k + 4 \sum_{jkl} \sum X_{ijkl} E_j E_k E_l + \dots$$

The third order nonlinear polarization, equation (46), is:

$$P_i^{NL} = 4 \sum_{jkl} \sum X_{ijkl} E_j E_k E_l$$

The total electric field consists of the four superimposed fields so that:

$$\begin{aligned}
 P_i &= 4 \sum_j \sum_k \sum_l \chi_{ijkl} (E_j^{\omega_1} + E_j^{\omega_2} + E_j^{\omega_p} + E_j^{\omega_c}) \\
 &\quad (E_k^{\omega_1} + E_k^{\omega_2} + E_k^{\omega_p} + E_k^{\omega_c}) \\
 &\quad (E_l^{\omega_1} + E_l^{\omega_2} + E_l^{\omega_p} + E_l^{\omega_c}) \\
 &= 4 \sum_j \sum_k \sum_l \sum_m \sum_n \sum_q \chi_{ijkl} E_j^{\omega_m} E_k^{\omega_n} E_l^{\omega_q} \tag{68}
 \end{aligned}$$

where

j, k and $l = x, y$ or z

m, n and $q = 1, 2, p$ or c

(The expansion of equation (68) yields 1728 terms!)

The product of the E-fields in equation (68) can be further expanded as follows:

$$\begin{aligned}
 E_j^{\omega_m} E_k^{\omega_n} E_l^{\omega_q} &= (1/2) \{ A_j^{\omega_m}(\mathbf{r}) \exp[i(\omega_m t - \mathbf{k}_m \cdot \mathbf{r})] \\
 &\quad + A_j^{\omega_m*}(\mathbf{r}) \exp[-i(\omega_m t - \mathbf{k}_m \cdot \mathbf{r})] \} \\
 &(1/2) \{ A_k^{\omega_n}(\mathbf{r}) \exp[i(\omega_n t - \mathbf{k}_n \cdot \mathbf{r})] \\
 &\quad + A_k^{\omega_n*}(\mathbf{r}) \exp[-i(\omega_n t - \mathbf{k}_n \cdot \mathbf{r})] \} \\
 &(1/2) \{ A_l^{\omega_q}(\mathbf{r}) \exp[i(\omega_q t - \mathbf{k}_q \cdot \mathbf{r})] \\
 &\quad + A_l^{\omega_q*}(\mathbf{r}) \exp[-i(\omega_q t - \mathbf{k}_q \cdot \mathbf{r})] \} \tag{69}
 \end{aligned}$$

(The expansion of equations (68) and (69) yields 13,824 terms!)

Thus the polarization contains many frequency components. However, the conservation of energy condition of interest here is

$\omega_c = \omega_1 + \omega_2 - \omega_p$ so the frequency components of the nonlinear polarization at ω_c are singled out:

$$\begin{aligned}
 P_i^{\omega_c} &= \omega_1 + \omega_2 - \omega_p (\mathbf{r}, t) = 3 \sum_j \sum_k \sum_l \chi_{ijkl} \{ A_j^{\omega_1} A_k^{\omega_2} A_l^{\omega_p*}(\mathbf{r}) \\
 &\quad \exp[i(\omega_1 + \omega_2 - \omega_p)t - (\mathbf{k}_1 + \mathbf{k}_2 - \mathbf{k}_p) \cdot \mathbf{r}] \\
 &\quad + A_j^{\omega_1*} A_k^{\omega_2*} A_l^{\omega_p}(\mathbf{r}) \\
 &\quad \exp[-i(\omega_1 + \omega_2 - \omega_p)t - (\mathbf{k}_1 + \mathbf{k}_2 - \mathbf{k}_p) \cdot \mathbf{r}] \} \} \tag{70}
 \end{aligned}$$

$$\begin{aligned}
P_i^{\omega_c} = \omega_c + \omega_m - \omega_m(\mathbf{r}, t) &= 3 \sum_j \sum_k \sum_l \chi_{ijkl} \\
&\quad \{ A_j^{\omega_c}(\mathbf{r}) A_k^{\omega_m}(\mathbf{r}) A_l^{\omega_m^*}(\mathbf{r}) \\
&\quad \exp[i(\omega_c t - \mathbf{k}_c \cdot \mathbf{r})] \\
&\quad + A_j^{\omega_c^*}(\mathbf{r}) A_k^{\omega_m^*}(\mathbf{r}) A_l^{\omega_m}(\mathbf{r}) \\
&\quad \exp[-i(\omega_c t - \mathbf{k}_c \cdot \mathbf{r})] \} \tag{71}
\end{aligned}$$

where $m = 1, 2, p$ or c , and $A_j^{\omega_1}$, $A_j^{\omega_1^*}$, $A_k^{\omega_2}$ and $A_k^{\omega_2^*}$ are not functions of \mathbf{r} because of the non-depleted pump assumption. The amplitudes of the polarization wave are (as in equation (53)):

$$\begin{aligned}
P_i^{(\omega_c)}(\mathbf{r}) &= 6 \sum_j \sum_k \sum_l \chi_{ijkl} A_j^{\omega_1} A_k^{\omega_2} A_l^{\omega_p^*}(\mathbf{r}) \\
&\quad + 6 \sum_j \sum_k \sum_l \sum_m \chi_{ijkl} A_j^{\omega_c}(\mathbf{r}) A_k^{\omega_m}(\mathbf{r}) A_l^{\omega_m^*}(\mathbf{r}) \\
P_i^{(\omega_c)^*}(\mathbf{r}) &= 6 \sum_j \sum_k \sum_l \chi_{ijkl} A_j^{\omega_1^*} A_k^{\omega_2^*} A_l^{\omega_p}(\mathbf{r}) \\
&\quad + 6 \sum_j \sum_k \sum_l \sum_m \chi_{ijkl} A_j^{\omega_1^*}(\mathbf{r}) A_k^{\omega_m^*}(\mathbf{r}) A_l^{\omega_m}(\mathbf{r}) \tag{72}
\end{aligned}$$

The Wave Equation

The wave equation developed from Maxwell's equations, equation (21), is in the following form:

$$\begin{aligned}
&\{-i[k_{cx} \partial A_i^{\omega_c}(\mathbf{r})/\partial x + k_{cy} \partial A_i^{\omega_c}(\mathbf{r})/\partial y + k_{cz} \partial A_i^{\omega_c}(\mathbf{r})/\partial z] \\
&\quad - (1/2) |\mathbf{k}_c|^2 A_i^{\omega_c}(\mathbf{r})\} \exp[i(\omega_c t - \mathbf{k}_c \cdot \mathbf{r})] \\
&\quad + \{i[k_{cx} \partial A_i^{\omega_c^*}(\mathbf{r})/\partial x + k_{cy} \partial A_i^{\omega_c^*}(\mathbf{r})/\partial y + k_{cz} \partial A_i^{\omega_c^*}(\mathbf{r})/\partial z] \\
&\quad - (1/2) |\mathbf{k}_c|^2 A_i^{\omega_c^*}(\mathbf{r})\} \exp[-i(\omega_c t - \mathbf{k}_c \cdot \mathbf{r})] \\
&\quad = (i \mu_0 \sigma \omega_c / 2) \{A_i^{\omega_c}(\mathbf{r}) \exp[i(\omega_c t - \mathbf{k}_c \cdot \mathbf{r})] \\
&\quad - A_i^{\omega_c^*}(\mathbf{r}) \exp[i(\omega_c t - \mathbf{k}_c \cdot \mathbf{r})]\} \\
&\quad - (\mu_0 \epsilon \omega_c^2 / 2) \{A_i^{\omega_c}(\mathbf{r}) \exp[i(\omega_c t - \mathbf{k}_c \cdot \mathbf{r})] \\
&\quad + A_i^{\omega_c^*}(\mathbf{r}) \exp[-i(\omega_c t - \mathbf{k}_c \cdot \mathbf{r})]\} \\
&\quad + \mu_0 \sigma^2 P_i^{\omega_c}(\mathbf{r}, t) / \partial t^2 \tag{73}
\end{aligned}$$

From equations (60) and (71):

$$\partial^2 P_i^{\omega_c}(\mathbf{r}, t) / \partial t^2 = -\omega_c^2 P_i^{\omega_c}(\mathbf{r}, t) \tag{101}$$

The same simplifying assumption made in the previous chapter is made here: the medium is transparent at ω_c so that $\sigma = 0$. Then, using

$|\mathbf{k}_c|^2 = \omega_c^2 \mu_0 \epsilon$, terms on either side of equation (73) synchronous with $\exp(i \omega_c t)$ can be equated:

$$\begin{aligned} -i[k_{cx} \partial A_i^{\omega c}(\mathbf{r})/\partial x + k_{cy} \partial A_i^{\omega c}(\mathbf{r})/\partial y + k_{cz} \partial A_i^{\omega c}(\mathbf{r})/\partial z] \exp(-i \mathbf{k}_c \cdot \mathbf{r}) \\ = -\mu_0 \omega_c^2 P_i^{\omega c}(\mathbf{r}, t) \\ k_{cx} \partial A_i^{\omega c}(\mathbf{r})/\partial x + k_{cy} \partial A_i^{\omega c}(\mathbf{r})/\partial y + k_{cz} \partial A_i^{\omega c}(\mathbf{r})/\partial z \\ = -i 6 \mu_0 \omega_c^2 \sum_j \sum_k \sum_l \chi_{ijkl} A_j^{\omega 1} A_k^{\omega 2} A_l^{\omega p*}(\mathbf{r}) \\ \exp[-i(\mathbf{k}_1 + \mathbf{k}_2 - \mathbf{k}_p - \mathbf{k}_c) \cdot \mathbf{r}] \\ + \sum_j \sum_k \sum_l \sum_m \chi_{ijkl} A_j^{\omega c}(\mathbf{r}) A_l^{\omega p*}(\mathbf{r}) A_l^{\omega m*}(\mathbf{r}) \end{aligned} \quad (75)$$

Since $\mathbf{E}_1(\mathbf{r}, t)$ and $\mathbf{E}_2(\mathbf{r}, t)$ are counterpropagating, $\mathbf{k}_1 + \mathbf{k}_2 = 0$ (2:555). (For an argument when $\mathbf{k}_1 + \mathbf{k}_2 \neq 0$, consult Reference 6 (pages 30-33).) Then, if $\mathbf{k}_c = -\mathbf{k}_p$ (the conjugate is counterpropagating to the probe), the exponential in equation (75) may be set to unity.

Another simplification made toward achieving a solution is: the amplitudes of the pumps are much greater than that of the probe or conjugate:

$$A_k^{\omega 1} A_1^{\omega 1*} + A_k^{\omega 2} A_1^{\omega 2*} \gg A_k^{\omega p}(\mathbf{r}) A_1^{\omega p*}(\mathbf{r}) + A^{\omega c}(\mathbf{r}) A^{\omega c*}(\mathbf{r}) \quad (76)$$

Then, equation (75) reduces to:

$$\begin{aligned} k_{cx} \partial A_i^{\omega c}(\mathbf{r})/\partial x + k_{cy} \partial A_i^{\omega c}(\mathbf{r})/\partial y + k_{cz} \partial A_i^{\omega c}(\mathbf{r})/\partial z \\ = -i 6 \mu_0 \omega_c^2 \sum_j \sum_k \sum_l \chi_{ijkl} A_j^{\omega 1} A_k^{\omega 2} A_l^{\omega p*}(\mathbf{r}) \\ + A_j^{\omega c}(\mathbf{r}) [A_k^{\omega 1} A_1^{\omega 1*} + A_k^{\omega 2} A_1^{\omega 2*}] \end{aligned} \quad (77)$$

The third simplification made is: since $\mathbf{E}^{\omega c}(\mathbf{r})$ and $\mathbf{E}^{\omega p}(\mathbf{r})$ are the only terms which are a function of position and they are a counterpropagating pair, let both travel in z , only. Then, equation (77) becomes:

$$\begin{aligned} dA_i^{\omega c}(z)/dz = -i 6 \omega_c (\mu_0/\epsilon)^{1/2} \sum_j \sum_k \sum_l \chi_{ijkl} \{ A_j^{\omega 1} A_k^{\omega 2} A_l^{\omega p*}(z) \\ + A_j^{\omega c}(z) [A_k^{\omega 1} A_1^{\omega 1*} + A_k^{\omega 2} A_1^{\omega 2*}] \} \end{aligned} \quad (78)$$

The final simplifying assumption is: often, one χ_{ijkl} will be much

greater than any of the others in the tensor. Assume the fields here are polarized along the appropriate axes to take advantage of that dominant susceptibility, $\chi^{(3)}$. Equation (78) becomes:

$$\begin{aligned} dA^{\omega C}(z)/dz = -i 6 \omega_c (\mu_0/\epsilon)^{1/2} \chi^{(3)} [A^{\omega 1} A^{\omega 2} A^{\omega P*}(z) \\ + A^{\omega C}(z) (|A^{\omega 1}|^2 + |A^{\omega 2}|^2)] \end{aligned} \quad (79)$$

(3:31)

By a similar development, the equation for $E^{\omega P}(z)$ is:

$$\begin{aligned} dA^{\omega P}(z)/dz = i 6 \omega (\mu_0/\epsilon)^{1/2} \chi^{(3)} [A^{\omega 1} A^{\omega 2} A^{\omega C*}(z) \\ + A^{\omega P}(z) (|A^{\omega 1}|^2 + |A^{\omega 2}|^2)] \end{aligned} \quad (80)$$

(3:30)

Solutions for the Amplitudes of the Probe and Conjugate

Assume the forms of the solutions to equations (79) and (80) to be:

$$\begin{aligned} A^{\omega C}(z) &= A^{\omega C*}(z) \exp[-i 6 \omega (\mu_0/\epsilon)^{1/2} \chi^{(3)} (|A^{\omega 1}|^2 + |A^{\omega 2}|^2) z] \\ A^{\omega P}(z) &= A^{\omega P*}(z) \exp[i 6 \omega (\mu_0/\epsilon)^{1/2} \chi^{(3)} (|A^{\omega 1}|^2 + |A^{\omega 2}|^2) z] \end{aligned} \quad (81)$$

then:

$$\begin{aligned} dA^{\omega C}(z)/dz &= (dA^{\omega C*}(z)/dz) \exp[-i 6 \omega (\mu_0/\epsilon)^{1/2} \chi^{(3)} (|A^{\omega 1}|^2 + |A^{\omega 2}|^2) z] \\ &\quad - i 6 \omega (\mu_0/\epsilon)^{1/2} \chi^{(3)} (|A^{\omega 1}|^2 + |A^{\omega 2}|^2) A^{\omega C}(z) \\ dA^{\omega P}(z)/dz &= (dA^{\omega P*}(z)/dz) \exp[i 6 \omega (\mu_0/\epsilon)^{1/2} \chi^{(3)} (|A^{\omega 1}|^2 + |A^{\omega 2}|^2) z] \\ &\quad + i 6 \omega (\mu_0/\epsilon)^{1/2} \chi^{(3)} (|A^{\omega 1}|^2 + |A^{\omega 2}|^2) A^{\omega P}(z) \end{aligned} \quad (82)$$

(3:33)

Inserting equations (82) into equations (79) and (80) gives:

$$\begin{aligned} -i 6 \omega (\mu_0/\epsilon)^{1/2} \chi^{(3)} A^{\omega 1} A^{\omega 2} A^{\omega P*}(z) \\ = dA^{\omega C*}(z)/dz \exp[-i 6 \omega (\mu_0/\epsilon)^{1/2} \chi^{(3)} (|A^{\omega 1}|^2 + |A^{\omega 2}|^2) z] \\ dA^{\omega C*}(z)/dz = -i 6 \omega (\mu_0/\epsilon)^{1/2} \chi^{(3)} A^{\omega 1} A^{\omega 2} A^{\omega P*}(z) \\ = i \kappa A^{\omega P*}(z) \end{aligned} \quad (83)$$

and:

$$\begin{aligned}
& i 6 \omega(\mu_0/\epsilon)^{1/2} \chi^{(3)} A^{\omega 1} A^{\omega 2} A^{\omega c*}(z) \\
& = dA^{\omega p*}(z)/dz \exp[i 6 \omega(\mu_0/\epsilon)^{1/2} \chi^{(3)} (|A^{\omega 1}|^2 + |A^{\omega 2}|^2)z] \\
dA^{\omega p*}(z)/dz & = i 6 \omega(\mu_0/\epsilon)^{1/2} \chi^{(3)} A^{\omega 1} A^{\omega 2} A^{\omega c,*}(z) \\
& = -i \kappa A^{\omega c,*}(z)
\end{aligned} \tag{84}$$

where

$$\kappa = -6 \omega(\mu_0/\epsilon)^{1/2} \chi^{(3)} A^{\omega 1} A^{\omega 2}$$

Note in equation (81) that the primed notation merely represented a phase shift. This phase shift will be inconsequential so the primed notation is dropped here. Then, equations (83) and (84) become:

$$\begin{aligned}
dA^{\omega c}(z)/dz & = i \kappa A^{\omega p*}(z) \\
dA^{\omega p}(z)/dz & = -i \kappa A^{\omega c*}(z)
\end{aligned} \tag{85}$$

(2:556, 3:36).

Yariv gives the solution to equations (85) (2:556, 3:36) as:

$$\begin{aligned}
A^{\omega p}(z) & = A^{\omega p}(0) \cos[|\kappa|(z - L)]/\cos(|\kappa|L) \\
A^{\omega c}(z) & = i A^{\omega p*}(0) \kappa^* \sin[|\kappa|(z - L)]/(|\kappa| \cos|\kappa|L)
\end{aligned} \tag{86}$$

using as boundary conditions that $E^P(0)$ is finite and $E^C(L) = 0$. The value of the probe wave at the output plane is given by:

$$A^{\omega p}(1) = A^{\omega p}(0)/\cos(|\kappa|L) \tag{87}$$

whereas the value of the conjugate wave reflected at the input plane is:

$$A^{\omega c}(0) = -i A^{\omega p*}(0) (\kappa^*/|\kappa|) \tan(|\kappa|L) \tag{88}$$

Figure 5 represents equations (86), (87) and (88) graphically.

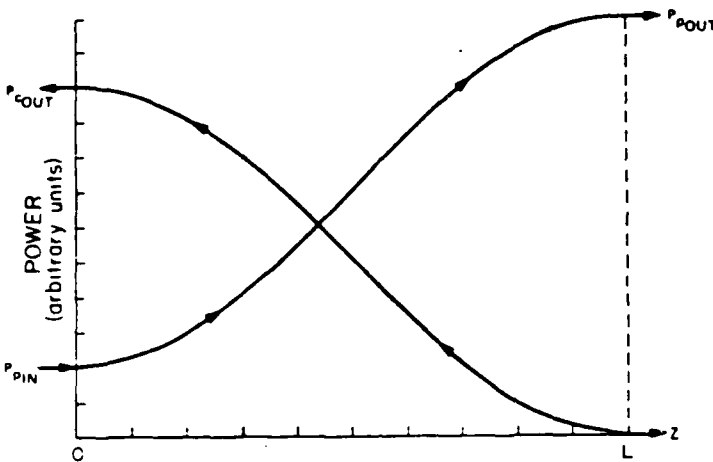


Figure 5. Intensities of the probe and conjugate waves in phase conjugation by degenerate four wave mixing (2:559, 3:37).

Summary

Optical phase conjugation by degenerate four wave mixing was shown to be a special case of the third order nonlinear processes discussed in the previous chapter. By applying the concepts of nonlinear polarization and the wave equation, it was shown that the probe and conjugate must counterpropagate to achieve phase match conditions and significant energy transfer from the pumps to the probe and conjugate waves. Finally, expressions for the amplitudes of the probe and conjugate as functions of position in the nonlinear medium were derived.

IV. The Photorefractive Effect

Introduction

The previous chapter showed that optical phase conjugation was possible by degenerate four wave mixing in which the conjugate light wave was generated by the third order nonlinear polarization of the medium. The amplitude of this polarization is directly proportional to the third order nonlinear susceptibility of the medium and the amplitude of each of the incident electric fields (equation (72)).

Table 1 lists the dominant third order susceptibilities for some exemplary media. Because the magnitude of these susceptibilities is very small, high intensity incident light is required to drive the medium into nonlinearity and produce phase conjugation. Therefore, an alternative technique for producing optical phase conjugation with lower intensity incident light would be desireable. Such a technique is through the use of photorefractive crystals.

Table I

Examples of third order nonlinear susceptibilities, χ_{xyyx} , at a wavelength of 694 nm (2:554)

Material	n	$\chi_{xyyx}(-\omega, \omega, \omega, -\omega)$ (10^{-34} MKS)
CS ₂	1.612	441
CCl ₄	1.454	6.2
Fused quartz	1.455	1.5
YAG	1.829	7.41
Benzene	1.493	68.9
LSO glass	1.505	2.26
ED-4 glass	1.557	2.8
SF-7 glass	1.631	9.8
BK-7 glass	1.513	2.26
LaSF-7 glass	1.91	12.4

The interference of the (coherent) pump and probe beams (a.k.a.

"write" beams) in a photorefractive crystal causes a spatially sinusoidal distribution of intensity as shown in Figure 6-a. A photorefractive crystal contains various sites in its lattice which accept and hold electrons with a low thermal probability of excitation. (The origin of these sites is uncertain. They may be naturally occurring impurities, doped impurities or defects in the crystal.) Under illumination, these charges are freed and the movement of either electrons or holes (depending on the crystal) occurs until the charge is retrapped in an area of the crystal that is not illuminated. In Figure 6-b, the location from which charges left corresponds to the interference maxima of Figure 6-a and the location where they are retrapped, to the interference minima.

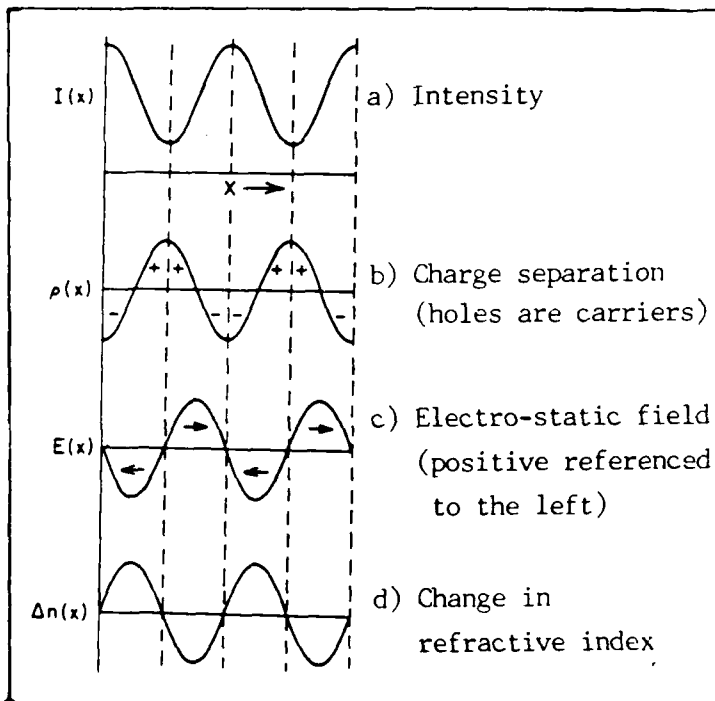


Figure 6. Illustration of the photorefractive effect (4:422)

The separation of opposite charges, either electrons or holes (whichever is the carrier) and the ions left behind, causes an electro-static field to form (Figure 6-c). This field modulates the

index of refraction of the crystal through the linear electro-optic (Pockel's) effect (Figure 6-d) (2:223,226).

For this "photorefractive effect", the electric field driving the nonlinearity of the crystal is the created space charge field. The magnitude of this field is proportional to the modulation index of the interfering beams. Since the modulation index is dependent on relative intensities rather than the incident intensity of either beam, phase conjugation can be produced from lower intensity incident light.

Phase conjugation in photorefractive crystals, then, differs from that of degenerate four wave mixing in that rather than being dependent on the INTENSITY of the incident beams, it is dependent on the RELATIVE intensity of the pump and probe beams.

Two models describing the photorefractive effect are Feinberg's Hopping Model and Kukhtarev's Solid State Model. Feinberg's model is based on the idea that a charge "hops" from site to site in the crystal and develops the probability of this charge movement. Kukhtarev's model is a more standard solid state development of charge transport.

Both models' solutions for a given sinusoidal illumination with small modulation index are a sinusoidal space charge field of the same spatial frequency as the illumination but out of phase with it. This space charge field is the basis for the development of "two beam coupling" and diffraction efficiency expressions in later chapters.

Feinberg's Hopping Model

The Model Itself

The "hopping" model is based on the idea that a charge may occupy any of a large number of sites in the crystal lattice. When the crystal is not illuminated, a charge is bound to a site. However, under

illumination, the charge is given enough energy to free it from any one site and it is free to "hop" from site to site. When the charge is re-bound at another (dark) site, the separation of the charge and the ionized site left behind causes an electro-static field to be set up which will modulate the index of refraction of the crystal.

Assumptions which are implicit in the model are:

1. Typical photorefractive material: charge is bound deep in a site in darkness but is free to hop to another site under illumination. (5:1298)
In other words, the charge cannot be thermally excited enough to hop from site to site. The implication of this is that once a grating is formed in the crystal, if the crystal is kept in darkness the grating will remain indefinitely. Although the grating does persist in darkness, it does eventually decay. (5:1297)
2. The number of sites that these charges can occupy is much greater than the number of charges available (5:1298). Thus, the model does not account for saturation effects. A charge is assumed to always have a place to migrate to.
3. The number of charge carriers excited into the conduction band is proportional to the incident intensity. Therefore, the hopping rate is also proportional to the intensity (5:1298).

Definitions necessary before setting up the model are:

w_n = probability that a site at position x_n is filled

dW_n/dt = probability per second of hopping into that site

Then:

$dW_n/dt \propto$ probability that the m^{th} site is filled and the charge has enough energy to hop to the n^{th} site (and the n^{th} site is open) minus the probability that the n^{th} site is filled and the charge has enough energy to leave (and the m^{th} site is open).

$$\propto I_m W_m \exp[C q (\phi_m - \phi_n)/k_B T] (1 - W_n) \\ - I_n W_n \exp[C q (\phi_n - \phi_m)/k_B T] (1 - W_m)$$

where

$I_{n(m)}$ = Intensity at site $n(m)$

C = Constant to assure model obeys statistical mechanics

q = Charge (Note that it is a positive charge in this form. It would be $-q$ for an electron.)

$\phi_{n(m)}$ = Potential at site $n(m)$

k_B = Boltzmann's constant

T = Lattice temperature

If the number of sites is much greater than the number of charges, then $W_{n(m)} \ll 1$ and the rate equation becomes:

$$dW_n/dt = - \sum_m D_{mn} [I_n W_n \exp(C \beta \phi_{nm}) - I_m W_m \exp(C \beta \phi_{mn})] \quad (89)$$

where

D_{mn} = Constant of proportionality

$$\beta = q/(k_B T)$$

$$\phi_{nm(mn)} = \phi_{n(m)} - \phi_{m(n)}$$

To determine C , under uniform intensity, the probability that a site is filled should be the same for all sites:

$$W_n \exp(\beta \phi_n) = W_m \exp(\beta \phi_m) \\ W_n / W_m = \exp(\beta \phi_{nm}) \quad (90)$$

and the probability of movement should be zero:

$$dW_n/dt = 0 \quad (91)$$

Then, from equations (89) and (91):

$$\begin{aligned} w_n \exp(C \beta \phi_{nn}) &= w_m \exp(C \beta \phi_{mm}) \\ w_n / w_m &= \exp(2C \beta \phi_{nn}) \end{aligned} \quad (92)$$

Therefore, from equation (90):

$$C = 1/2$$

(5:1298)

The model is expressed mathematically as (5:1298):

$$dw_n/dt = - \sum_m D_{mn} [w_n I_n \exp(\beta \phi_{nn}/2) - w_m I_m \exp(\beta \phi_{mm}/2)] \quad (93)$$

Solution to the Model

More assumptions made to achieve a solution to the model are:

4. Sites are equally rather than randomly spaced. The rms distance between sites is 1 (5:1299). This allows:

$$x_m = x_n + 1 \quad (94)$$

5. There are many adjacent sites (and hopping opportunities) within each spatial wavelength ($kl \ll 1$). This allows:

$$\begin{aligned} D_{mn} &= 0 \text{ except for nearest-neighbor sites} \\ &= D \text{ for nearest-neighbor sites.} \end{aligned} \quad (95)$$

This removes the summation from the hopping probability equation.

(5:1299)

The model is now in the form:

$$dw_n/dt = -D [w_n I_n \exp(\beta \phi_{nn}/2) - w_m I_m \exp(-\beta \phi_{mm}/2)] \quad (96)$$

- Consider this special case: Two light waves interfere as in Figure 7. The electric field of each wave can be written as (5:1298):

$$\begin{aligned} E_1 &= E_1 \hat{e}_1 \exp(i k_1 \cdot x) \\ E_2 &= E_2 \hat{e}_2 \exp(i k_2 \cdot x) \end{aligned} \quad (97)$$

and the interference as (5:1299):

$$I_{n(m)} = G_0 [1 + m \cos k \cdot x_{n(m)}] \quad (98)$$

where

$$G_0 = |E_1|^2 + |E_2|^2$$

m = modulation index

$$= 2 E_1 E_2^* \hat{e}_1 \hat{e}_2^* / G_0$$

$$= G/G_0$$

$$\mathbf{k} = \mathbf{k}_1 - \mathbf{k}_2$$

Further assumptions toward a solution are:

6. Small modulation conditions will only be considered (5:1299):

$$m \ll 1 \quad (99)$$

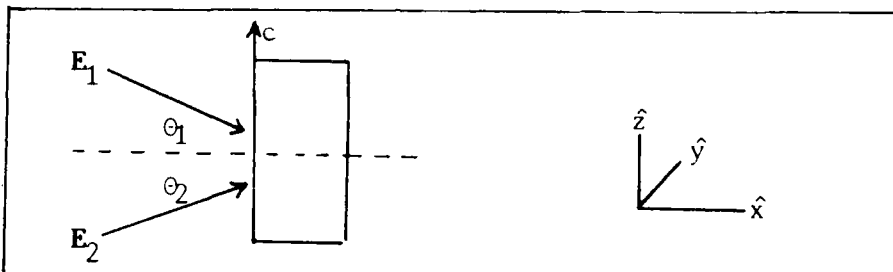


Figure 7. Orientation of interfering beams and crystal (5:1298)

7. The form of the solutions (following the form of the interference above) is (5:1299):

$$\begin{aligned} w_n &= w_{0n} + \operatorname{Re} W \exp(i\mathbf{k} \cdot \mathbf{x}_n) \\ \phi_n &= \phi_{0n} + \operatorname{Re} \phi \exp(i\mathbf{k} \cdot \mathbf{x}_n) \end{aligned} \quad (100)$$

where

w_{0n} = Unmodulated probability site n is filled

ϕ_{0n} = Potential due to external or intrinsic fields (everything but charge migration)

W = Charge distribution amplitude

ϕ = Potential distribution amplitude

Kukhtarev will show assumption 7 is good if assumption 6 already exists.

However, both Feinberg's and Kukhtarev's models are often extended to cases where the modulation index approaches unity and the resulting

field is still assumed to be spatially sinusoidal following the interference fringes. The field may not be sinusoidal under such conditions. This problem is addressed to some extent in the development of Kukhtarev's model.

Equations (100) are not independent. From Poisson's equation (6:164):

$$\nabla \cdot \mathbf{D} = \rho_v q \quad (101)$$

where

\mathbf{D} = Electric displacement vector

= $\epsilon_0 \epsilon \cdot \mathbf{E}$

ϵ_0 = Permittivity of free space

ϵ = Static dielectric tensor

$\mathbf{E} = -\nabla \phi$

$\nabla = ik$ (for plane waves)

$q\rho_v$ = Charge distribution

= $\rho W q$

ρ = Average density of sites (number per unit volume)

Then, the charge and potential distributions are related by:

$$\begin{aligned} -ik \cdot \epsilon \cdot ik \phi &= \rho q W / \epsilon_0 \\ \phi &= \rho q W / \epsilon \epsilon_0 k^2 \end{aligned} \quad (102)$$

(5:1299)

Final simplifying assumptions made toward achieving a solution are:

8. First order series expansion of exponential will be used (5:1299):

$$\exp(\beta \phi_{nm}/2) = 1 + \beta \phi_{nm}/2 \quad (103)$$

This is reasonable since $\beta \sim 1/40$ eV at room temperature, typical internal fields are < 50 kV/cm and $l \sim 1/10^6$ cm so $\beta \phi_{nm}/2 \ll 1$.

The hopping probability equation (96) becomes:

$$\begin{aligned}
d/dt [W_0 + \operatorname{Re} W \exp(i\mathbf{k} \cdot \mathbf{x}_n)] &= -D \{ [W_0 + \operatorname{Re} W \exp(i\mathbf{k} \cdot \mathbf{x}_n)] \\
&\quad [G_0 + \operatorname{Re} G \exp(i\mathbf{k} \cdot \mathbf{x}_n)] \\
&\quad \{1 + (\beta/2) [\Delta\Phi_0 + \operatorname{Re} \Phi \exp(i\mathbf{k} \cdot \mathbf{x}_n) \\
&\quad - \operatorname{Re} \Phi \exp[i\mathbf{k} \cdot (\mathbf{x}_n + 1)]]\} \\
&\quad - \{W_0 + \operatorname{Re} W \exp[i\mathbf{k} \cdot (\mathbf{x}_n + 1)]\} \\
&\quad \{G_0 + \operatorname{Re} G \exp[i\mathbf{k} \cdot (\mathbf{x}_n + 1)]\} \\
&\quad \{1 - (\beta/2) [\Delta\Phi_0 + \operatorname{Re} \Phi \exp(i\mathbf{k} \cdot \mathbf{x}_n) \\
&\quad - \operatorname{Re} \Phi \exp[i\mathbf{k} \cdot (\mathbf{x}_n + 1)]]\}\} \} \quad (104)
\end{aligned}$$

where

$$\Delta\Phi_0 = \Phi_{0n} - \Phi_{0m}$$

Equating synchronous terms [in $\exp(i\mathbf{k} \cdot \mathbf{x}_n)$] from both sides (5:1299):

$$\begin{aligned}
dW/dt &= -D \{ (W_0 G_0 + W G/2)(\beta \Phi/4)[1 - \exp(ikl)] \\
&\quad + (W_0 G/2 + W G_0/2)(1 + \beta \Delta \Phi_0/2) + (W G/4)(\beta \Phi/4) \\
&\quad [1 - \exp(-ikl)] \\
&\quad + (W_0 G_0 + W G/2)(\beta \Phi/4)[1 - \exp(ikl)] \\
&\quad - (W_0 G/2 + W G_0/2) \exp(ikl) (1 - \beta \Delta \Phi_0/2) \\
&\quad + (W G/4) \exp(2ikl) (\beta \Phi/4)[1 - \exp(-ikl)] \} \quad (105)
\end{aligned}$$

After expanding the exponentials to their second order (reasonable given assumption 5):

$$\exp(ikl) = 1 + ikl - (kl)^2/2 \quad (106)$$

and making the substitutions:

$$w = \text{Normalized charge wave amplitude}$$

$$= W/W_0$$

$$m = G/G_0$$

Feinberg gives the final form as (5:1299):

$$\begin{aligned}
dw/dt &= -D G_0 [(w + m)(k^2 l^2 - ikl \beta \Delta \Phi_0) + \Phi \beta k^2 l^2] \\
&= -\Gamma [(w + m)(\alpha^2 + i\alpha f) + w] \quad (107)
\end{aligned}$$

where

Γ = Characteristic hopping rate

$$= D G_0 k_0^2 l^2$$

k_0 = Characteristic wave vector

$$= [(\rho \omega_0 q^2 / (\epsilon \epsilon_0 k_B T))^{1/2}]$$

= Normalized grating wave vector

$$= k/k_0$$

f = Uniform e-field strength normalized by the characteristic field

$$= -\Delta\phi_0 / (l f_0)$$

f_0 = Characteristic field

$$= k_0 k_B T/q$$

The solution to this differential equation (107) is:

$$\frac{dw}{w(\alpha^2 + 1 + i\alpha f) + m(\alpha^2 + i\alpha f)} = -\Gamma dt$$
$$w = \frac{\exp[-\Gamma (\alpha^2 + 1 + i\alpha f) t] - m(\alpha^2 + i\alpha f)}{\alpha^2 + 1 + i\alpha f} \quad (108)$$

or solving for the potential amplitude, ϕ , using equation (102):

$$\phi = \frac{\omega_0 \rho q [\exp[-\Gamma (\alpha^2 + 1 + i\alpha f) t] - m(\alpha^2 + i\alpha f)]}{\epsilon \epsilon_0 k^2 (\alpha^2 + 1 + i\alpha f)} \quad (109)$$

Electric Field Modulating the Index of Refraction

In the linear electro-optic effect, the index of refraction of a crystal may be modulated by an internal dc electric field. In photorefractive crystals, this (space charge) E-field is the (negative of the) gradient of the quasistatic potential due to internal charge migration.

From equation (109), the steady state solution for the potential amplitude is:

$$\begin{aligned}\phi &= \frac{-W_0 \rho q m (\alpha^2 + i\alpha f)}{\epsilon \epsilon_0 k^2 (\alpha^2 + 1 + i\alpha f)} \\ &= \frac{-f_0 m}{k} \left(\frac{\alpha + if}{\alpha^2 + 1 + i\alpha f} \right) \quad (110)\end{aligned}$$

The space charge field, \mathbf{E}_{SC} , is (5:1304):

$$\begin{aligned}\mathbf{E}_{SC}(\mathbf{x}) &= -\nabla \phi(\mathbf{x}) \\ &= -\nabla [\phi_0 + \operatorname{Re} \phi \exp(i\mathbf{k} \cdot \mathbf{x})] \\ &= i k f_0 m \left(\frac{\alpha + if}{\alpha^2 + 1 + i\alpha f} \right) \exp(i\mathbf{k} \cdot \mathbf{x}) \quad (111)\end{aligned}$$

Note that the space charge field should be in the direction of \mathbf{k} given the form of the potential (equation (100)).

Since this is a complex expression, it may be expressed in magnitude-phase form. The significance of this form is evident in later chapters where the diffraction efficiency and phase conjugate reflectivity are dependent on the magnitude of \mathbf{E}_{SC} and the energy transfer in steady state two beam coupling is dependent on the phase shift between the grating and the intensity fringes.

The amplitude of the space charge field is given by:

$$\begin{aligned}|\mathbf{E}_{SC}(\mathbf{x})| &= k f_0 m \left[\frac{\alpha^2 + f^2}{(\alpha^2 + 1)^2 + (\alpha f)^2} \right]^{1/2} \\ &= k m E_q \left[\frac{E_D^2 + E_0^2}{(E_D + E_q)^2 + E_0^2} \right]^{1/2} \quad (112)\end{aligned}$$

where

$$\begin{aligned}E_q &= \text{Limiting value of the space charge field} \\ &= f_0 / \alpha \\ &= \rho W_0 q / (\epsilon \epsilon_0 k) \text{ (Proportional to the trapped charge density)}\end{aligned}$$

E_D = Diffusion field (assumed parallel (or antiparallel) to \mathbf{k})

$$= f_0 \alpha$$

$$= k_B T k/q$$

E_0 = Applied field (also assumed parallel (or antiparallel to \mathbf{k})

$$= f f_0$$

To find the phase shift, ψ , between the space charge field and the intensity interference pattern, the space charge field is separated into its real and imaginary parts:

$$\begin{aligned} E_{SC}(x) &\propto \frac{-f + i\alpha}{\alpha^2 + 1 + i\alpha f} \\ &\propto \frac{f + i\alpha (1 + \alpha^2 + f^2)}{(\alpha^2 + 1)^2 + (\alpha f)^2} \end{aligned} \quad (113)$$

$$\begin{aligned} \psi &= \tan^{-1} \alpha (1 + \alpha^2 + f^2)/f \\ &= \tan^{-1} \frac{E_D E_Q + E_D^2 + E_0^2}{E_Q E_Q} \end{aligned} \quad (114)$$

With no applied field ($E_0 = 0$), $\tan \psi = \infty$, and the phase shift is $\pi/2$.

As the applied field grows large ($E_0 = \infty$), $\tan \psi = \infty$, and the phase shift is again, $\pi/2$. Again, these forms are used in the papers mentioned above.

The space charge field, then, can be written in the form:

$$F_{SC}(x) = \hat{k} m E_Q \left[\frac{E_D^2 + E_0^2}{(E_D + E_Q)^2 + E_0^2} \right]^{1/2} \text{Re } \exp(i\psi) \exp(i\mathbf{k} \cdot \mathbf{x}) \quad (115)$$

This is the form for the space charge field found in other papers such as those by Fischer et al. (7:520), Valley and Klein (8:115), and Gunter (9:252).

Modulated Optical Susceptibility

The space charge field causes a modulation of the optical susceptibility, $X(x)$, of the form:

$$\mathbf{X}(\mathbf{x}) = \operatorname{Re} \mathbf{X} \exp(i\mathbf{k} \cdot \mathbf{x}) \quad (116)$$

The derivation for the form of the amplitude of the modulated susceptibility follows:

$$\begin{aligned} \mathbf{P} &= \mathbf{P}_L + \mathbf{P}_{NL} \\ &= \epsilon_0 \chi^{(1)} \mathbf{E}^{(\omega)} + 2 \mathbf{d} \cdot \mathbf{E}_{SC} \cdot \mathbf{E}^{(\omega)} \\ &= \epsilon_0 [\chi^{(1)} + 2 \mathbf{d} \cdot \mathbf{E}_{SC} / \epsilon_0] \cdot \mathbf{E}^{(\omega)} \end{aligned} \quad (117)$$

The electric displacement vector is:

$$\begin{aligned} \mathbf{D} &= \epsilon_0 \mathbf{E} + \mathbf{P} \\ &= \epsilon_0 \mathbf{E}^{(\omega)} + \epsilon_0 [\chi^{(1)} + 2 \mathbf{d} \cdot \mathbf{E}_{SC} / \epsilon_0] \cdot \mathbf{E}^{(\omega)} \\ &= \epsilon_0 [\mathbf{I} + \chi^{(1)} + 2 \mathbf{d} \cdot \mathbf{E}_{SC} / \epsilon_0] \mathbf{E}^{(\omega)} \\ &= \epsilon_0 [\epsilon + 2 \mathbf{d} \cdot \mathbf{E}_{SC} / \epsilon_0] \cdot \mathbf{E}^{(\omega)} \end{aligned} \quad (118)$$

since:

$$\epsilon = \mathbf{I} + \chi^{(1)} \quad (119)$$

but:

$$\mathbf{D} = \epsilon_0 (\mathbf{b} + \Delta\mathbf{b})^{-1} \cdot \mathbf{E}^{(\omega)} \quad (120)$$

where

\mathbf{b} = Impermeability tensor

$\Delta\mathbf{b} = \mathbf{R} \cdot \mathbf{E}_{SC}$

\mathbf{R} = Linear electro-optic tensor

Therefore:

$$\epsilon + 2 \mathbf{d} \cdot \mathbf{E}_{SC} / \epsilon_0 = (\mathbf{b} + \mathbf{R} \cdot \mathbf{E}_{SC})^{-1} \quad (121)$$

The first order series expansion of the right side is:

$$(\mathbf{b} + \mathbf{R} \cdot \mathbf{E}_{SC})^{-1} = \mathbf{b}^{-1} - \mathbf{b}^{-1} \cdot \mathbf{R} \cdot \mathbf{E}_{SC} \cdot \mathbf{b}^{-1} \quad (122)$$

and:

$$\epsilon = \mathbf{b}^{-1} \quad (123)$$

Therefore:

$$2 \mathbf{d} \cdot \mathbf{E}_{SC} = -\epsilon_0 \epsilon \cdot \mathbf{R} \cdot \mathbf{E}_{SC} \cdot \epsilon \quad (124)$$

As shown earlier, the space charge field is related to the potential by:

$$E_{SC}(x) = -i \mathbf{k} \phi \exp(i\mathbf{k} \cdot \mathbf{x}) \quad (125)$$

so the amplitude of the modulated optical susceptibility, X , takes the form (5:1299):

$$\begin{aligned} X &= 2 \mathbf{d} \cdot \mathbf{E}_{SC} \\ &= i \epsilon_0 \mathbf{\epsilon} \cdot \mathbf{R} \cdot \mathbf{k} \cdot \mathbf{\epsilon} \phi \end{aligned} \quad (126)$$

Summary

Feinberg et al. developed a model for the photorefractive effect based on the probability that a certain site in the crystal lattice was filled by a charge. The fruition of this model in the case of spatially periodic illumination (interference fringes) shows the space charge field set up in the medium for small modulation fringes is spatially sinusoidal with the same frequency as the illumination, amplitude given by equation (113) and shifted in phase from the illumination with shift given by equation (114). This field modulates the optical susceptibility of the medium as given by equations (116) and (126).

Kukhtarev Solid State Model

Kukhtarev et al. (10:949-960) developed a model for the photorefractive process based more in conventional solid state physics than Feinberg's hopping model. Other papers such as Kogelnik (11:2909-2945), Vahey (12:3510-3515), Fisher (7:519-521) and even Feinberg (5:1297-1305) develop theories in which an initial assumption is that the spatial distribution of electrons (and thus the index grating) is proportional to the incident intensity pattern. Kukhtarev clearly points out he makes no such assumption to begin with, yet, in the end this is shown to be the case. (10:950).

Background to the Model

The same interference pattern as Feinberg considered is set up in the crystal as in Figure 8. The incident waves, \tilde{E}_1^+ , are assumed to be

polarized in the plane of incidence (10:951).

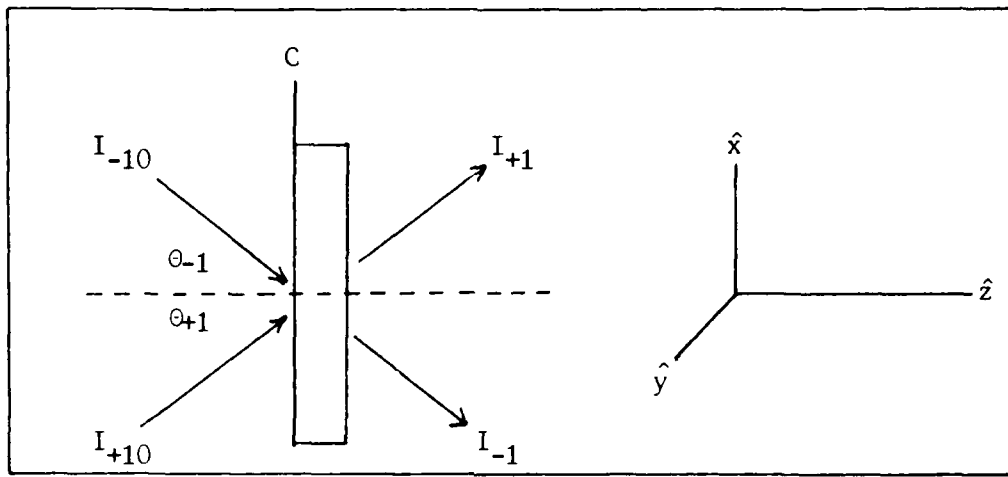


Figure 8. Geometry for formation of an index grating in photorefractive crystals (10:951).

Probabilities considered when developing the model are:

$$\text{Electron transitions from donors to conductivity band} = (sI + \beta)(N_D - N_D^+) \quad (127)$$

where

s = Cross section of photoionization

I = Light intensity

$$= c |\mathbf{E}|^2 \epsilon^{1/2} / (4\pi)$$

c = Velocity of light

ϵ = High frequency dielectric constant

$\epsilon_i(I) = i^{\text{th}}$ component of ϵ which is a function of intensity through the linear electro-optic effect

$$= \epsilon_i(1 + \Delta\epsilon_i)$$

$$\Delta\epsilon_i = r_{ik} \epsilon_i E_k(I) \quad (i, k = x, y \text{ or } z)$$

$$= \frac{2 \Delta\kappa_i}{\kappa_i}$$

r_{ik} = Component of electro-optic tensor, R

$E_k(I) = k^{\text{th}}$ component of space charge field

ϵ_i = i^{th} component of refractive index (written as n in other places and elsewhere in this paper)

$$= \epsilon_i^{1/2}$$

β = Rate of thermal generation

N_D = concentration of donors

N_D^+ = Concentration of ionized donors

and

$$\text{Ionized donors capturing electrons} = \gamma_R n N_D^+ \quad (128)$$

where

γ_R = Recombination constant

n = Concentration of carriers

(10:951)

The change in the concentration of carriers with time is given by:

$$dn/dt = dN_D^+/dt - \nabla j/e \quad (129)$$

where

$$dN_D^+/dt = (sI + \beta)(N_D - N_D^+) - \gamma_R n N_D^+$$

$$j = e\mu n [E - (T/e)\nabla \ln n] + pI\hat{e}_c$$

e = Electronic charge

μ = Electron mobility

E = Electric field modulating the index of refraction

T = Temperature

pI = Photovoltaic current

p = Photovoltaic constant

\hat{e}_c = Unit vector along c-axis

The wave equation is:

$$\nabla^2 E + (1/c^2) d^2(\epsilon E)/dt^2 = 0 \quad (130)$$

(10:951)

The electric field of the two interfering beams may be written as:

$$\mathbf{E} = (4\pi/c\varepsilon^{1/2}) \{ \hat{\mathbf{e}}_{+1} I_{+1}^{1/2} \exp[i(\phi_{+1} + k_x x - k_z z)] + \hat{\mathbf{e}}_{-1} I_{-1}^{1/2} \exp[i(\phi_{-1} - k_x x - k_z z)] \} \quad (131)$$

where

$\hat{\mathbf{e}}_{\pm 1}$ = Polarization vectors

$k_{x,z}$ = Wave vector components

$\phi_{\pm 1}$ = Phases of interfering beams

(10:951)

The electron generation rate, including both thermal and photo-generation, is given by:

$$f = \beta + sI \\ = (\beta + sI_0)[1 + M_0 \cos |2k_x x + \Phi(z)|] \quad (132)$$

where

$$I_0 = I_{+1} + I_{-1}$$

$$M_0 = 2(I_{+1} I_{-1})^{1/2} (\hat{\mathbf{e}}_{+1} \cdot \hat{\mathbf{e}}_{-1}) / [I_0(1 + \sigma_d/\sigma_p)] \\ = m/(1 + \sigma_d/\sigma_p)$$

m = Modulation index

$$= 2(I_{+1} I_{-1})^{1/2} \cos(\phi_{+1} + \phi_{-1})/I_0$$

$$\sigma_d/\sigma_p = \text{Ratio of dark and photo-conductivities} \\ = \beta/(sI_0)$$

$\Phi(z)$ = Phase difference of interfering beams

$$= \phi_{+1} - \phi_{-1}$$

(10:951-952)

Steady State Solution

The space-charge field, $\Delta E(x, I)$ is now solved for and shown to be sinusoidal and proportional to the incident interference pattern.

In the case of linear recombination, there are more donors than free carriers and more free carriers than the generation rate-recombination ratio:

$$N_D, N_D - N_A \gg n \gg f/\gamma_R \quad (133)$$

where

$$\begin{aligned} N_A &= \text{Trap concentration} \\ (10:952) \end{aligned}$$

The spatial change in the E-field is given by:

$$\begin{aligned} dE/dx &= [p/(e\mu)] d(1/n)/dx + (J/e\mu) d(1/n)/dx + (T^2/e) d^2 \ln n / dx^2 \\ &= (4\pi e/\epsilon_0)(N_A - fN_D/\gamma_R n) \\ E &= [J/(e\mu n)] + (T/e)d \ln n / dx + pI/(e\mu n) \end{aligned} \quad (134)$$

where

J = Constant current associated with the averaged e-field, $\langle E \rangle$, and applied voltage, V .

$$\begin{aligned} \langle E \rangle &= 1/d \int_0^d E \, dx \\ &= JR + V/d \end{aligned}$$

d = Length of crystal in x-direction

R = Resistivity of external circuit

(10:952)

Case 1

If the space charge screening length, l_T , and the length of electron tightening by the external field, l_E , are much greater than the fringe spacing, L :

$$l_T, l_E \gg L \quad (135)$$

where

$$l_T = [\epsilon_0 \pi T / (e^2 N_A)]^{1/2}$$

$$l_E = \epsilon_0 E_0 / (2eN_A)$$

$$E_0 = V/d$$

then the carrier concentration is:

$$\begin{aligned} n &= N_D(\beta + sI_0) / (N_A \gamma_R) \\ &= n_d + n_p \end{aligned} \quad (136)$$

and the space charge field is given by:

$$\begin{aligned} E &= \langle E \rangle + (4\pi e/\epsilon_0) [N_A - fN_D/(\gamma_R n)] dx \\ &= \langle E \rangle - [2\pi e N_A / (\epsilon_0 |k_x|)] M_0 \sin |2k_x x + \phi(z)| \\ &= \langle E \rangle - E_q M_0 \sin |2k_x x + \phi(z)| \end{aligned} \quad (137)$$

where

E_q = Limiting value of the space charge field (comparable to Feinberg's limiting value).

$$= 2\pi e N_A / (\epsilon_0 |k_x|)$$

(10:952)

Thus, if the charge transport lengths are much longer than the fringe spacing, the space charge field is sinusoidal and of the same frequency as the interference fringes but shifted $\pi/2$ from them. This condition is analogous to Feinberg's $\pi/2$ shift for a very large applied external field.

Case 2

If the space charge screening length, l_T , and the length of electron tightening by external field, l_E , are much less than the fringe spacing, L:

$$l_T, l_E \ll L \quad (138)$$

then the carrier concentration is:

$$n = \langle n \rangle \{1 + M \cos [2k_x x + \phi(z)]\} \quad (139)$$

where

$\langle n \rangle$ = Average carrier concentration (from crystal neutrality)

$$= N_D (sI_0 + sI_0)/(\gamma_R N_A)$$

$$M = M_0 (1 - \xi_T - \xi_E)$$

$$\xi_T = (l_T/L)^2$$

$$\xi_E = l_E/L$$

and the space charge field is given by:

$$\begin{aligned}
E &= (J/e\mu n) + (T/e) (d \ln n/dx) + [pI/(e\mu n)] \\
&= \frac{[J/(e\mu n)] - E_D M \sin [2k_x x + \phi(z)] + E_P \{1 + m \cos [2k_x x + \phi(z)]\}}{1 + M \cos [2k_x x + \phi(z)]} \\
&\quad (140)
\end{aligned}$$

where

E_D = Diffusion field (comparable to Feinberg's diffusion field

$$= 2k_x T/e$$

E_P = Photovoltaic field

$$= pI_0/(e\langle n \rangle)$$

(10:953)

The average field, $\langle E \rangle$, is found by averaging over one period after making the variable substitution, $\xi = 2k_x x + \phi(z)$:

$$\begin{aligned}
\langle E \rangle &= 1/\Lambda \int_0^\Lambda E dx \\
&= 1/(2\pi) \xi [J/(e\mu n)] \int_0^{2\pi} (1 + M \cos \xi)^{-1} d\xi \\
&\quad - E_D M \int_0^{2\pi} [(sin \xi)/(1 + M \cos \xi)] d\xi \\
&\quad + E_P \int_0^{2\pi} [(1 + m \cos \xi)/(1 + M \cos \xi)] d\xi \\
&= J/[e\mu n(1 + M^2)^{1/2}] + E_P [m/M + (M - m)/[M(1 - m^2)^{1/2}]] \quad (141)
\end{aligned}$$

The current, J , is then:

$$\begin{aligned}
J &= e\mu n(1 - M^2)^{1/2} \{\langle E \rangle - E_P \{m/M + (M - m)/[M(1 - m^2)^{1/2}]\}\} \\
&= e\mu n(1 - M^2)^{1/2} (\langle E \rangle - E_P^0) \\
&= \sigma_\perp E_0 \quad (142)
\end{aligned}$$

where

$$\begin{aligned}
E_P^0 &= E_P \{m/M + (M - m)/[M(1 - m^2)^{1/2}]\} \\
&\cong E_P
\end{aligned}$$

σ_\perp = Transverse conductivity

$$= e\mu n (1 - M^2)^{1/2}$$

$$= \langle \sigma \rangle (1 - M^2)^{1/2}$$

$\langle \sigma \rangle$ = Average conductivity

$$\begin{aligned}
 E_0 &= \text{Effective field causing macroscopic current} \\
 &= \langle E \rangle - E_p
 \end{aligned}$$

(10:953)

Equation (140) takes the form:

$$E = \frac{E_0 (1 - M^2)^{1/2} - E_D M \sin(2k_x x + \Phi) + E_p [1 - m \cos(2k_x x + \Phi)]}{1 + M \cos(2k_x x + \Phi)} \quad (143)$$

The Fourier series representation of this equation is in the form:

$$E = \langle E \rangle + \sum E_n \exp(i n 2k_x x) \quad (144)$$

where

$$n = \pm 1, 2, \dots$$

For which Kukhtarev gives the Fourier coefficients as:

$$\begin{aligned}
 E_n &= [E_0 + E_p(1 - m/M) - iE_D] \{[(1 + M^2)^{1/2} - 1]/M\}^n \exp(i n \Phi) \\
 &= \Delta E \{[(1 + M^2)^{1/2} - 1]/M\}^n \exp[i(n\Phi + \psi)]
 \end{aligned} \quad (145)$$

when written in magnitude-phase form where

ΔE = Amplitude of electric field grating (comparable to Feinberg's space charge field (equation (112)))

$$= \{[E_0 + E_p(1 - m/M)]^2 + E_D^2\}^{1/2}$$

ψ = Phase shift between the space charge field and interference pattern (comparable to Feinberg's phase shift (equation (114)))

$$= \tan^{-1} \{E_D/[E_0 + E_p(1 - m/M)]\}$$

(10:953)

If the Fourier series can be limited to first order, only, the E-field will be spatially sinusoidal. This can be achieved if the term $[(1 + M^2)^{1/2} - 1]/M$ is small so raising it to any power other than unity adds an insignificant contribution to the series.

For small modulation conditions, m , M_0 and M are all small and:

$$\lim_{m \rightarrow 0} [(1 + M^2)^{1/2} - 1]/M = 0 \quad (146)$$

so limiting the Fourier series to the first order is a good approximation. As the modulation index, m , increases toward unity,

however, M could also approach unity under the right conditions. In this case:

$$\lim_{m \rightarrow 1} [(1 + M^2) - 1]/M = .41421 \quad (147)$$

which raised to the second, third and fourth powers are .17157, .07163 and .029437, respectively. These are by no means relatively insignificant contributions.

It is possible to have small M even if the modulation index, m , is unity, however. If the ratio of dark and photo-conductivities, $\sigma_d/\sigma_p = \beta/sI_0$, is large, or if the space charge screening length, l_T , or the length of electron tightening by external field, l_E , (which are still assumed here to be much less than the fringe spacing, L) begin approaching the fringe spacing, M can be reduced.

Electro-Static Field in Terms of Incident Intensity

The first order approximation of the Fourier series (equation (144)) will be considered appropriate by assuming small modulation, $M \ll 1$, exists. Equation (145), in terms of the incident intensities, becomes:

$$\begin{aligned} E_1 &= [E_0 + E_p (1 - m/M) - iE_D] \{(1 + M^2)^{1/2} - 1\}/M^2 \exp(i\phi) 2 \cos 2\theta \\ &\quad (I_{+1} I_{-1})^{1/2} (1 - \xi_T - \xi_E)/I_0 \\ &= [(I_{+1} I_{-1})^{1/2}/I_0](A + iB) \exp(i\phi) \end{aligned} \quad (148)$$

where

$$\begin{aligned} \lim_{m \rightarrow 0} [(1 + M^2)^{1/2} - 1]/M^2 &= 1/2 \\ A &= [E_0 + E_p (1 - m/M)] (1 - \xi_T - \xi_E)(\cos 2\theta)/(1 + \sigma_d/\sigma_p) \\ B &= -E_D (\cos 2\theta) (1 - \xi_T - \xi_E)/(1 + \sigma_d/\sigma_p) \end{aligned}$$

(10:954)

Index Grating

For certain crystal orientations, the index of refraction modulated by the linear electro-optic (Pockel's) effect is given by (this is by no means a general form, see Appendix A for specific examples):

$$n = n_{\text{original}} \pm (1/2) n_{\text{orig}}^3 r_{\text{appropriate}} E \quad (149)$$

If the electric field, E , is in the form of equations (144) and (148), the change in the refractive index takes the form:

$$\begin{aligned} \Delta n &= \pm (1/2) n_{\text{orig}}^3 r_{\text{approp}} |\langle E \rangle + [I_{+1} I_{-1}]^{1/2}/I_0](A + iB) \\ &\quad \exp[i(\phi + 2k_x x)]| \\ &= \pm (1/2) n_{\text{orig}}^3 r_{\text{approp}} \{ \langle E \rangle + [(I_{+1} I_{-1})^{1/2}/I_0](A^2 + B^2) \\ &\quad \cos(2k_x x + \phi + \psi) \} \end{aligned} \quad (150)$$

(10:954)

Summary

Without assuming it to be the case, Kukhtarev has shown the space-charge field to be sinusoidally varying and proportional to the incident interference pattern for small modulation index or charge transport lengths greater than the fringe spacing. Assuming this field to be sinusoidal may not be correct for conditions other than these and must be looked at on an individual basis.

For the form of the modulated index of refraction given in equation (149), the index grating is shown to be spatially sinusoidal and proportional to the interference fringes, as well.

Summary

Both Feinberg and Kukhtarev developed models for the photorefractive effect which, for spatially sinusoidally varying incident intensity and under correct conditions such as small modulation, concluded the electro-static field set up in the medium is also sinusoidal with the same frequency as the interference fringes but shifted in phase from them. This field then modulates the index of refraction of the medium.

It will be shown in a later chapter that diffraction off this index

grating produces the phase conjugate of one of the input beams. The usefulness of phase conjugation by the photorefractive effect is that conjugation is possible with lower intensity incident light than by degenerate four wave mixing.

In the photorefractive effect, the crystal is driven into nonlinearity by the space charge field set up in the medium rather than by the electric fields of the incident light as in four wave mixing. Both Feinberg (equation (126)) and Kukhtarev (equation (151)) show that the magnitude of the index grating is dependent on this field and the elements of the linear electro-optic tensor, R. Table 2 lists the elements of the electro-optic tensors of several media.

Table II
Linear electro-optic coefficients, r (2:230-233)

Substance	Symmetry	Wavelength λ (μm)	Electro-optic Coefficients ^a		Index of Refraction n_r	$n^2 r$ (10^{-12} m/V)	Dielectric Constant ^b $\epsilon (\epsilon_0)$
			r_{41}	(10^{-12} m/V)			
CdTe	43m	1.0	(T) $r_{41} = 4.5$		$n = 2.84$	103	(S) $\epsilon = 9.4$
		3.39	(T) $r_{41} = 6.8$				
		10.6	(T) $r_{41} = 6.8$				
		23.35	(T) $r_{41} = 5.47$				
		27.95	(T) $r_{41} = 5.04$				
GaAs	43m	0.9	$r_{41} = 1.1$		$n = 3.60$	51	(S) $\epsilon = 13.2$
		1.15	(T) $r_{41} = 1.43$				
		3.39	(T) $r_{41} = 1.24$				
		10.6	(T) $r_{41} = 1.51$				
GaP	43m	0.55-1.3	(T) $r_{41} = -1.0$		$n = 3.66-3.08$	15	(S) $\epsilon = 10$
		0.633	(S) $r_{41} = -1.97$				
		1.15	(S) $r_{41} = -1.10$				
		3.39	(S) $r_{41} = -0.97$				
β -ZnS (sphalerite)	43m	0.4	(T) $r_{41} = 1.1$		$n = 2.52$	18	(T) $\epsilon = 16$ (S) $\epsilon = 12.5$
		0.5	(T) $r_{41} = 1.81$				
		0.6	(T) $r_{41} = 2.1$				
		0.633	(S) $r_{41} = -1.6$				
		3.39	(S) $r_{41} = -1.4$				
ZnSe	43m	0.548	(T) $r_{41} = 2.0$		$n = 2.66$	25	(T) $\epsilon = 9.1$ (S) $\epsilon = 9.1$
		0.633	(S) $r_{41} = 2.0$				
		10.6	(T) $r_{41} = 2.2$				
ZnTe	43m	0.589	(T) $r_{41} = 4.51$		$n = 3.06$	108	(T) $\epsilon = 10.1$ (S) $\epsilon = 10.1$
		0.616	(T) $r_{41} = 4.27$				
		0.633	(T) $r_{41} = 4.04$				
		(S) $r_{41} = 4.3$					
		0.690	(T) $r_{41} = 3.97$				
		3.41	(T) $r_{41} = 4.2$				
		10.6	(T) $r_{41} = 3.9$				

$\text{Bi}_{1-x}\text{GeO}_3$	23	0.666	(T) $r_{41} = 3.22$		$n_r = 2.54$	53	
$\text{Bi}_{1-x}\text{SiO}_3$	23	0.633	$r_{41} = 5.0$		$n_r = 2.54$	82	
CdS	6mm	0.589	(T) $r_{41} = 3.7$	(T) $r = 4$	$n_r = 2.501$		(T) $\epsilon_r = 9.35$
		0.633	(T) $r_{41} = 1.6$	(T) $r = 4.8$	$n_r = 2.519$		(T) $\epsilon_r = 10.33$
		1.15	(T) $r_{41} = 3.1$	(T) $r = 6.2$	$n_r = 2.460$		(S) $\epsilon_r = 9.02$
			(T) $r_{41} = 3.2$		$n_r = 2.477$		
			(T) $r_{41} = 2.0$		$n_r = 2.320$		(S) $\epsilon_r = 9.53$
		3.39	(T) $r_{41} = 3.5$	(T) $r = 6.4$	$n_r = 2.276$		
			(T) $r_{41} = 2.9$		$n_r = 2.292$		
CdSe	6mm		(T) $r_{41} = 2.0$				
		10.6	(T) $r_{41} = 2.45$	(T) $r = 5.2$	$n_r = 2.226$		
			(T) $r_{41} = 2.75$		$n_r = 2.239$		
			(T) $r_{41} = 1.7$				
ZnO	6mm	0.633	(S) $r_{41} = 1.4$		$n_r = 1.990$		$\epsilon_1 = \epsilon_2 = 8.15$
			(S) $r_{41} = 2.6$		$n_r = 2.006$		$\approx \epsilon_1$
		3.39	(S) $r_{41} = 0.96$		$n_r = 1.902$		
α -ZnS (wurtzite)	6mm	0.633	(S) $r_{41} = 0.9$		$n_r = 1.916$		
			(S) $r_{41} = 1.8$				
$\text{Pb}_{1-x}\text{La}_{x/2}\text{O}_3$ ($\text{Ti}_{1-x}\text{Zr}_{x/2}\text{O}_3$) (PLZT)	∞ m	0.546	$n_r^2 r_{41} = n_r^2 r_{11} = 2320$		$n_r = 2.55$		

Table II (continued)

Substance	Symmetry	Wavelength λ (μm)	Electro-optic Coefficients ^a		Index of Refraction n	$n^2 r$ ($10^{-12} \text{ m}^2/\text{V}$)	Dielectric Constant ^b ϵ (ϵ_0)
			r_{11}	r_{22}			
LiIO_3	6	0.633	(S) $r_{11} = 4.1$ (S) $r_{41} = 1.4$	(S) $r_{33} = 6.4$ (S) $r_{33} = 3.3$	$n_s = 1.8830$ $n_c = 1.7367$		
Ag_3AsS	3m	0.633	(S) $n^2 r = 70$ (S) $n^2 r_{22} = 29$		$n_s = 3.019$ $n_c = 2.739$		
LiNbO_3 ($T = 1230^\circ\text{C}$)	3m	0.633	(T) $r_{11} = 9.6$ (T) $r_{22} = 6.8$ (T) $r_{33} = 30.9$ (T) $r_{41} = 32.6$ (T) $r_{41} = 21.1$	(S) $r_{11} = 8.6$ (S) $r_{22} = 3.4$ (S) $r_{33} = 30.8$ (S) $r_{41} = 28$	$n_s = 2.286$ $n_c = 2.200$		(T) $\epsilon_s = \epsilon_c = 78$ (T) $\epsilon_s = \epsilon_c = 32$ (S) $\epsilon_s = \epsilon_c = 43$ (S) $\epsilon_s = \epsilon_c = 28$
		1.15	(T) $r_{22} = 5.4$ (T) $r_{41} = 19$		$n_s = 2.229$ $n_c = 2.150$		
		3.39	(T) $r_{22} = 3.1$ (T) $r_{41} = 18$	(S) $r_{11} = 28$ (S) $r_{22} = 3.1$ (S) $r_{33} = 6.5$ (S) $r_{41} = 23$	$n_s = 2.136$ $n_c = 2.073$		
LiTaO_3	3m	0.633	(T) $r_{11} = 8.4$ (T) $r_{22} = 30.5$ (T) $r_{33} = -0.2$ (T) $r_{41} = 22$	(S) $r_{11} = 7.5$ (S) $r_{22} = 33$ (S) $r_{33} = 20$ (S) $r_{41} = 1$	$n_s = 2.176$ $n_c = 2.180$		(T) $\epsilon_s = \epsilon_c = 51$ (T) $\epsilon_s = 45$ (S) $\epsilon_s = \epsilon_c = 41$ (S) $\epsilon_s = 43$
		3.39	(S) $r_{11} = 27$ (S) $r_{22} = 4.5$ (S) $r_{33} = 15$ (S) $r_{41} = 0.3$		$n_s = 2.060$ $n_c = 2.065$		
AgGaS	42m	0.633	(T) $r_{41} = 4.0$ (T) $r_{41} = 3.0$		$n_s = 2.553$ $n_c = 2.507$		

CsH_2AsO_4 (CDA)	42m	0.55	(T) $r_{41} = 14.8$ (T) $r_{41} = 18.2$		$n_s = 1.572$ $n_c = 1.550$		
KH_2PO_4 (KDP)	42m	0.546	(T) $r_{41} = 8.77$ (T) $r_{41} = 10.3$		$n_s = 1.5115$ $n_c = 1.4698$		(T) $\epsilon_s = \epsilon_c = 42$ (T) $\epsilon_s = 21$
		0.633	(T) $r_{41} = 8$ (T) $r_{41} = 11$		$n_s = 1.5074$ $n_c = 1.4669$		(S) $\epsilon_s = \epsilon_c = 44$ (S) $\epsilon_s = 21$
		3.39	(T) $r_{41} = 9.7$ (T) $n^2 r_{41} = 33$				
KD_2PO_4 (KD*P)	42m	0.546	(T) $r_{41} = 26.8$ (T) $r_{41} = 8.8$		$n_s = 1.5079$ $n_c = 1.4683$		(T) $\epsilon_s = 50$ (S) $\epsilon_s = \epsilon_c = 58$
		0.633	(T) $r_{41} = 24.1$		$n_s = 1.502$ $n_c = 1.462$		(S) $\epsilon_s = 48$
$(\text{NH}_4)_2\text{H}_2\text{PO}_4$ (ADP)	42m	0.546	(T) $r_{41} = 23.76$ (T) $r_{41} = 8.56$		$n_s = 1.5266$ $n_c = 14808$		(T) $\epsilon_s = \epsilon_c = 56$ (T) $\epsilon_s = 15$
		0.633	(T) $r_{41} = 23.41$ (T) $n^2 r_{41} = 27.6$		$n_s = 1.5220$ $n_c = 14773$		(S) $\epsilon_s = \epsilon_c = 58$ (S) $\epsilon_s = 14$
$(\text{NH}_4)_2\text{D}_2\text{PO}_4$ (AD*P)	42m	0.633	(T) $r_{41} = 40$ (T) $r_{41} = 10$		$n_s = 1.516$ $n_c = 1.475$		
BaTiO_3 ($T = 395\text{ K}$)	4mm	0.546	(T) $r_{41} = 1640$ (T) $r_{41} = 108$	(S) $r_{41} = 820$ (S) $r_{41} = 23$	$n_s = 2.437$ $n_c = 2.365$		(T) $\epsilon_s = \epsilon_c = 3600$ (T) $\epsilon_s = 135$
$\text{KTa}_x\text{Nb}_{1-x}\text{O}_3$ (KTN , $x = 0.35$ $T = 40\text{--}60^\circ\text{C}$)		0.633	(T) $r_{41} = 8000$ ($T = 28$) (T) $r_{41} = 500$ ($T = 28$) (T) $r_{41} = 3000$ ($T = 16$) (T) $r_{41} = 700$ ($T = 16$)		$n_s = 2.318$ $n_c = 2.277$ $n_s = 2.318$ $n_c = 2.281$		
$\text{Ba}_{1-x}\text{Sr}_x\text{Nb}_2\text{O}_6$ ($T = 395\text{ K}$)	4mm	0.633	(T) $r_{41} = 67$ (T) $r_{41} = 1340$	(T) $r_{41} = 42$ (S) $r_{41} = 1090$	$n_s = 2.3117$ $n_c = 2.2987$		$\epsilon_s = 3400$ (15 MHz)

V. Steady State Two-Beam Coupling

The previous chapter described two theoretical models for the photorefractive effect. In this chapter and the one following, various figures of merit for the photorefractive effect are presented. These figures of merit are important because they are a quantification of those aspects of the photorefractive effect which play a significant role in optical phase conjugation.

The first of these figures of merit is "two beam coupling". It has been observed experimentally that when two beams write an index grating in a photorefractive crystal and propagate through this grating, one of the writing beams may experience a gain in intensity while the other experiences a corresponding loss.

Initially, this coupling effect appears not to have a place in phase conjugation. However, when self-pumped phase conjugate mirrors are considered, two-beam coupling becomes an important issue. Self-pumped phase conjugation occurs when a single beam is incident on a photorefractive crystal. This beam is defocused (13:46-51) or "fanned" in the crystal and reflected back to interfere with the original beam by either external mirrors (14:689-691) or internal reflections off the crystal faces (15:486-488). These reflected beams become the pumps for four wave mixing and get their energy from the original beam through two-beam coupling (14:688-691)(15:486-488)(16:548-553).

Two theories of two beam coupling are presented. The first is developed from Feinberg's Hopping Model. The second assumes a sinusoidal index grating exists in the medium due to modulation by the electro-static field in an "index ellipsoid"-type argument. (See Appendix A for details on the index ellipsoid.) Both theories show that

as long as there is a phase shift between the interference fringes and index grating, ψ , increased intensity can occur for one of the writing beams, with decreased intensity of the other, provided the crystal orientation is correct.

Feinberg's Hopping Model

This derivation of an expression for two beam coupling is a continuation of the development of the hopping model in the previous chapter. Assumption 6 made in developing the model was that small modulation conditions would only be considered ($m \ll 1$). The implication of this is that one writing beam is much weaker than the other. For this development, then:

$$\text{Beam 2} \gg \text{Beam 1}$$

The nonlinear polarization of the medium due to the modulated susceptibility (equation (153)) and the superposition of the two electric fields is:

$$\begin{aligned} P_{NL} &= X \cdot E \\ &= X \cdot [(E_1/2)\hat{e}_1 + (E_2/2)\hat{e}_2] \\ &\approx X \cdot \hat{e}_2 E_2/2 \end{aligned} \quad (151)$$

where, from equations (110) and (126), the susceptibility, X , is:

$$X = i \epsilon_0 \epsilon_\omega \cdot R \cdot k \cdot \epsilon_\omega \frac{W_0 \rho q}{\epsilon \epsilon_0 k^2} \frac{2 E_1 E_2^* \hat{e}_1 \cdot \hat{e}_2^*}{|E_1|^2 + |E_2|^2} \frac{\alpha^2 + i\alpha f}{\alpha^2 + 1 + i\alpha f} \quad (152)$$

(5:1300).

From Maxwell's equations, with $\sigma = 0$ and the SVEA similar to previous development, the wave equation is in the form:

$$\begin{aligned} k_{1x} \frac{\partial E_1}{\partial x} + k_{1y} \frac{\partial E_1}{\partial y} + k_{1z} \frac{\partial E_1}{\partial z} \\ + i|\mathbf{k}_1|^2 E_1/2 - i \mu_0 \epsilon \omega^2 E_1/2 = (i \mu_0 \omega^2 E_2/4) X \cdot e_2 \\ \exp[i(\mathbf{k}_1 - \mathbf{k}_2 + \mathbf{k}_2 - \mathbf{k}_1) \cdot \mathbf{x}] \end{aligned} \quad (153)$$

If there is no driving term (the nonlinear polarization) then:

$$k_{1x} \partial E_1 / \partial x + k_{1y} \partial E_1 / \partial y + k_{1z} \partial E_1 / \partial z = 0 \quad (154)$$

But with the driving term, the modulated susceptibility, X , alters the dispersion relation for \mathbf{k}_1 as (5:1300):

$$\begin{aligned} \mathbf{k}_1 &= \mathbf{k}_1(\omega) + \delta \mathbf{k}_1 \\ |\mathbf{k}_1|^2 &= |\mathbf{k}_1(\omega)|^2 + 2 \mathbf{k}_1(\omega) \cdot \delta \mathbf{k}_1 + |\delta \mathbf{k}_1|^2 \\ &\approx |\mathbf{k}_1(\omega)|^2 + 2 \mathbf{k}_1(\omega) \cdot \delta \mathbf{k}_1 \end{aligned} \quad (155)$$

if $|\delta \mathbf{k}_1| \ll |\mathbf{k}_1(\omega)|$.

Two assumptions are made in order to achieve a solution:

1. Assume that the changes in \mathbf{k}_1 , $\delta \mathbf{k}_1$, are much smaller than the unperturbed portion, $\mathbf{k}_1(\omega)$ (already used in equation (155)) (5:1300):

$$|\delta \mathbf{k}_1| \ll |\mathbf{k}_1(\omega)| \quad (156)$$

2. Assume $k_{1x} \partial E_1 / \partial x + k_{1y} \partial E_1 / \partial y + k_{1z} \partial E_1 / \partial z \approx 0$ as in non-driven case (equation (154)).

Equation (153) then becomes:

$$\begin{aligned} i|\mathbf{k}_1|^2(\omega) + 2 \mathbf{k}_1(\omega) \cdot \delta \mathbf{k}_1 |E_1/2 - i\mu_0 \epsilon \omega^2 E_1/2 \\ = (i\mu_0 \omega^2 |E_2/4) (\mathbf{X} \cdot \hat{\mathbf{e}}_2) \end{aligned} \quad (157)$$

Using $\mu_0 \epsilon_0 = 1/c^2$ and expanding \mathbf{X} where $|E_2| \gg |E_1|$ so that

$|E_2|^2 / (|E_1|^2 + |E_2|^2) = 1$, then (5:1300):

$$\begin{aligned} \mathbf{k}_1 \cdot \delta \mathbf{k}_1 &= [\omega^2 / (4c^2 \epsilon_0)] (E_2/E_1) \hat{\mathbf{e}}_1^* \cdot \mathbf{X} \cdot \hat{\mathbf{e}}_2 \\ &= \frac{i\omega^2 f_0}{2c^2} \frac{\alpha + if}{\alpha^2 + 1 + iaf} (\hat{\mathbf{e}}_1^* \cdot \epsilon_\omega \cdot \mathbf{R} \cdot \mathbf{k} \cdot \epsilon_\omega \cdot \hat{\mathbf{e}}_2) (\hat{\mathbf{e}}_1 \cdot \hat{\mathbf{e}}_2^*) \end{aligned} \quad (158)$$

If \mathbf{k}_1 is approximately parallel to $\delta \mathbf{k}_1$ then:

$$|\delta \mathbf{k}_1| = \frac{i\omega^2 f_0}{2c^2 |\mathbf{k}_1|} \frac{(1 + \alpha^2) \alpha + \alpha f^2 + if}{(1 + \alpha^2)^2 + (\alpha f)^2} (\hat{\mathbf{e}}_1^* \cdot \epsilon_\omega \cdot \mathbf{R} \cdot \mathbf{k} \cdot \epsilon_\omega \cdot \hat{\mathbf{e}}_2) (\hat{\mathbf{e}}_1 \cdot \hat{\mathbf{e}}_2^*) \quad (159)$$

and the propagation vector alteration, $\delta \mathbf{k}_1$, causes either growth or decay in E_1 described as:

$$\begin{aligned} \mathbf{E}_1'(\mathbf{x}) &= \mathbf{E}_1 \exp[i(\mathbf{k}_1 + \delta\mathbf{k}_1) \cdot \mathbf{x}] \\ &= \mathbf{E}_1 \exp[i(\mathbf{k}_1 + \operatorname{Re} \delta\mathbf{k}_1) \cdot \mathbf{x}] \exp(-\operatorname{Im} \delta\mathbf{k}_1 \cdot \mathbf{x}) \end{aligned} \quad (160)$$

The intensity becomes (5:1300,1301):

$$\begin{aligned} I_1'(\mathbf{x}) &= |\mathbf{E}_1|^2 \exp(-2 \operatorname{Im} \delta\mathbf{k}_1 \cdot \mathbf{x}) \\ I_1(\mathbf{x}) + \Delta I_1(\mathbf{x}) &= |\mathbf{E}_1|^2 (1 - 2 \operatorname{Im} \delta\mathbf{k}_1 \cdot \mathbf{x}) \end{aligned} \quad (161)$$

using the first order series expansion for the exponent.

The fractional intensity gain for \mathbf{E}_1 over some interaction distance, L , can be written as (5:1302):

$$\begin{aligned} \Delta I_1(\mathbf{x})/I_1(\mathbf{x}) &= -2 \operatorname{Im} \delta\mathbf{k}_1 \cdot \hat{\mathbf{r}} L \\ &= \frac{-\omega^2 f_0 L}{c^2 k_1} \frac{\alpha(1 + \alpha^2 + f^2)}{(1 + \alpha^2)^2 + (qf)^2} (\hat{\mathbf{e}}_1^* \cdot \epsilon_\omega \cdot \mathbf{R} \cdot \mathbf{k} \cdot \epsilon_\omega \cdot \hat{\mathbf{e}}_2) (\hat{\mathbf{e}}_1 \cdot \hat{\mathbf{e}}_2^*) \end{aligned} \quad (162)$$

Note that from equation (114), if there is no phase shift between the interference pattern and the index grating, ψ , the numerator of equation (162) is also zero. Thus, there is no energy transfer between the beams under this condition.

A comparison of the functional dependence of equation (162) to experimental data is made in the applications chapter (VII).

Examples

The following are examples of the form the relative intensity gain, equation (162), would take for two specific crystals, BaTiO₃ and BSO.

$$\begin{aligned} \text{BaTiO}_3 \\ (\hat{\mathbf{e}}_1^* \cdot \epsilon_\omega \cdot \mathbf{R} \cdot \mathbf{k} \cdot \epsilon_\omega \cdot \hat{\mathbf{e}}_2) (\hat{\mathbf{e}}_1 \cdot \hat{\mathbf{e}}_2^*) &= [(n_o^4 r_{13} k_z e_{2x} + n_o^2 n_e^2 r_{51} k_x e_{2z})^2 \\ &\quad + (n_o^4 r_{13} k_z e_{zy} + n_o^2 n_e^2 r_{51} k_y e_{2z})^2 \\ &\quad + (n_o^2 n_e^2 r_{51} k_x e_{2x} + n_o^2 n_e^2 r_{51} k_y e_{2y})^2 \\ &\quad + n_e^4 r_{33} k_z e_{2z})^2] \\ (e_{1x} e_{2x} + e_{1y} e_{2y} + e_{1z} e_{2z}) \end{aligned} \quad (163)$$

where

e_1^* is a mathematical expression used here to clear dot product of directionality and leave only its magnitude. This is done because it was assumed the stimulus ($\mathbf{x} \cdot \hat{e}_2$) and the response (\hat{e}_1') were of the same polarization.

\hat{e}_1 = Unit polarization vector of input wave, \mathbf{E}_1

$$= e_{1x}\hat{x} + e_{1y}\hat{y} + e_{1z}\hat{z} \text{ (see Figure 9 for orientation of directional cosines)}$$

\hat{e}_2 = Unit polarization vector of input wave, \mathbf{E}_2

$$= e_{2x}\hat{x} + e_{2y}\hat{y} + e_{2z}\hat{z}$$

ϵ_ω = Dielectric tensor for BaTiO₃

$$= \begin{pmatrix} n_o^2 & 0 & 0 \\ 0 & n_o^2 & 0 \\ 0 & 0 & n_e^2 \end{pmatrix}$$

R = Contracted electro-optic coefficient tensor for BaTiO₃

$$= \begin{pmatrix} 0 & 0 & r_{13} \\ 0 & 0 & r_{13} \\ 0 & 0 & r_{33} \\ 0 & r_{51} & 0 \\ r_{51} & 0 & 0 \\ 0 & 0 & 0 \end{pmatrix}$$

\mathbf{k} = Direction vector of grating

$$= \mathbf{k}_1 - \mathbf{k}_2$$

$$= k_x\hat{x} + k_y\hat{y} + k_z\hat{z}$$

\mathbf{k}_1 = Propagation vector of input \mathbf{E}_1 wave

$$= k_{1x}\hat{x} + k_{1y}\hat{y} + k_{1z}\hat{z}$$

$$k_{1x} = k_1 \cos \alpha_1 \cos \theta_1$$

$$k_{1y} = k_1 \cos \alpha_1 \sin \theta_1$$

$$k_{1z} = -k_1 \sin \alpha_1$$

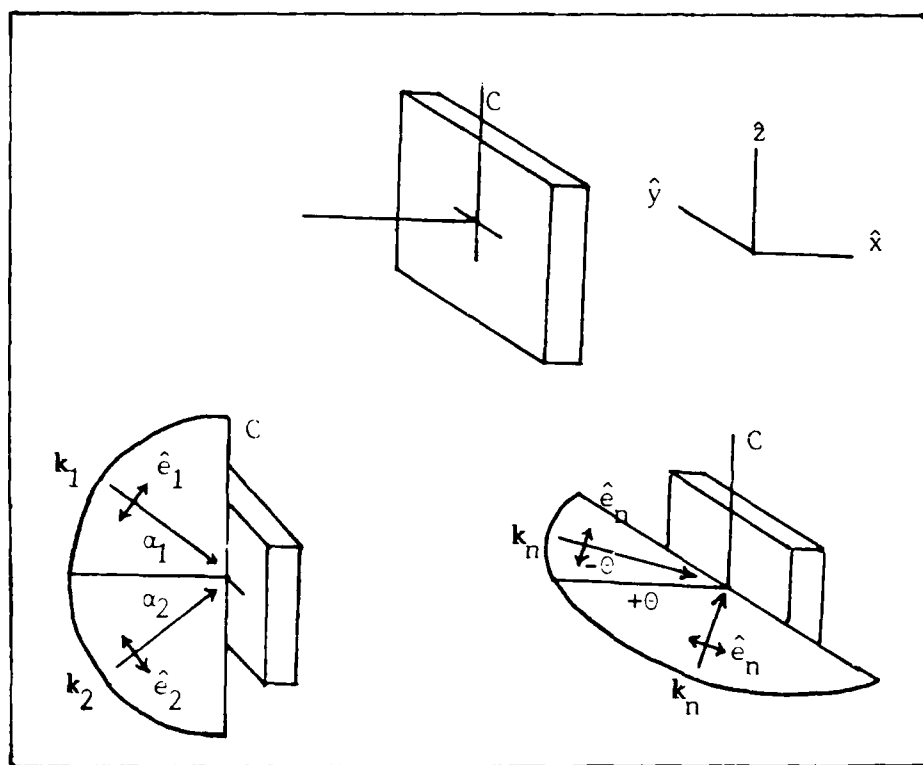
\mathbf{k}_2 = Propagation vector of input \mathbf{E}_2 wave

$$= k_{2x}\hat{x} + k_{2y}\hat{y} + k_{2z}\hat{z}$$

$$k_{2x} = k_2 \cos \alpha_2 \cos \theta_2$$

$$k_{2y} = k_2 \cos \alpha_2 \sin \theta_2$$

$$k_{2z} = k_2 \sin \alpha_2$$



a) Vertical Polarization

b) Horizontal Polarization

$$e_{1x} = \sin \alpha_1$$

$$e_{1x} = \sin \theta_1$$

$$e_{1y} = 0$$

$$e_{1y} = \cos \theta_1$$

$$e_{1z} = \cos \alpha_1$$

$$e_{1z} = 0$$

$$e_{2x} = \sin \alpha_2$$

$$e_{2x} = \sin \theta_2$$

$$e_{2y} = 0$$

$$e_{2y} = \cos \theta_2$$

$$e_{2z} = \cos \alpha_2$$

$$e_{2z} = 0$$

Figure 9. Orientation of angles used in directional cosine terms for polarization vectors, \hat{e}_1 and \hat{e}_2 , and propagation vectors \mathbf{k}_1 and \mathbf{k}_2 .

BSO(Bi₁₂SiO₂₀)

$$(\hat{e}_1^* \cdot \epsilon_{\omega} \cdot R \cdot k \cdot \epsilon_{\omega} \cdot \hat{e}_2) (\hat{e}_1 \cdot \hat{e}_2^*) = n^4 r_{41} [(k_z e_{2y} + k_y e_{2z})^2 + (k_z e_{2x} + k_x e_{2z})^2 + (k_y e_{2x} + k_x e_{2y})^2]^{1/2} (e_{1x} e_{2x} + e_{1y} e_{2y} + e_{1z} e_{2z}) \quad (164)$$

where

ϵ_{ω} = Dielectric tensor for BSO

$$= \begin{pmatrix} n^2 & 0 & 0 \\ 0 & n^2 & 0 \\ 0 & 0 & n^2 \end{pmatrix}$$

R = Contracted electro-optic coefficient tensor for BSO

$$= \begin{pmatrix} 0 & 0 & 0 \\ 0 & 0 & 0 \\ 0 & 0 & 0 \\ r_{41} & 0 & 0 \\ 0 & r_{41} & 0 \\ 0 & 0 & r_{41} \end{pmatrix}$$

Two Beam Coupling Assuming a Sinusoidal Index Grating Exists

Many authors such as Kukhtarev (10:954-956), Vahey (12:3510-3515) and White (17:10) assume an index grating has been set up in a photorefractive medium and derive expressions for the growth or decay of the writing beams propagating through this grating. Basically, each development is similar with each author including his own details in the picture. The derivation done here closely follows Vahey's derivation but is aimed at attaining White's solution which is more readily applicable.

Derivation

Given a sinusoidal index grating exists in the medium as derived in the previous chapter, in the correct crystal configuration, that grating may be represented as in equation (149) where the E-field is given by Feinberg's space-charge field (equation (115)) (7:519,520)(17:10):

$$\begin{aligned} n(E) &= n_{\text{appropriate}} \pm (1/2) n_{\text{approp}}^3 r_{\text{approp}} m \text{Eq} \\ &\quad \{(E_D^2 + E_0^2)/[(E_D + Eq)^2 + E_0^2]\}^{1/2} \cos(\mathbf{k} \cdot \mathbf{r} + \psi) \\ &= n_0 + n_I m \cos(\mathbf{k} \cdot \mathbf{r} + \psi) \end{aligned} \quad (165)$$

where

$$\begin{aligned} n_I &= \pm(1/2)n_{\text{approp}}^3 r_{\text{approp}} E_q \{(E_D^2 + E_0^2)/[(E_D + E_q)^2 + E_0^2]\}^{1/2} \\ &\quad (\text{see Appendix A for definition of } \pm) \\ m &= 2(I_1 I_2)^{1/2}/(I_1 + I_2) \\ \psi &= \tan^{-1}[(E_D E_q + E_D^2 + E_0^2)/(E_0 E_q)] \text{ (equation (114))} \end{aligned}$$

(The geometry follows Figure 7.)

Wave Equation

The scalar wave equation for this geometry is:

$$\nabla^2 \mathbf{E} + k^2 \mathbf{E} = 0 \quad (166)$$

where

$$\begin{aligned} \mathbf{E} &= A_1 \hat{\mathbf{e}}_1 \exp(i\mathbf{k}_1 \cdot \mathbf{r}) + A_1^* \hat{\mathbf{e}}_1^* \exp(-i\mathbf{k}_1 \cdot \mathbf{r}) + A_2 \hat{\mathbf{e}}_2 \exp(i\mathbf{k}_2 \cdot \mathbf{r}) \\ &\quad + A_2^* \hat{\mathbf{e}}_2^* \exp(-i\mathbf{k}_2 \cdot \mathbf{r}) \\ &= A_1(x) \exp[i(k \cos \theta_x - k \sin \theta_z)] + \text{c.c.} \\ &\quad + A_2(x) \exp[i(k \cos \theta_x + k \sin \theta_z)] + \text{c.c.} \end{aligned}$$

c.c. = Complex conjugate

$$k^2 = \omega^2 n^2(E)/c^2$$

$$\begin{aligned} n^2(E) &= n_0^2 + 2n_0 n_I m \cos(\mathbf{k} \cdot \mathbf{r} + \psi) + n_I^2 m^2 \cos^2(\mathbf{k} \cdot \mathbf{r} + \psi) \\ &\approx n_0^2 + n_0 n_I m \{\exp[i(2k \sin \theta_z + \psi)] \\ &\quad + \exp[-i(2k \sin \theta_z + \psi)]\} \end{aligned}$$

After applying the Slowly Varying Envelope Approximation (SVEA),

equation (166) becomes:

$$\begin{aligned}
 & 2(\partial A_1 / \partial x)(ik \cos \theta) \exp[i(k \cos \theta x - k \sin \theta z)] + c.c. \\
 & + A_1(-k^2 \cos^2 \theta) \exp[i(k \cos \theta x - k \sin \theta z)] + c.c. \\
 & + 2(\partial A_2 / \partial x)(ik \cos \theta) \exp[i(k \cos \theta x + k \sin \theta z)] + c.c. \\
 & + A_2(-k^2 \cos^2 \theta) \exp[i(k \cos \theta x + k \sin \theta z)] + c.c. \\
 & - k^2 \sin^2 \theta E + (\omega^2 n_0^2 / c^2) E \\
 & + (\omega^2 n_0 n_I m / c^2) \{ A_1 \exp[i(k \cos \theta x + k \sin \theta z + \psi)] + c.c. \\
 & + A_1 \exp[i(k \cos \theta x - 3k \sin \theta z - \psi)] + c.c. \\
 & + A_2 \exp[i(k \cos \theta x + 3k \sin \theta z + \psi)] + c.c. \\
 & + A_2 \exp[i(k \cos \theta x - k \sin \theta z - \psi)] + c.c. \} = 0
 \end{aligned} \tag{167}$$

Grouping terms in equation (167) synchronous with $\exp[i(k \cos \theta x - k \sin \theta z)]$ yields:

$$\begin{aligned}
 & 2(\partial A_1 / \partial x)(ik \cos \theta) + A_1(-k^2 \cos^2 \theta) - k^2 \sin^2 \theta A_1 + \omega^2 n_0^2 A_1 / c^2 \\
 & + \omega^2 n_0 n_I m A_2 \exp(-i\psi) / c^2 = 0
 \end{aligned} \tag{168}$$

Since:

$$\omega^2 n_0^2 A_1 / c^2 - k^2(\sin^2 \theta + \cos^2 \theta) A_1 = 0 \tag{169}$$

after rewriting the exponential, equation (169) becomes:

$$\begin{aligned}
 & \partial A_1 / \partial x - ik n_I m A_2 \exp(-i\psi) / (2n_0 \cos \theta) = 0 \\
 & \partial A_1 / \partial x - k n_I m A_2 \sin \psi / (2n_0 \cos \theta) \\
 & - ik n_I m A_2 \cos \psi / (2n_0 \cos \theta) = 0
 \end{aligned} \tag{170}$$

The real part of equation (170) yields:

$$\begin{aligned}
 \partial A_1 / \partial x &= k n_I (I_1 I_2)^{1/2} A_2 (\sin \psi) / [n_0 (I_1 + I_2) \cos \theta] \\
 &= (1/A_1) (dI_1 / dx)
 \end{aligned} \tag{171}$$

by definition. Then:

$$\begin{aligned}
 dI_1 / dx &= k n_I I_1 I_2 (\sin \psi) / [n_0 (I_1 + I_2) \cos \theta] \\
 dI_1 / dr &= 2 \Gamma I_1 I_2 / (I_1 + I_2)
 \end{aligned} \tag{172}$$

where

$$r = x/\cos \theta$$

$$\Gamma = \pi n_I \sin \psi / \lambda$$

A similar development for $\exp[i(k \cos \theta x + k \sin \theta z)]$ yields:

$$dI_2/dr = -2\Gamma I_1 I_2 / (I_1 + I_2) \quad (173)$$

White (17:10) points out that linear absorption, α , is crucial to the photorefractive effect so his coupled equations are in the form:

$$\begin{aligned} dI_1/dr &= -\alpha I_1 + 2\Gamma I_1 I_2 / (I_1 + I_2) \\ dI_2/dr &= -\alpha I_2 - 2\Gamma I_1 I_2 / (I_1 + I_2) \end{aligned} \quad (174)$$

Solution to the Coupled Wave Equations

White gives the solutions to equations (174) as (17:10) (10:954):

$$\begin{aligned} I_1(r) &= I_1(0) \exp(-\alpha r) [I_1(0) + I_2(0)] / [I_1(0) + I_2(0) \exp(-2\Gamma r)] \\ I_2(r) &= I_2(0) \exp(-\alpha r) [I_1(0) + I_2(0)] / [I_1(0) \exp(2\Gamma r) + I_2(0)] \end{aligned} \quad (175)$$

Note that the term responsible for the gain or loss of intensity, Γ , contains the change in the index of refraction, n_I , which is proportional to the magnitude of the space-charge field and the phase shift between the incident interference fringes and the space-charge field, ψ . If there is no phase shift, $\psi = 0$, only the linear absorption loss remains in equation (175) so no energy transfer between the two beams occurs.

Summary

"Two beam coupling" is one of the figures of merit for the photorefractive effect as applied to optical phase conjugation. It describes the phenomenon of intensity growth (or corresponding loss) in one of the incident beams writing an index grating in a photorefractive crystal.

Two theoretical expressions were developed to describe two beam coupling. The first (equation (162)) is an extension of Feinberg's

Hopping Model for the photorefractive effect developed in the previous chapter. The second (equation (175)) assumed an index grating existed and could be described by an index ellipsoid-type expression. It solved the wave equation for light propagating through the grating.

Although expressions (162) and (175) are unique, they both indicate that if no spatial phase shift exists between the interference fringes and the index grating, no beam coupling will occur. A comparison of these two expressions occurs in the applications chapter (VII) for specific crystal orientations of Bismuth Silicate (BSO).

VI. Diffraction Efficiency and Phase Conjugate Reflectivity

The second and third figures of merit quantifying the aspects of the photorefractive effect important to optical phase conjugation are diffraction efficiency and phase conjugate reflectivity. Diffraction efficiency is the amount of power in a wave diffracted off a grating at the Bragg angle compared to the amount of power in the wave incident on the grating. Phase conjugate reflectivity, in the photorefractive phase conjugation geometry shown in Figure 10, is the power in the conjugate wave compared to the power in the probe wave. The probe wave and one of the pump waves, E_1 , write an index grating in the crystal. The counterpropagating pump wave, E_3 , diffracts off the grating as E_4 , the phase conjugate of the probe.

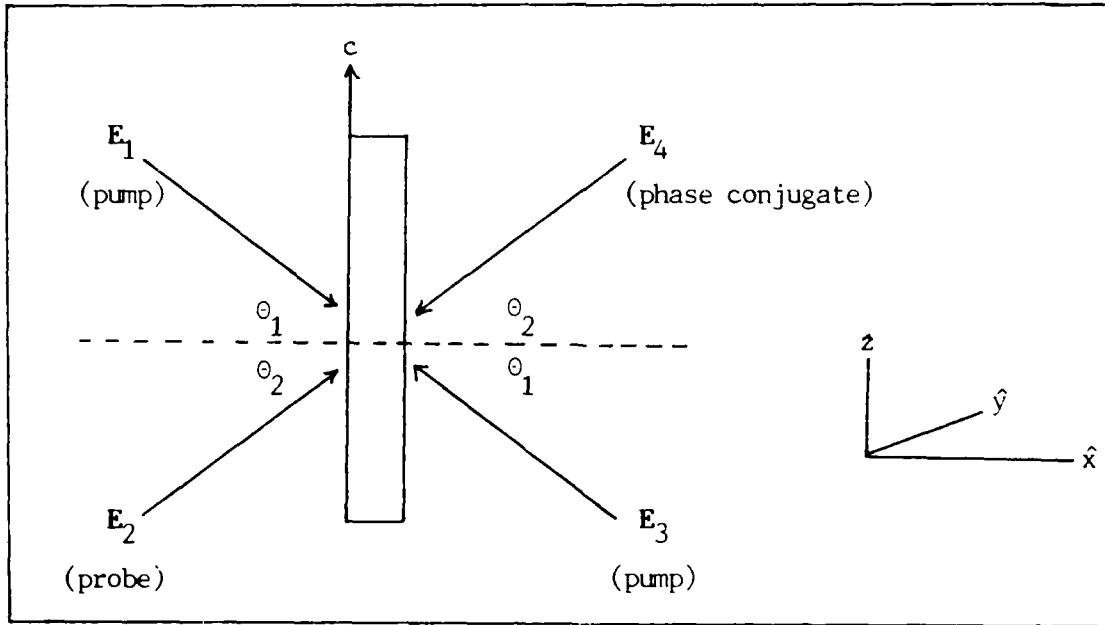


Figure 10. Geometry of optical phase conjugation in photorefractive crystals.

As for two beam coupling, two theories for both diffraction efficiency and phase conjugate reflectivity are presented. The first for

each is again an extension of Feinberg's Hopping Model. The second for each again assumes an index grating exists in the medium due to modulation by the electro-static field.

Feinberg's Hopping Model

Development

The interference of two optical waves in a photorefractive crystal (E_1 and E_2 in Figure 10) causes charge migration and the steady state potential distribution as described in Chapter IV. When a third optical wave (5:1300)

$$E_3 = E_3 \hat{e}_3 \operatorname{Re} \exp[i(\mathbf{k}_3 \cdot \mathbf{x} - \omega t)] \quad (176)$$

is scattered off the modulated optical susceptibility set up by the potential distribution and E_3 is counterpropagating to E_1 , the scattered wave, E_4 , will be the phase conjugate of E_2 .

The Wave Equation

The solution for the four wave mixing will be derived through Maxwell's wave equation with the expression for the nonlinear polarization (nonlinear susceptibility) given by (equation(151)). The wave equation is (equation (15)):

$$\nabla^2 \mathbf{E} = \mu_0 \sigma \partial \mathbf{E} / \partial t + \mu_0 \epsilon \partial^2 \mathbf{E} / \partial t^2 + \mu_0 \partial^2 \mathbf{P}_{NL} / \partial t^2$$

As in the second and third order mixing derivations, a number of simplifying assumptions will be made to make the equation soluble:

1. The media is non-conducting ($\sigma = 0$). Then:

$$\begin{aligned} -\nabla^2 E_4 \exp[i(\mathbf{k}_4 \cdot \mathbf{x} - \omega t)] - \mu_0 \epsilon (\partial^2 / \partial t^2) E_4 \exp[i(\mathbf{k}_4 \cdot \mathbf{x} - \omega t)] \\ = \mu_0 (\partial^2 / \partial t^2) P_3(\mathbf{x}, t) \end{aligned} \quad (177)$$

where:

$$\begin{aligned} (\partial^2 / \partial x^2) E_4(\mathbf{x}, t) &= (\partial^2 E_4 / \partial x^2) \exp[i(\mathbf{k}_4 \cdot \mathbf{x} - \omega t)] \\ &+ i 2k_{4x} (\partial E_4 / \partial t) \exp[i(\mathbf{k}_4 \cdot \mathbf{x} - \omega t)] \\ &- k_{4x}^2 E_4 \exp[i(\mathbf{k}_4 \cdot \mathbf{x} - \omega t)] \end{aligned} \quad (178)$$

Similarly for y and z :

$$\begin{aligned} (\partial^2/\partial t^2) \mathbf{E}_4(\mathbf{x}, t) &= -\omega^2 \mathbf{E}_4(\mathbf{x}, t) \\ (\partial^2/\partial t^2) \mathbf{P}_3(\mathbf{x}, t) &= -\omega^2 \mathbf{P}_3(\mathbf{x}, t) \end{aligned} \quad (179)$$

and the nonlinear polarization is in the form (5:1300):

$$\begin{aligned} \mathbf{P}_3(\mathbf{x}, t) &= \mathbf{X}(\mathbf{x}) \cdot \mathbf{E}_3(\mathbf{x}, t) \\ &= E_3/2 \operatorname{Re} \mathbf{X} \cdot \hat{\mathbf{e}}_3 \exp[i((\mathbf{k}_1 - \mathbf{k}_2 + \mathbf{k}_3) \cdot \mathbf{x} - \omega t)] \end{aligned} \quad (180)$$

2. Assume the Slowly Varying Envelope Approximation (SVEA):

$$\partial^2/\partial x^2 = \partial^2/\partial y^2 = \partial^2/\partial z^2 = 0$$

The wave equation becomes:

$$\begin{aligned} &2i k_{4x} (\partial \mathbf{E}_4 / \partial x) \exp[i(\mathbf{k}_4 \cdot \mathbf{x} - \omega t)] - k_{4x}^2 \mathbf{E}_4 \exp[i(\mathbf{k}_4 \cdot \mathbf{x} - \omega t)] \\ &+ 2i k_{4y} (\partial \mathbf{E}_4 / \partial y) \exp[i(\mathbf{k}_4 \cdot \mathbf{x} - \omega t)] - k_{4y}^2 \mathbf{E}_4 \exp[i(\mathbf{k}_4 \cdot \mathbf{x} - \omega t)] \\ &+ 2i k_{4z} (\partial \mathbf{E}_4 / \partial z) \exp[i(\mathbf{k}_4 \cdot \mathbf{x} - \omega t)] - k_{4z}^2 \mathbf{E}_4 \exp[i(\mathbf{k}_4 \cdot \mathbf{x} - \omega t)] \\ &+ \mu_0 \epsilon \omega^2 \mathbf{E}_4 \exp[i(\mathbf{k}_4 \cdot \mathbf{x} - \omega t)] \\ &= (-\mu_0 \omega^2/2) E_3 \mathbf{X}(\mathbf{x}) \cdot \hat{\mathbf{e}}_3 \exp[i((\mathbf{k}_1 - \mathbf{k}_2 + \mathbf{k}_3) \cdot \mathbf{x} - \omega t)] \end{aligned} \quad (181)$$

By multiplying both sides by $(-i/2) \exp[-i(\mathbf{k}_4 \cdot \mathbf{x} - \omega t)]$, using the identity, $\mathbf{k}_4^2 = \mu_0 \epsilon \omega^2$ and if $\mu_0 = \mu$, then:

$$\begin{aligned} k_{4x} \partial \mathbf{E}_4 / \partial x + k_{4y} \partial \mathbf{E}_4 / \partial y + k_{4z} \partial \mathbf{E}_4 / \partial z \\ = (i \mu_0 \omega^2/4) E_3 \mathbf{X}(\mathbf{x}) \cdot \hat{\mathbf{e}}_3 \exp[i \Delta \mathbf{k} \cdot \mathbf{x}] \end{aligned} \quad (182)$$

where:

$$\Delta \mathbf{k} = \mathbf{k}_1 - \mathbf{k}_2 + \mathbf{k}_3 - \mathbf{k}_4 \quad (183)$$

3. The scattered beam, \mathbf{E}_3 , is not depleted by the mixing, then:

$$\mathbf{E}_3(\mathbf{x}) = \mathbf{E}_3 \quad (184)$$

Solution

The form of the solution is assumed to be:

$$\mathbf{E}_4 = \mathbf{K} \exp(i \Delta \mathbf{k} \cdot \mathbf{x}) + \mathbf{C} \quad (185)$$

... : \mathbf{E}_4 is the amplitude of $\mathbf{E}_4(\mathbf{x})$, only.)

$$\partial E_4 / \partial x = i \Delta k_x K \exp(i \Delta k \cdot x) \quad (186)$$

with similar forms for y and z . Equation (182) becomes:

$$i K \Delta k \cdot k_4 \exp(i \Delta k \cdot x) = (i \mu_0 \omega^2 / 4) E_3 \mathbf{x} \cdot \hat{\mathbf{e}}_3 \exp(i \Delta k \cdot x) \quad (187)$$

Therefore:

$$K = \mu_0 \omega^2 E_3 \mathbf{x} \cdot \hat{\mathbf{e}}_3 / (4 \Delta k \cdot k_4) \quad (188)$$

To solve for the constant, C , if there is no interaction length in the medium, no nonlinear polarization occurs and no new wave, E_4 , is produced:

$$\begin{aligned} E_4(0,0,0) &= 0 \\ &= K + C \\ C &= -K \end{aligned} \quad (189)$$

The conjugate wave which is the fourth wave of the four wave mixing process can then be expressed (after minor manipulation) as:

$$E_4 = \frac{\mu_0 \omega^2 E_3 \mathbf{x} \cdot \hat{\mathbf{e}}_3}{4 \Delta k \cdot k_4} \frac{\exp(i \Delta k \cdot x/2) - \exp(-i \Delta k \cdot x/2)}{\exp(-i \Delta k \cdot x/2)} \quad (190)$$

or, over interaction length, L , as:

$$E_4(L) = \frac{i L \mu_0 \omega^2 E_3 \mathbf{x} \cdot \hat{\mathbf{e}}_3}{4 k_4 \exp(-i \Delta k L/2)} \frac{\sin(\Delta k L/2)}{\Delta k L/2} \quad (191)$$

The power per unit area radiated by the nonlinear polarization takes the form:

$$\begin{aligned} P^{(4)}/\text{Area} &= 1/2 (\epsilon/\mu_0)^{1/2} |E_4|^2 \\ &= \frac{1}{2} \left(\frac{\epsilon}{\mu_0}\right)^{1/2} \frac{L^2 \mu_0^2 \omega^4 |E_3|^2 |\hat{\mathbf{e}}_4^* \cdot \mathbf{x} \cdot \hat{\mathbf{e}}_3|^2}{16 k_4^2} \left[\frac{\sin(\Delta k L/2)}{\Delta k L/2}\right]^2 \end{aligned} \quad (192)$$

Under conservation of momentum, $\Delta k = 0$ so that $(\sin x)/x = 1$ in the preceding expression for any significant power transfer.

Diffraction Efficiency

The power per unit area of the pump wave, E_3 , is:

$$P^{(3)}/\text{Area} = (1/2)(\epsilon/\mu_0)^{1/2} |E_3|^2 \quad (193)$$

The ratio of the power radiated by the nonlinear polarization to the input power of E_3 is the diffraction efficiency, η , and from equations (192) and (193) is given by:

$$\begin{aligned}\eta &= |L \mu_0 \omega^2 \hat{e}_4^* \cdot \mathbf{x} \cdot \hat{e}_3 / (4 k_4)|^2 \\ &= \left(\frac{L \omega f_0}{4 n_4 c k} \right)^2 \frac{2I_1 I_2}{(I_1 + I_2 + I_3)^2} \frac{\alpha^2 + f^2}{(\alpha^2 + 1)^2 + (\alpha f)^2} |\hat{e}_4^* \cdot \epsilon_\omega \cdot R \cdot \mathbf{k} \cdot \epsilon_\omega \cdot \hat{e}_3|^2 \\ &= \left(\frac{L \omega}{4 n_4 c k} \right)^2 \frac{2I_1 I_2}{(I_1 + I_2 + I_3)^2} E_q^2 \frac{E_D^2 + E_0^2}{(E_D + E_q)^2 + E_0^2} |\hat{e}_4^* \cdot \epsilon_\omega \cdot R \cdot \mathbf{k} \cdot \epsilon_\omega \cdot \hat{e}_3|^2\end{aligned}\quad (194)$$

using $\mu_0 \omega/k_4 = 1/(n_4 c \epsilon_0)$ and where the modulation index is:

$$m = 2(I_1 I_2)^{1/2} / (I_1 + I_2 + I_3) \quad (195)$$

Note that Feinberg includes I_3 , the third incident intensity, in the denominator of this form of the modulation index expression which does not appear in the usual forms (5:1299,1300).

Feinberg's form of diffraction efficiency, then, is proportional to the square of the magnitude of the created space-charge field.

Phase Conjugate Reflectivity

The power per unit area of the probe wave, E_2 , is:

$$P^{(2)}/\text{Area} = (1/2)(\epsilon/\mu_0)^{1/2} |E_2|^2 \quad (196)$$

The ratio of the power radiated by the nonlinear polarization to the input power of E_2 is the phase conjugate reflectivity, R , and from equations (192) and (196) is given by:

$$\begin{aligned}R &= |E_4|^2 / |E_2|^2 \\ &= |L \omega \hat{e}_4^* \cdot \mathbf{x} \cdot \hat{e}_3 / (4 n_4 c \epsilon_0)|^2 (I_3/I_2) \\ &= \left(\frac{L \omega f_0}{4 n_4 c k} \right)^2 \frac{2I_1 I_3}{(I_1 + I_2 + I_3)^2} \frac{\alpha^2 + f^2}{(\alpha^2 + 1)^2 + (\alpha f)^2} |\hat{e}_4^* \cdot \epsilon_\omega \cdot R \cdot \mathbf{k} \cdot \epsilon_\omega \cdot e_3|^2 \\ &= \left(\frac{L \omega}{4 n_4 c k} \right)^2 \frac{2I_1 I_3}{(I_1 + I_2 + I_3)^2} E_q^2 \frac{E_D^2 + E_0^2}{(E_D + E_q)^2 + E_0^2} |\hat{e}_4^* \cdot \epsilon_\omega \cdot R \cdot \mathbf{k} \cdot \epsilon_\omega \cdot e_3|^2\end{aligned}\quad (197)$$

Feinberg's form of the phase conjugate reflectivity, like the diffraction efficiency, is proportional to the square of the magnitude of the space-charge field.

Examples

The following are examples of the form the diffraction efficiency and phase conjugate reflectivity expressions (equations (194) and (197)) would take for two specific crystals, BaTiO₃ and BSO.

BaTiO₃

$$|\hat{e}_4^* \cdot \epsilon_{\omega} \cdot R \cdot k \cdot e_3|^2 = (n_o^4 r_{13} k_z e_{3x} + n_o^2 n_e^2 r_{51} k_x e_{3z})^2 + (n_o^4 r_{13} k_z e_{3y} + n_o^2 n_e^2 r_{51} k_y e_{3z})^2 + (n_o^2 n_e^2 r_{51} k_x e_{3x} + n_o^2 n_e^2 r_{51} k_y e_{3y} + n_e^4 r_{33} k_z e_{3z})^2 \quad (198)$$

where

\hat{e}_4^* , as used here, is a mathematical expression, as in the two beam coupling examples, to clear the dot product of directionality and leave only its magnitude. It was assumed, here, that the stimulus ($X \cdot e_3$) and the response (\hat{e}_4) were of the same polarization.

\hat{e}_3 = Unit polarization vector of pump wave, E_3

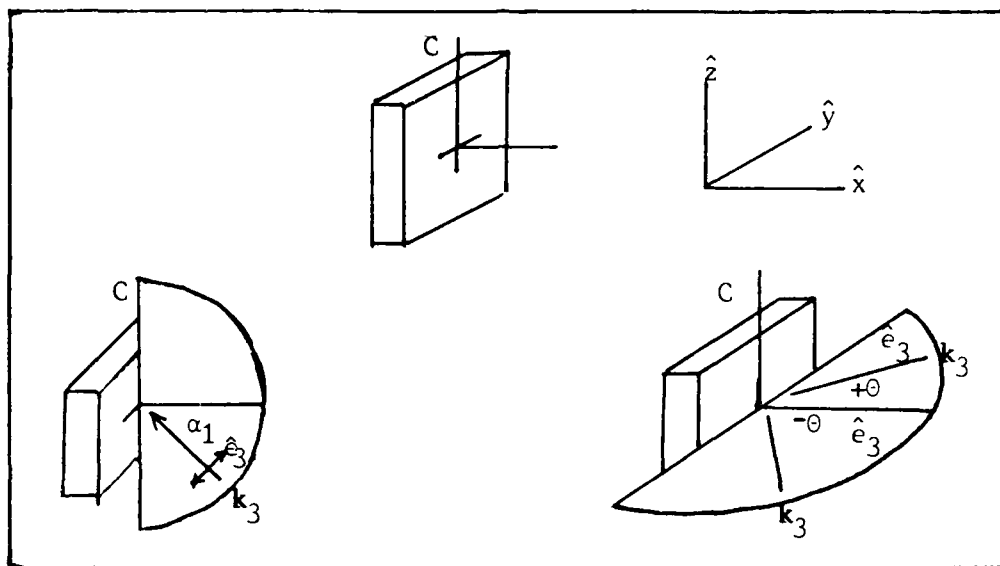
= $e_{3x} \hat{x} + e_{3y} \hat{y} + e_{3z} \hat{z}$ (see Figure 11 for orientation of directional cosines)

k = Direction vector of grating

ϵ_{ω} = Dielectric tensor for BaTiO₃

R = Contracted electro-optic coefficient tensor for BaTiO₃

See two beam coupling examples for details on directional cosines, the dielectric tensor and the electro-optic coefficient tensor for BaTiO₃.



a) Vertical polarization

b) Horizontal polarization

$$e_{3x} = \sin \alpha_1$$

$$e_{3y} = 0$$

$$e_{3z} = \cos \alpha_1$$

$$e_{3x} = \sin \theta$$

$$e_{3y} = \cos \theta$$

$$e_{3z} = 0$$

Figure 11. Orientation of angles used in directional cosines of polarization vector, \hat{e}_3 .

BSO ($\text{Bi}_{12}\text{SiO}_{20}$)

$$|\hat{e}_4^* \cdot \epsilon_\omega \cdot R \cdot k \cdot \epsilon_\omega \cdot \hat{e}_3|^2 = n^8 r_{41}^2 [(k_z e_{3y} + k_y e_{3z})^2 + (k_z e_{3x} + k_x e_{3z})^2 + (k_y e_{3x} + k_x e_{3y})^2] \quad (199)$$

where

ϵ_ω = Dielectric tensor for BSO

R = Contracted electro-optic coefficient tensor for BSO

See two beam coupling examples for details on the dielectric tensor and the electro-optic coefficient tensor for BSO.

Diffraction Efficiency Assuming a Sinusoidal Index Grating Exists

This derivation is aimed at attaining the form of diffraction efficiency used by Kukhtarev (10:955) and Gunter (9:250). It is assumed that a sinusoidal index grating exists in the medium as derived in

Chapter IV, the geometry follows Figure 7 and the crystal is oriented so equation (165) is applicable for the modulated index. Then using the wave equation (166), the same derivation as in the previous chapter can be made but with electric fields replaced by primed electric fields representing beams of the same frequency as the writing beams incident at the Bragg angle (10:955) but with small enough intensity that they do not effect the index grating (9:250). Then equations (172) and (173) can be written as:

$$\begin{aligned} dI_1'/dx &= 2\Gamma I_1' I_2' / (I_1' + I_2') \\ dI_2'/dx &= -2\Gamma I_1' I_2' / (I_1' + I_2') \end{aligned} \quad (200)$$

where

$$\Gamma = \pi n_I \cos \theta / \lambda$$

$I_{1,2}'$ = Intensity of beams of the same frequency as the writing beams, $I_{1,2}$, incident at the Bragg angle but with small enough intensity that they do not effect the index grating

But n_I is as defined in equation (186) as in Kukhtarev's development of Chapter IV (10:954).

The solution to the coupled equations (200) for diffraction efficiency, η , with boundary condition $I_2'(0) = 0$ since the diffraction of I_1' is I_2' , is given by Kukhtarev as:

$$\begin{aligned} \eta &= I_2'(x)/I_1'(0) \\ &= \frac{2\beta_0 \exp(\Gamma' x/2) [\cosh(\Gamma' x/2) - \cos(\gamma x)]}{(1 + \beta_0) [1 + \beta_0 \exp(\Gamma' x)]} \end{aligned} \quad (201)$$

where

$$\beta_0 = I_2(0)/I_1(0)$$

$$\Gamma' = (-2\pi/\lambda) n_{orig}^3 r_{approp} \cos \theta B$$

$$\gamma = (-\pi/\lambda) n_{orig}^3 r_{approp} \cos \theta A$$

with A and B as defined after equation (148) of Chapter IV (10:955).

(Note the intensities in β_0 are of the writing beams.)

In this form, the diffraction efficiency is proportional to the exponential of the diffusion field, only.

Phase Conjugate Reflectivity Assuming a Sinusoidal Index Grating Exists

The optical phase conjugation geometry of Figure 10 is assumed. At this point, no index grating exists in the medium but the probe and pump (E_1) will write one. The scalar wave equation (166) is :

$$\nabla^2 E + k^2 E = 0$$

where E is the superposition of the four electric fields:

$$\begin{aligned} E = & A_1(r) \exp[i(k_1 \cos \theta_1 x - \omega t)] + c.c. \\ & + A_2(r) \exp[i(k_2 \cos \theta_2 x - \omega t)] + c.c. \\ & + A_3(r) \exp[-i(k_1 \cos \theta_1 x + \omega t)] + c.c. \\ & + A_4(r) \exp[-i(k_2 \cos \theta_2 x + \omega t)] + c.c. \end{aligned} \quad (202)$$

and where

$$\partial E / \partial y = \partial E / \partial z = 0$$

$$k^2 = \omega^2 n^2(E) / c^2$$

Here, $n(E)$ takes the same form as equation (165), however, initially, each pair of beams in Figure 10 will be allowed to interfere with one another and create a grating. Equation (165) then takes the form (7:519):

$$\begin{aligned} n(E) = & n_0 + [n_I \exp(i\psi_1)/2] (A_1^* A_2 + A_3^* A_4^*) \exp(ik_1 \cdot r) / I_0 + c.c. \\ & + [n_{II} \exp(i\psi_2)/2] (A_1 A_4^* + A_3 A_2^*) \exp(ik_2 \cdot r) / I_0 + c.c. \\ & + [n_{III} \exp(i\psi_3)/2] A_1 A_3^* \exp(ik_1 \cdot r) / I_0 + c.c. \\ & + [n_{IV} \exp(i\psi_4)/2] A_4^* A_2 \exp(ik_2 \cdot r) / I_0 + c.c. \\ = & n_0 + \Delta n \end{aligned} \quad (203)$$

where

$$n_{I,II,III,IV} = n_{approp}^3 r_{approp} E_q \{ (E_D^2 + E_0^2) / [(E_D + E_q)^2 + E_0^2] \}^{1/2}$$

(using Feinberg's space-charge field.)

$\psi_{I,II,III,IV}$ = Appropriate phase shift between that set of
interference fringes and index grating

$$\mathbf{k}_I = \mathbf{k}_2 - \mathbf{k}_1$$

$$\mathbf{k}_{II} = \mathbf{k}_1 + \mathbf{k}_2$$

$$\mathbf{k}_{III} = 2\mathbf{k}_1$$

$$\mathbf{k}_{IV} = 2\mathbf{k}_2$$

$$I_0 = I_1 + I_2 + I_3 + I_4$$

If it is assumed that the change in the index is small compared to
the background index, $\Delta n \ll n_0$, then:

$$\begin{aligned} n^2(E) &= n_0^2 + 2 n_0 \Delta n + \Delta n^2 \\ &\approx n_0^2 + 2 n_0 \Delta n \end{aligned} \quad (204)$$

By using equations (202), (203) and (204) in the wave equation and applying the Slowly Varying Envelope Approximation (SVEA), the terms synchronous with $\exp[i(k_1 \cos \theta_1 x - \omega t)]$ in the wave equation are:

$$\begin{aligned} 2k_1 \cos \theta_1 dA_1/dx &= [i \omega^2 n_0 n_I^* \exp(-i \psi_I) (A_1 A_2^* + A_3 A_4^*) A_2 \\ &\quad + i \omega^2 n_0 n_{II} \exp(i \psi_{II}) (A_1 A_4^* + A_3 A_2^*) A_4 \\ &\quad + i \omega^2 n_0 n_{III} \exp(i \psi_{III}) (A_1 A_3^*) A_3] / (c^2 I_0) \end{aligned} \quad (205)$$

Now it is assumed that although all these gratings are created, only one will give rise to strong beam coupling. This grating is created by the interference of beams 1 and 2, and, 3 and 4 and characterized by $n_I \exp(i \psi_I)$ (7:520), then equation (205) becomes:

$$dA_1/dx = i \omega n_I^* \exp(-i \psi_I) (A_1 |A_2|^2 + A_3^* A_4 A_2) / (2 c \cos \theta_1 I_0) \quad (206)$$

Similarly, for terms synchronous with $\exp[i(k_1 \cos \theta_1 x + \omega t)]$:

$$dA_3^*/dx = i \omega n_I^* \exp(-i \psi_I) (A_1 A_2^* + A_3^* A_4) A_4^* / (2 c I_0 \cos \theta_1) \quad (207)$$

with $\exp[-i(k_2 \cos \theta_2 x + \omega t)]$:

$$dA_4/dx = -i \omega n_I^* \exp(-i \psi_I) (A_1 A_2^* + A_3^* A_4) A_3 / (2 c I_0 \cos \theta_2) \quad (208)$$

and with $\exp[-i(k_2 \cos \theta_2 x - \omega t)]$:

$$dA_2^*/dx = -i \omega n_I^* \exp(-i \psi_I) (A_1 A_2^* + A_3^* A_4) A_1^* / (2 c I_0 \cos \theta_2) \quad (209)$$

If in Figure 10, $\theta_1 = \theta_2 = \theta$ so the grating vector is in the \hat{z} direction only, then in equations (206), (207), (208) and (209):

$$\gamma = -i \omega n_I^* \exp(-i \omega_I) / (2 c \cos \theta) \quad (210)$$

To further simplify the expressions toward achieving a solution, the following constants are defined (18:313):

$$\begin{aligned} c &= A_1 A_3 + A_2 A_4 \\ d_1 &= |A_1|^2 + |A_2|^2 \\ d_2 &= |A_3|^2 + |A_4|^2 \end{aligned} \quad (211)$$

The coupled equations (206), (207), (208) and (209) become (18:314):

$$\begin{aligned} dA_1/dx &= (-\gamma/I_0)[A_1 d_1 - A_1(I_1 + I_3) + A_2^* c] \\ dA_3^*/dx &= (-\gamma/I_0)[A_1 c^* - A_3^*(I_1 + I_3) + A_3^* d_2] \\ dA_4/dx &= (\gamma/I_0)[A_4 d_2 - A_4(I_4 + I_2) + A_2^* c] \\ dA_2^*/dx &= (\gamma/I_0)[A_4 c^* - A_2^*(I_4 + I_2) + A_2^* d_1] \end{aligned} \quad (212)$$

Equations (212) may be rearranged as (18:314):

$$\begin{aligned} (d/dx)(A_1/A_3^*) &= (-A_1/A_3^{*2}) dA_3^*/dx + (1/A_3^*) dA_1/dx \\ &= (-\gamma/I_0)[c + (d_1 - d_2)(A_1/A_3^*) - c^* (A_1/A_3^*)^2] \\ (d/dx)(A_4/A_2^*) &= (-A_4/A_2^{*2}) dA_2^*/dx + (1/A_2^*) dA_4/dx \\ &= (\gamma/I_0)[c + (d_2 - d_1)(A_4/A_2^*) - c^* (A_4/A_2^*)^2] \end{aligned} \quad (213)$$

By partial fraction expansion, the solutions to equations (213) are (18:314):

$$\begin{aligned}
A_1/A_3^* &= [\Delta + (\Delta^2 + 4|c|^2)^{1/2}] J \exp(-\mu x) \\
&\quad + [\Delta + (\Delta^2 + 4|c|^2)^{1/2}] (1/J) \exp(\mu x) \\
&\quad - 2c^* [J \exp(-\mu x) - (1/J) \exp(\mu x)]^{-1} \\
A_4/A_2^* &= [\Delta + (\Delta^2 + 4|c|^2)^{1/2}] K \exp(-\mu x) \\
&\quad + [-\Delta + (\Delta^2 + 4|c|^2)^{1/2}] (1/K) \exp(\mu x) \\
&\quad - 2c^* [K \exp(-\mu x) - (1/K) \exp(\mu x)]^{-1} \quad (214)
\end{aligned}$$

where

$$\Delta = d_2 - d_1$$

J, K = Constants of integration

$$\mu = \gamma(\Delta^2 + 4|c|^2)^{1/2}/(2 I_0 c^*)$$

The phase conjugate reflectivity, R, can now be solved using equations (211) and (214) with boundary citations: $I_1(0)$; $I_2(0)$; $I_3(1)$; and $I_4(1) = 0$ where l is the crystal length in x. From these equations:

$$\Delta = I_3(l) - I_1(0) - I_2(0) \quad (215)$$

and Cronin-Golomb gives the solution for phase conjugate reflectivity as (18:314):

$$\begin{aligned}
R &= I_4(0)/I_2(0) \\
&= \frac{I_3(1) - I_3(l) A_1(l)/A_3^*(l) + I_2(0) A_4(0)/A_2^*(0)}{I_2(0) A_1(0)/A_3^*(0)} \\
&= 4|c|^2 |T|^2 / |\Delta T + (\Delta^2 + 4|c|^2)^{1/2}|^2 \quad (216)
\end{aligned}$$

where

$$T = \tanh \mu l$$

and $|c|^2$ is found by the equation:

$$\begin{aligned}
[|c|^2 - I_1(0) I_3(1)] |\Delta T + (\Delta^2 + 4|c|^2)^{1/2}|^2 + 4|c|^2 |T|^2 I_2(0) I_3(1) \\
+ 2|c|^2 I_2(0) (\Delta^2 + 4|c|^2)^{1/2} (T + T^*) = 0 \quad (217)
\end{aligned}$$

The functional relationships of this form of the phase conjugate reflectivity have been buried in the derivation and are not nearly as

obvious as in Feinberg's form.

Summary

Diffraction efficiency and phase conjugate reflectivity are the last two figures of merit for the photorefractive effect as applied to optical phase conjugation. Two theoretical expressions were derived for each of these figures of merit.

The first expressions for each (equations (194) for diffraction efficiency and (197) for phase conjugate reflectivity) were an extension of Feinberg's Hopping Model. They showed that both these figures of merit were proportional to the square of the magnitude of the electro-static field set up in the crystal. (Thus, proportional to the square of the magnitude of the index grating, as well.)

The second expressions for each (equations (201) for diffraction efficiency and (216) for phase conjugate reflectivity) assumed an index grating existed in the crystal and solved for the light diffracted off it. The diffraction efficiency was shown in equation (201) to be proportional to the exponential of the magnitude of the diffusion field, only. The phase conjugate reflectivity expression (216) is very complicated and functional dependencies are not easily obtained.

Although all three figures of merit, two beam coupling, diffraction efficiency and phase conjugate reflectivity, are considered important to optical phase conjugation, the optimum crystallographic orientation of for each separate figure may be different in a given crystal. A specific example of this is addressed in the applications chapter.

VII. Applications of the Theory

The previous two chapters developed theoretical expressions for steady state two beam coupling, diffraction efficiency and phase conjugate reflectivity since these are the figures of merit which will quantify the photorefractive effect as it applies to optical phase conjugation. In this chapter, this theory is applied to experimentally observed phenomena with the theoretical predictions compared to experimental results to determine the accuracy of the models.

Three main types of applications will be considered. The first compares the functional relationships of the figures of merit to experimental data. The second investigates the directionality of energy transfer in steady state two beam coupling. It has been determined experimentally which writing beam will gain intensity for a specific crystal orientation. The two beam coupling expressions developed here will be applied to predict this direction. Finally, the theoretical expressions will be applied to specific crystallographic orientations to determine which orientations are optimum for two beam coupling and diffraction efficiency.

Relationships Between Feinberg's $\Delta I_1/I_1$, n and R , and E_0 , Δ , k and ρW_0

The expressions Feinberg developed for intensity gain in steady state two beam coupling, $\Delta I_1/I_1$ (equation (162)), diffraction efficiency, n (equation (194)), and phase conjugate reflectivity, R (equation (197)), are all functions of several variables. The functional behavior of these expressions with respect to some of these variables is investigated in this section.

$\Delta I_1/I_1$ as a Function of the External E-field, E_0

From equation (162), the intensity gain in two beam coupling can be written in the form:

$$\Delta I_1/I_1 \propto (1 + \alpha^2 + f^2)/[(1 + \alpha^2)^2 + (\alpha f)^2] \quad (217)$$

where $f = E_0/f_0$. Setting the first derivative of equation (217) equal to zero, $d(\Delta I_1/I_1)/df = 0$, yields an inflection point at $f = 0$.

Evaluating the second derivative of equation (217) at $f = 0$, $d^2(\Delta I_1/I_1)/df^2|_{f=0}$, yields a positive result. Therefore, the point $f = 0$ ($E_0 = 0$) is a minimum of the intensity gain equation.

In his paper, Gunter, uses an expression for two beam coupling intensity gain, γ_0 (9:252), which can be defined as:

$$\gamma_0 = 1 + \Delta I_1/I_1 \quad (218)$$

Figure 12 plots experimental points of γ_0 versus E_0 for BSO crystals and shows minima at $E_0 = 0$.

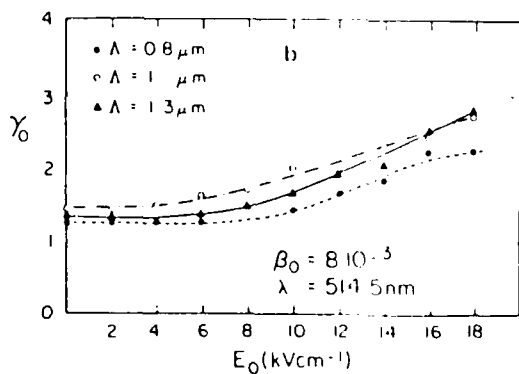


Figure 12. Electric field dependence of two beam coupling intensity gain for BSO (9:263)

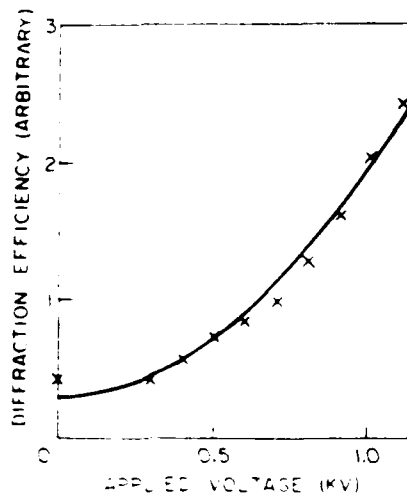
η and R as a Function of the External E-field, E_0

From equations (194) and (197), both the diffraction efficiency and the phase conjugate reflectivity can be written in the form:

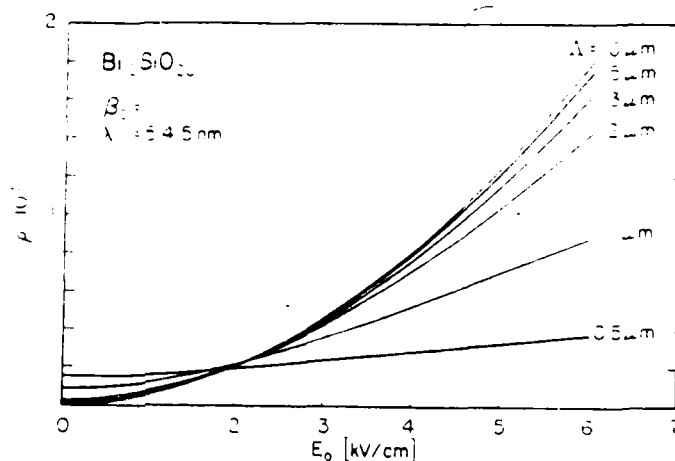
$$\eta, R \propto (\alpha^2 + f^2)/[(\alpha^2 + 1)^2 + (\alpha f)^2] \quad (219)$$

The minimum of equation (219) with respect to f is at $f = 0$. Therefore,

$E_0 = 0$ is a minimum of both the diffraction efficiency and phase conjugate reflectivity. Figure 13-a is an experimental plot by Feinberg of η versus E_0 for BaTiO_3 and shows a minimum at $E_0 = 0$. Gunter's symbol for phase conjugate reflectivity is ρ (9:257). Figure 13-b has experimental plots by Gunter for ρ versus E_0 in BSO crystals. They have minima at $E_0 = 0$.



a.



b.

Figure 13. a.) Diffraction efficiency as a function of applied voltage in BaTiO_3 (5:1304)
b.) Phase conjugate reflectivity versus applied field for BSO (9:281)

$\eta^{1/2}$ as a Function of External E-field, E_0

Because Gunter's plot for diffraction efficiency versus external field in BSO appears as $\eta^{1/2}$ versus E_0 , equation (194) is now written in the form:

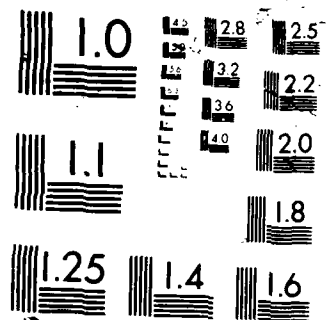
$$\eta^{1/2} \propto (\alpha^2 + f^2)^{1/2} / [(\alpha^2 + 1)^2 + (\alpha f)^2]^{1/2}$$

The minimum of equation (220) with respect to f is at $f = 0$. Thus, $E_0 = 0$ is a minimum of the square-root of diffraction efficiency.

Figure 14 is an experimental plot by Gunter of $\eta^{1/2}$ versus E_0 for BSO and has minima at $E_0 = 0$.

AD-A188 856 NONLINEAR OPTICAL PRINCIPLES AND THE PHOTOREFRACTIVE 2/2
EFFECT APPLIED TO OP. (U) AIR FORCE INST OF TECH
WRIGHT-PATTERSON AFB OH SCHOOL OF ENGI.. M A MARCINIAK
UNCLASSIFIED DEC 87 AFII/GEO/ENP/87D-3 F/G 9/3 NL

END
DATE
TIME
8-
T



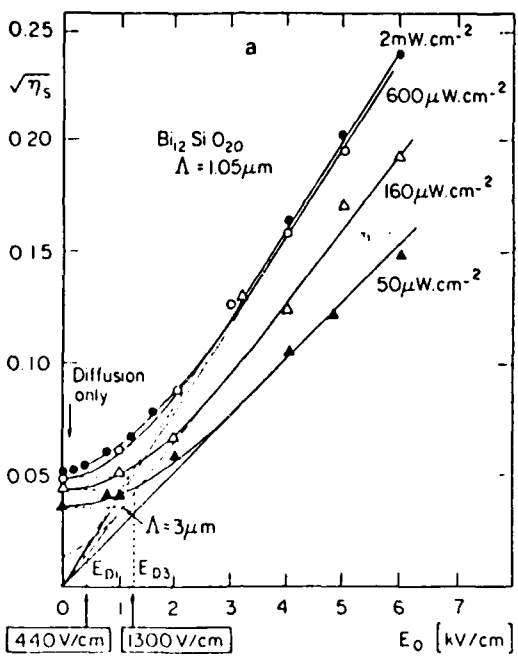


Figure 14. Electric field dependence of diffraction efficiency, $\eta^{1/2}$, for BSO (9:263)

η and R as a Function of Fringe Spacing, Λ

From equations (194) and (197), both the diffraction efficiency and phase conjugate reflectivity can be written as:

$$\begin{aligned}\eta, R &\propto (\alpha^2 + f^2)/[(\alpha^2 + 1)^2 + (\alpha f)^2] \\ &\propto (f^2 \Lambda^4 + A \Lambda^2)/[\Lambda^4 + A(2 + f^2) \Lambda^2 + A^2]\end{aligned}\quad (221)$$

where

$$\alpha = 2\pi/k_0 \Lambda$$

$$A = (2\pi/k_0)^2$$

A minimum of equation (221) with respect to Λ occurs at $\Lambda = 0$. If there is no applied field ($E_0 = 0$, $f = 0$) in equation (221), an inflection point occurs at $\Lambda = 2\pi/k_0$ which is a minimum if $A = 4\pi^2 \epsilon_0 k_B T / \rho W_0 q^2 < 1/5^{1/2}$ and a maximum if $4\pi^2 \epsilon_0 k_B T / \rho W_0 q^2 > 1/5^{1/2}$.

Figure 15-a plots experimental points of η versus Λ and Figure 15-b,

ρ versus Λ , for BSO. (Both graphs by Gunter.) Both graphs have minima at $\Lambda = 0$. In the cases where $E_0 = 0$, they have a single maximum before tailing off asymptotically toward zero.

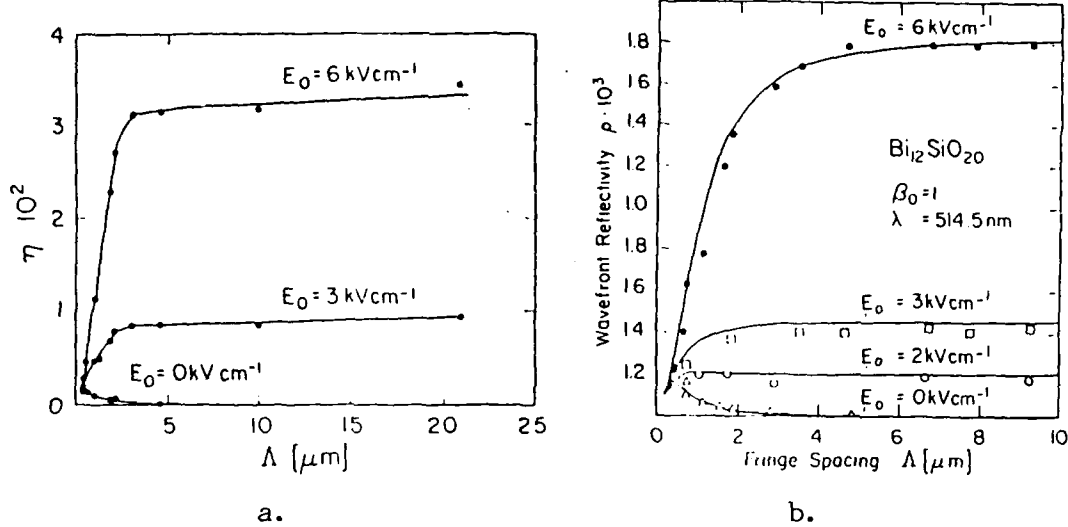


Figure 15. a.) Fringe spacing dependence of diffraction efficiency for BSO (9:262)
 b.) Phase conjugate reflectivity versus fringe spacing for BSO. Solid lines: theoretical. Points: experimental (9:280)

$\Delta I_1/I_1$ as a Function of Grating Vector, k

From equation (162), the intensity gain for two beam coupling may be written in the form:

$$\Delta I_1/I_1 \propto \alpha^2(1 + \alpha^2 + f^2)/[(1 + \alpha^2)^2 + (\alpha f)^2] \quad (222)$$

where $\alpha = k/k_0$. Equation (222) has a minimum with respect to α at $\alpha = 0$ ($k = 0$).

Figure 16 is Feinberg's theoretical plot of equation (162) and experiment plot of $\Delta I_1/I_1$ versus k for BaTiO_3 . It should have minima at $k = 0$.

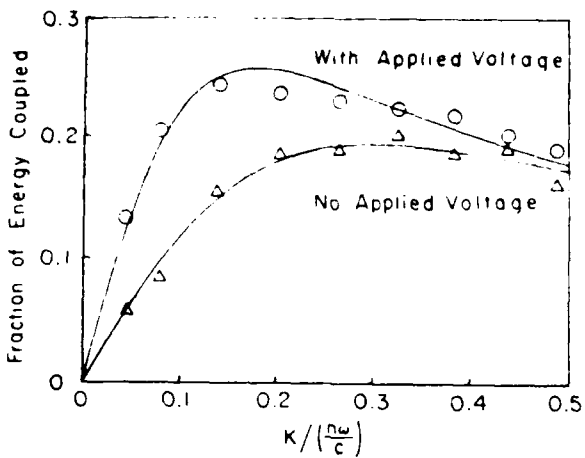


Figure 16. Intensity gain for two beam coupling in BaTiO₃ as a function of grating wave vector, \mathbf{k} . Triangles and circles are experimental data, solid lines are theoretical fit to equation (162) (5:1302)

η as a Function of Grating Vector, \mathbf{k}

From equation (194), the diffraction efficiency can be written in the form:

$$\eta \propto (\alpha^2 + f^2)/[(\alpha^2 + 1)^2 + (\alpha f)^2] \quad (223)$$

where $\alpha = k/k_0$. Equation (223) has an inflection point with respect to α at $\alpha = 0$ ($k = 0$). This point is a maximum if

$$|f| = |E_0 q/(k_0 k_B T)| > .64 \text{ and a minimum if } |E_0 q/(k_0 k_B T)| < .64.$$

If there is no applied field in equation (223) ($E_0 = 0$, $f = 0$), it has a maximum at $\alpha = 1$ ($k = [\rho W_0 q^2 / (\epsilon \epsilon_0 k_B T)]^{1/2}$).

Figure 17 is a theoretical plot of equation (194) for BaTiO₃ and contains the inflection points mentioned here.

If the experimental geometries in Figures (7) and (8) are considered, the grating vector, \mathbf{k} , may be written as:

$$\mathbf{k} = (4\pi n v/c) \sin \theta \quad (224)$$

if the angles of incidence are equal. ($\theta_1 = \theta_2 = \theta$ in Figure (7), $\theta_{+1} = \theta_{-1} = \theta$ in Figure (8)). The maximum of the diffraction efficiency curve in Figure 17 at $k = k_0$ ($\alpha = 1$), then would imply

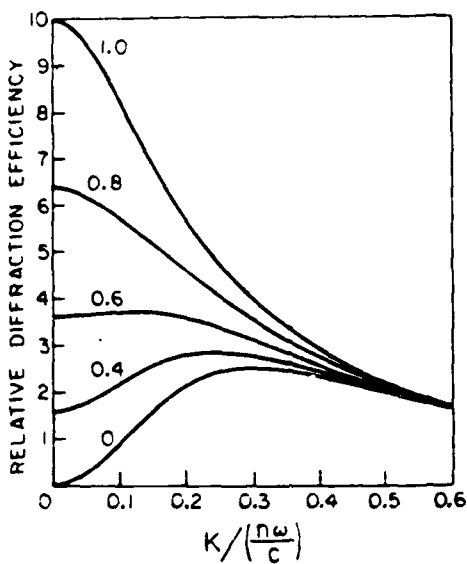


Figure 17. Theoretical plot of diffraction efficiency, η , as a function of grating wave vector, k (5:1304)

maximum diffraction efficiency at:

$$\sin \theta = [\rho W_0 / (\epsilon \epsilon_0 k_B T)]^{1/2} [q c / (4\pi n v)] \quad (225)$$

Feinberg states in his article:

In general, the charge density available for migration will depend on the optical frequency of the writing beams. (4:427)

From equation (225), if the angle of maximum efficiency is constant for various optical frequencies then the density of filled trap sites, ρW_0 , is proportional to the square of the optical frequency, v . Feinberg continues:

However, the following rather strange fact is noted: for many materials, studied in different laboratories, the diffraction efficiency always seems to peak for the same full crossing angle of about 40° in air. According to the model used here, this implies a similar number density of charges (10^{16} cm^{-3}) for all these quite different materials, a rather suspect coincidence. (4:427)

The following subsection investigates diffraction efficiency as a function of charge density.

η as a Function of Charge Density, ρW_0

From equation (194) for diffraction efficiency, η as a function of charge density can be written as:

$$\eta \propto \frac{x^2}{(A + x)^2 + B^2} \quad (226)$$

where

x = Charge density

$$= \rho W_0$$

$$A = k^2 \epsilon \epsilon_0 k_B T / q^2$$

$$B = k \Delta \Phi_0 \epsilon \epsilon_0 / (lq)$$

Equation (226) has a minimum at $x = 0$ and a maximum at $x = -(A^2 + B^2)/A$.

It is reasonable to have minimum diffraction efficiency when there is no charge density. The maximum occurs at:

$$\rho W_0 = [-\epsilon \epsilon_0 / (k_B T)] [(k_l k_B T + i q \Delta \Phi_0) / (q l)]^2 \quad (227)$$

$R^{1/2}$ as a Function of Spatial Frequency, $1/\Lambda$

Because Gunter's plot for phase conjugate reflectivity versus spatial frequency in BSO is in the form, $\rho^{1/2}$ versus $1/\Lambda$, equation (197) will be written in the form:

$$R^{1/2} \propto (\alpha^2 + f^2)^{1/2} / [(\alpha^2 + 1)^2 + (\alpha f)^2]^{1/2} \quad (228)$$

where $\alpha = 2\pi / (k_0 \Lambda)$. Equation (228) has a minimum with respect to α at $\alpha = 0$ ($1/\Lambda = 0$). If there is no applied field in equation (228) ($E_0 = 0$, $f = 0$), it has a maximum at $\alpha = 1$ ($1/\Lambda = [1/(2\pi)][\rho W_0 q^2 / (\epsilon \epsilon_0 k_B T)]^{1/2}$).

Figure 18 has both minima and maxima at $1/\Lambda = 0$ depending on the applied external field, E_0 .

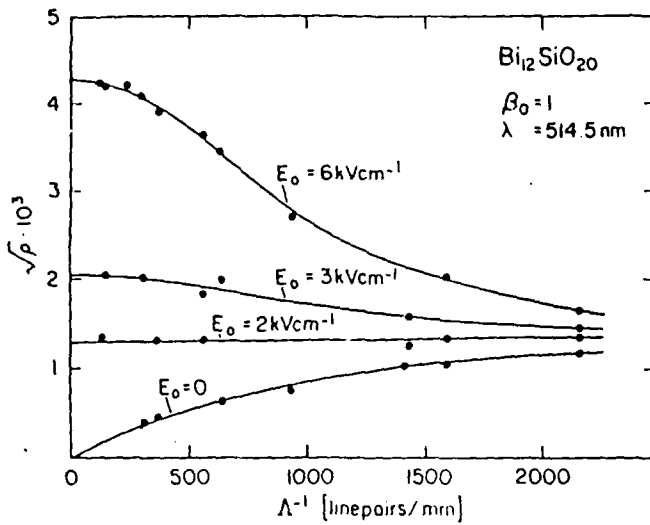


Figure 18. (Square root of) phase conjugate reflectivity as a function of spatial frequency, $1/\Lambda$ (9:280)

Can the Direction of Energy Transfer in Steady State Two-Beam Coupling be Predicted?

The direction of the energy transfer in the steady state two-beam coupling described in Chapter V has been observed to be dependent on the orientation of the crystal's c-axis relative to the incident beams (4:431). Figure 19 shows the direction of energy transfer in BaTiO_3 . The theory developed in Chapter V will be applied to two crystals, BaTiO_3 and BSO, to determine if coupling can be predicted.

Feinberg's Model

The fractional intensity gain expression developed by Feinberg in Chapter V (equation (162)) took the form:

$$\Delta I_1(x)/I_1(x) \propto (e_1^* \cdot \epsilon_\omega^* \cdot R \cdot k \cdot \epsilon_\omega \cdot \hat{e}_2) \quad (229)$$

The contracted electro-optic coefficient tensor, R , is referenced to the primary coordinate system (PCS) of the crystal so k must be referenced to the same coordinate system in order to perform the dot product.

Initially, since k is defined from the interference expression (equation (98)), it appears k can be defined as either $\pm k$ without any

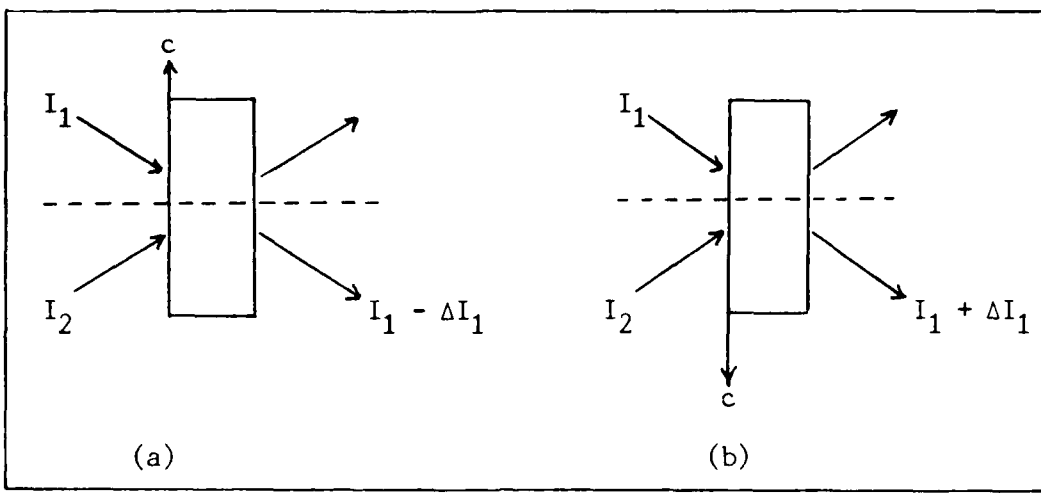


Figure 19. Directional two-beam coupling as observed in BaTiO_3 (a photorefractive crystal with positive charge carriers.) (3:432)

consequences ($\mathbf{k} = \mathbf{k}_1 - \mathbf{k}_2$ or $\mathbf{k} = \mathbf{k}_2 - \mathbf{k}_1$). However, from the defined space-charge field expression (equation (115)), a unique direction is given to \mathbf{k} and that is in the same direction as a positive phase shift, ψ . The space-charge field may be written in the form:

$$\mathbf{E}_{sc}(\mathbf{x}) = \hat{\mathbf{k}} [m \rho W_0 q / (\epsilon \epsilon_0 k)] |1/[1 + \rho W_0 q^2 / (\epsilon \epsilon_0 k_B T k^2)]| \cos(\mathbf{k} \cdot \mathbf{x} + \pi/2) \quad (230)$$

if there is no applied field ($E_0 = 0$) so the phase shift is $\pi/2$ ($\psi = \pi/2$). In this form, it can be seen that the direction of the grating shift is determined by the sign of the carrier, q .

Mathematically, the phase shift is $\pi/2$ for both positive and negative carriers. However, a negative carrier will change the sign of the magnitude of \mathbf{E}_{sc} (or give it a π phase charge) and give it the appearance of a $-\pi/2$ phase shift. Figure 20 exemplifies this.

From Figure 20, it is seen that \mathbf{k} is always in the direction opposite that of the positive E-field. Since \mathbf{R} and \mathbf{k} are the only terms in the gain expression (equations (163) and (164)) which contain directionality, when the space-charge field is reference to the same

coordinate system as R , $R \cdot k$ is always a negative expression and $\Delta I_1/I_1$ (equation (162)) positive.

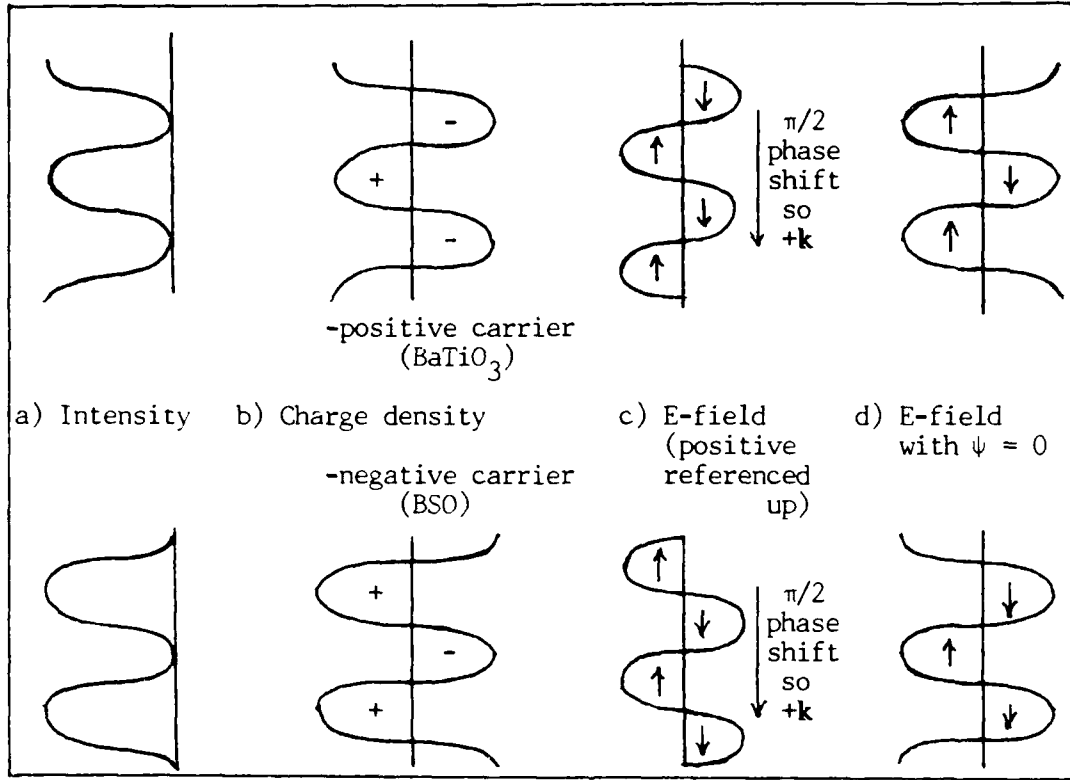


Figure 20. Illustration of the photorefractive effect for positive and negative carriers under diffusion only ($E_0 = 0$) showing direction of phase shift.

Feinberg's model for steady state two-beam coupling may define the magnitude of the coupling, but it does not describe the directionality.

Application of Two Beam Coupling Assuming a Sinusoidal Index Grating Exists

The expressions for the intensities, I_1 and I_2 developed by White in Chapter V, equations (175), can be written in the forms:

$$I_1(r) \propto 1/[I_1(0) + I_2(0) \exp(-2\Gamma r)]$$

$$I_2(r) \propto 1/[I_1(0) \exp(2\Gamma r) + I_2(0)] \quad (231)$$

From these forms it can be seen that I_1 is directly related to Γ and I_2 is inversely related to Γ .

Γ is proportional to n_I (after equation (172)), the modulated index

(after equation (165)). For a space-charge field in z only, n_I is inversely proportional to that field, E_z , for all polarizations. Therefore, I_1 is inversely related to E_z and I_2 is directly related to E_z .

In Figure 19, positive E_z is taken to be in the direction of the c-axis for both configurations (a) and (b). However, the orientation of E_z to the propagation vectors \mathbf{k}_1 and \mathbf{k}_2 is the opposite in (a) and (b). Since configuration (a) is used in the development of Chapter V, a direct substitution for BaTiO_3 from Appendix A into equations (231) shows that I_1 should be decreasing as it propagates and I_2 increasing.

In Figure 19-b, the effects of flipping the crystal is that E_z now looks like $-E_z$ in the Appendix A expressions. Substitution into equations (231) shows that I_1 should increase as it propagates while I_2 decreases.

The same argument can be applied to the BSO expressions in Appendix A though not as simply since the PCS is rotated and the index ellipsoid is expanded along one new axis but contracted along the other.

Polarizations must be tracked to determine the index a beam encounters but the direction of coupling is still attainable.

Summary

The expression for steady state two beam coupling developed from Feinberg's hopping model gives the magnitude of the gain or loss of intensity by the beams but it does not indicate which beam is gaining or losing. The direction of the coupling can, however, be predicted from a development in which an index grating is assumed to exist and the solution for propagation through this grating is found through the wave equation. By using this solution and the proper index ellipsoid relationship, the direction of coupling as well as its magnitude can be

found.

Why is There Better Two Beam Coupling and Diffraction Efficiency Crystallographic Orientations in BSO?

It has been observed that there are different crystallographic orientations of Bismuth Silicate (BSO) which are optimum for energy transfer in two beam coupling and diffraction efficiency for vertically polarized incident light. Figure 21 presents these optimum orientations. For maximum beam coupling, the space charge field is formed perpendicular to the 001 face, while for maximum diffraction efficiency, it is perpendicular to the 110 face (21:131-133).

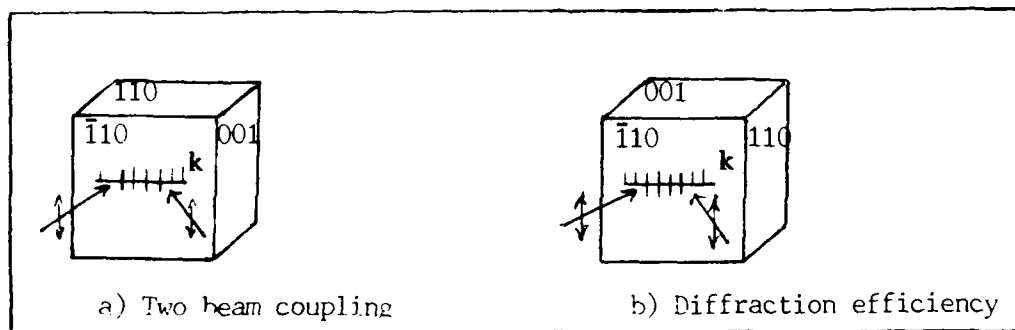


Figure 21. Optimum crystallographic orientations in BSO (19:132).

The theory developed in Chapters V and VI will be applied to BSO to determine if these optimum orientations can be predicted.

Feinberg's Model

From crystallography, the primary coordinate system (PCS) of BSO with no applied electric field is shown in Figure 22 (19:30-40).

From equations (162) and (164), the intensity gain for one of the beams in steady state two beam coupling in BSO can be written in the form:

$$\Delta I_1/I_1 \propto [(k_z e_{2y} + k_y e_{2z})^2 + (k_z e_{2x} + k_x e_{2z})^2 + (k_y e_{2x} + k_x e_{2y})^2] (e_{1x} e_{2x} + e_{1y} e_{2y} + e_{1z} e_{2z}) \quad (232)$$

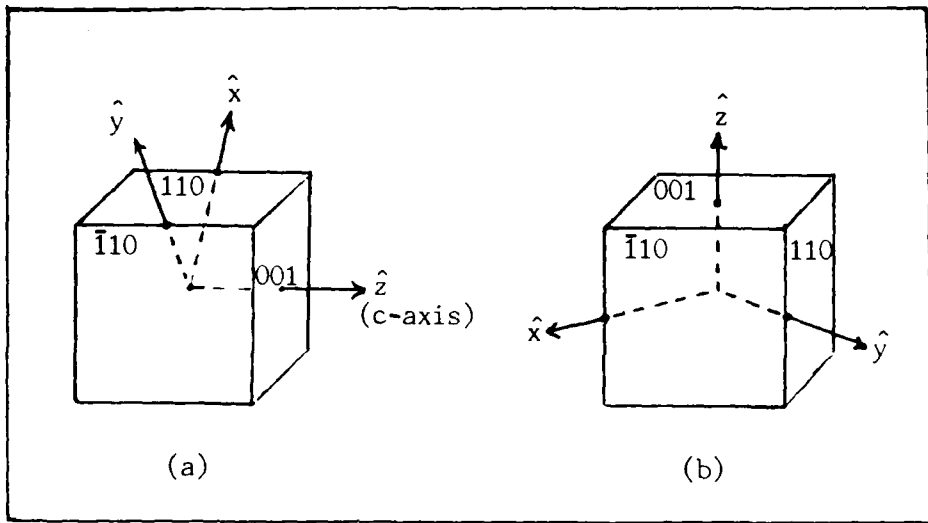


Figure 22. PCS in BSO with no applied field.

From equations (194) and (199), the diffraction efficiency in BSO can be written in the form:

$$\eta \propto (k_z e_{3y} + k_y e_{3z})^2 + (k_z e_{3x} + k_x e_{3z})^2 + (k_y e_{3x} + k_x e_{3y})^2 \quad (233)$$

In the optimum two beam coupling orientation (Figures 21-a and 22-a), the grating direction vector, \mathbf{k} , is in the \hat{z} direction only. Vertically polarized light with unit polarization vectors, \hat{e}_1 , \hat{e}_2 and \hat{e}_3 has only \hat{x} and \hat{y} components which are $1/2^{1/2}$ each. Equations (232) and (233), for this orientation become:

$$\frac{\Delta I_1}{I_1} \propto k \quad \eta \propto k^2 \quad (234)$$

In the optimum diffraction efficiency orientation (Figures 21-b and 22-b), the grating vector, \mathbf{k} , has $k_x \hat{x}$ and $k_y \hat{y}$ components where k_x and k_y are $k/2^{1/2}$. Vertically polarized light has $e_z \hat{z}$ components only, so equations (232) and (233) become the same as equations (234).

The relationships for two beam coupling and diffraction efficiency from Feinberg's hopping model, then, do not adequately predict optimum crystal orientations for vertical input polarizations.

An Index Ellipsoid Approach

The PCS of BSO without an applied field was shown in Figure 22. The direction of the \mathbf{k} vectors and thus the space charge fields are shown in Figure 21. For Figures 21-a and 22-a, the E-field is applied in the \hat{z} direction only. From Appendix A, the new indices of refraction are:

$$n' = n \pm (1/2) n^3 r_{41} E_{SC} \quad (235)$$

with new PCS resulting from a rotation about the z-axis of -135° (Figure 23-a) (20:132).

In Figures 21-b and 22-b, the space-charge field has \hat{x} and \hat{y} components so the index ellipsoid is:

$$(x^2 + y^2 + z^2)/n^2 + 2r_{41} E_x yz + 2r_{41} E_y xz = 1 \quad (236)$$

in the PCS of the crystal without an applied field. The eigenvalues can be found by solving the determinant:

$$\begin{vmatrix} (1/n^2) - \lambda & 0 & r_{41} E_{SC}/2^{1/2} \\ 0 & (1/n^2) - \lambda & r_{41} E_{SC}/2^{1/2} \\ r_{41} E_{SC}/2^{1/2} & r_{41} E_{SC}/2^{1/2} & (1/n^2) - \lambda \end{vmatrix} = 0 \quad (237)$$

where

λ = Eigenvalue

$$= 1/n'^2$$

n' = New indices of refraction

With this applied field, the crystal becomes biaxial with indices of refraction on the axes of the new PCS being n and $n \pm (1/2) n^3 r_{41} E_{SC}$.

The axes rotation between the old and new PCS is found by solving:

$$\begin{vmatrix} (1/n^2) - \lambda_i & 0 & r_{41} E_{SC}/2^{1/2} \\ 0 & (1/n^2) - \lambda_i & r_{41} E_{SC}/2^{1/2} \\ r_{41} E_{SC}/2^{1/2} & r_{41} E_{SC}/2^{1/2} & (1/n^2) - \lambda_i \end{vmatrix} \begin{bmatrix} a_{11} \\ a_{12} \\ a_{13} \end{bmatrix} = 0 \quad (238)$$

where

λ_i = Eigenvalues solved for in equation (237)

a_{ij} = Elements of rotation matrix

$$= \cos \theta_{ij}$$

θ_{ij} = Angle of rotation between old i^{th} axis and new j^{th} axis

The axes rotation is shown in Figure 23-b (19:132)

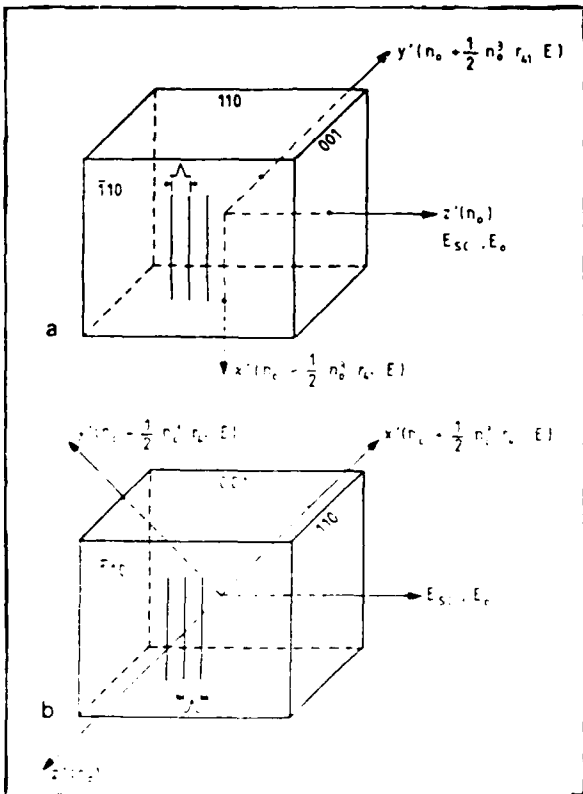


Figure 23. New primary coordinate system and indices of refraction in BSO with applied space-charge fields (a) $E_{SC} = |E_{SC}|^2$

$$(b) E_{SC} = (|E_{SC}|/2^{1/2})\hat{x} + (|E_{SC}|/2^{1/2})\hat{y} \quad (19:132)$$

For diffraction efficiency which is dependent on the magnitude of the index grating, in the Figure 23-a orientation, vertically polarized light is polarized along \hat{x}' only and sees index, $n - (1/2) n^3 r_{41} E_{SC}$. In the Figure 23-b orientation, vertically polarized light has both \hat{e}_x' and \hat{e}_y' components which see $n + (1/2) n^3 r_{41} E_{SC}$ and $n - (1/2) n^3 r_{41} E_{SC}$, respectively. At points where the maxima or minima of each component coincide, the summation of the components gives

a modulated index of $\pm n^3 r_{41} E_{SC}$ (19:132).

Therefore, the Figure 23-b orientation can be predicted to be the better of the two for diffraction efficiency.

For two beam coupling, the Figure 23-a orientation is precisely the configuration assumed for the Chapter V derivation so significant energy transfer can be assumed. In the Figure 23-b configuration, however, since the polarization components are split between two indices, one of which has a $+n_I$ term (as described in equation (165)) and the other $-n_I$, one component would tend to gain energy (as in equations (175)) while the other would lose energy. Each component, then, tends to compensate for the other and energy transfer is not efficient (19:132).

Therefore, the Figure 23-b orientation can be predicted to be the better for energy transfer in two beam coupling of the two.

AFIT Crystal

Another pair of crystal orientations which has one orientation better for two beam coupling and another for diffraction efficiency can be analyzed by considering beams incident on the 110 face. The incident light is vertically polarized and forms a \mathbf{k} vector oriented as shown in Figure 24.

In the Figure 24-a orientation, the space charge field is in the \hat{z} direction so the analysis is identical to the Figures 21-a, 22-a, and 23-a developments in the preceding subsections. The new PCS and appropriate indices of refraction are shown in Figure 25-a.

For the Figure 25-b orientation, the space charge field has both \hat{x} and \hat{y} components, however, these components are of opposite sign. The index ellipsoid in the PCS of the crystal without an applied field is in the form:

$$(x^2 + y^2 + z^2)/n^2 + 2r_{41} E_{SC}/2^{1/2} xz - 2r_{41} E_{SC}/2^{1/2} yz = 1 \quad (239)$$

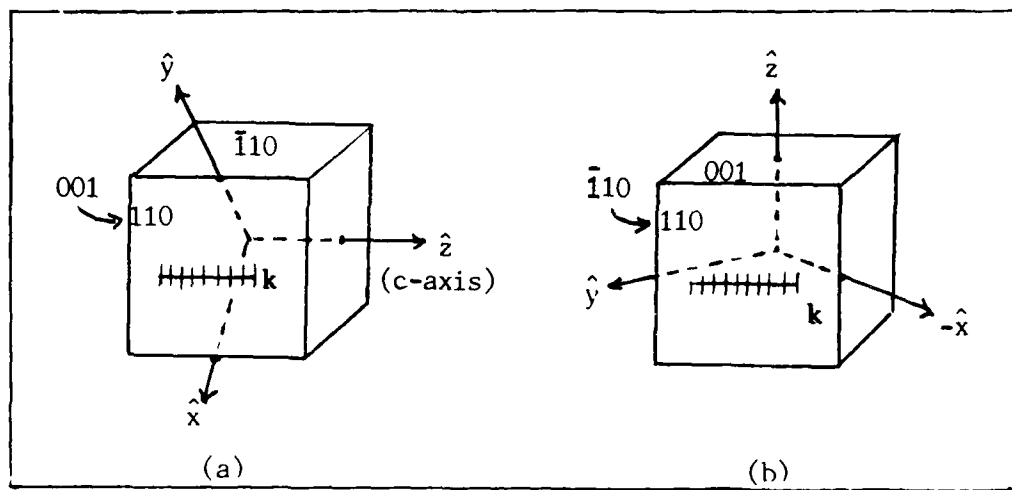


Figure 24. Potential incident light and grating vector orientations when only the 110 face of BSO is available for illumination.

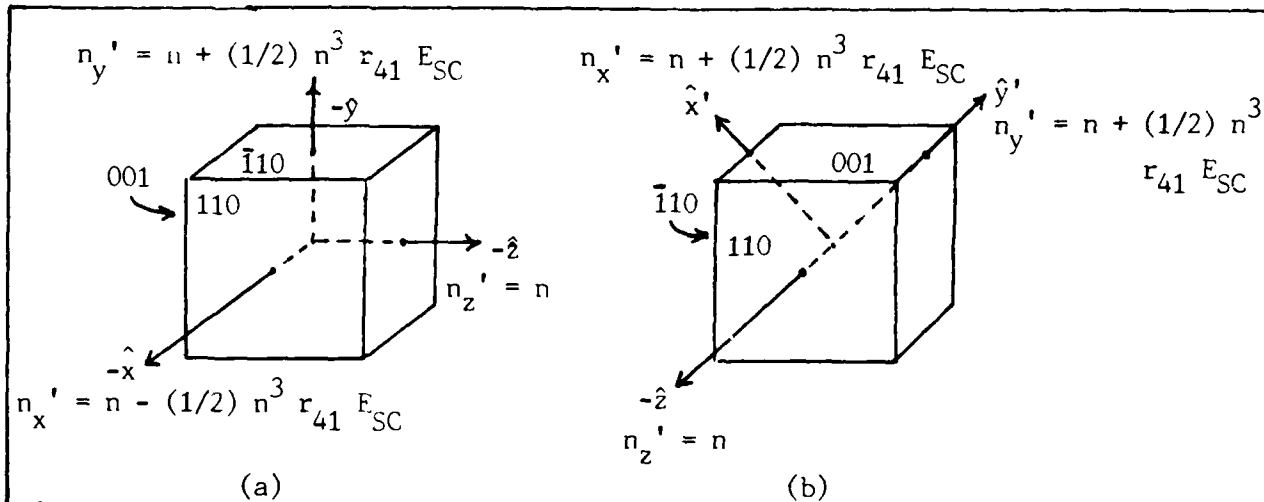


Figure 25. New PCS and appropriate indices of refraction for a BSO crystal illuminated on the 110 face such that the applied space-charge field is (a) $E_{SC} = E_{SC} \hat{z}$ and
(b) $E_{SC} = (-|E_{SC}|/2^{1/2})\hat{x} + (|E_{SC}|/2^{1/2})\hat{y}$.

The new indices of refraction and angles of rotation can be found by a derivation similar to that in the previous subsection. The new indices and PCS are shown in Figure 25-b.

By similar analysis as in the previous subsection, optically

polarized light incident on Figure 24-a orientation sees index $n + (1/2) n^3 r_{41} E_{SC}$ and should provide significant energy transfer. The same light incident on Figure 24-b orientation has components which see $n \pm (1/2)n^3 r_{41} E_{SC}$. At points where the maxima and minima of these components coincide, therefore, the total modulated index is $\pm n^3 r_{41} E_{SC}$ and this configuration should produce better diffraction efficiency. However, because of the change in sign of the modulated indices, the energy transfer in two beam coupling should be minimal.

Summary

Just as in the preceding section, Feinberg's hopping model appears to be fine for predicting the space-charge field and phase shift between the index grating and interference fringes but the expressions he develops from the model for diffraction efficiency and steady state two beam coupling do not adequately predict these effects for various crystal orientations. The directionality of these effects, however, can be accurately predicted by using an index ellipsoid approach.

Summary

Three applications of the three figures of merit, two beam coupling, diffraction efficiency and phase conjugate reflectivity, were performed in this chapter. The first application compared the functional relationships of the figures of merit developed by Feinberg to experimental data. These comparisons showed Feinberg's expressions to adequately predict the functional relationships of empirical data.

The second application was to predict the direction of energy transfer in two beam coupling. Feinberg's expressions proved inadequate in this respect. However, the expressions obtained in Chapter V by assuming an index grating existed in the medium did accurately predict the experimentally observed directionality.

The final application was to determine why one crystallographic orientation of BSO was better for two beam coupling while another was better for diffraction efficiency. Again, Feinberg's expressions could not predict this difference. This time, however, an index ellipsoid approach was used and the experimental observations were accurately predicted.

VIII. Conclusions and Recommendations

Conclusions

Optical phase conjugation is a nonlinear optical process which, from a set of incident light beams, produces a beam which acts as the time reversal of one of the incident beams. This process has application potential because phase aberrations added to the incident wavefront as it propagates through some medium would then be removed from the time reversed wavefront propagating through that same medium (provided the medium remained unchanged).

The first type of optical phase conjugation was by degenerate four wave mixing. Three electro-magnetic waves all of the same frequency, are incident on a nonlinear material oriented properly. They cause the polarization of the medium in both the linear and the nonlinear orders. The third order nonlinear polarization generates a new E-M wave whose amplitude is given through Maxwell's wave equation. By the conservation of energy and momentum, this wave must be of the same frequency as the incident light and counterpropagating to the probe if the two pump beams are counterpropagating in order for it to attain significant energy.

Since it is the electric fields of the incident light which drive the medium into nonlinearity and large E-fields are required to do this, high intensity incident light is required to produce optical phase conjugation by degenerate four wave mixing. A technique for producing phase conjugation with lower intensity incident light would then be desirable. This technique is through the use of photorefractive crystals.

Photorefractive crystals have various sites in their lattice. When under illumination, charges trapped at these sites are free to move from

site to site and finally be rebound at a location which is not illuminated. When two incident coherent light beams are interfered in a photorefractive crystal, the fringe pattern causes a depletion of charges at the interference maxima and a high concentration of charges at the minima. This separation of charge produces an electro-static field in the crystal which modulates the index of refraction of the crystal by the linear electro-optic (Pockel's) effect.

When a photorefractive crystal is oriented properly, a third light beam which is counter propagating to one of the incident (interfering) beams diffracts off the index grating. The diffracted beam counterpropagates to the other incident (interfering) beam and is the phase conjugate of that beam. Even if low intensity incident light is considered, their interference still produces a fringe pattern which induces an electro-static field. Since it is this induced field (rather than the E-fields of the incident light) which drives the crystal nonlinearity, optical phase conjugation may occur in photorefractive crystals with very low intensity incident light.

Two models of the photorefractive effect are Feinberg's Hopping Model and Kukhtarev's Solid State Model. Feinberg's Model is based on the idea that a charge "hops" from site to site in the crystal and develops the probability of this charge movement. Kukhtarev's model is a more standard development of charge transport. The significance of Kukhtarev's model is that he derives the conditions for which spatially sinusoidal incident light (interference fringes) produces an electro-static field which is also sinusoidal with the same spatial frequency as the fringe pattern.

Both Feinberg and Kukhtarev concluded that, for incident interfering waves with a small modulation index, the electro-static field would be

sinusoidal of the same spatial frequency as the interference pattern but spatially shifted in phase from it.

The spatial phase shift between the interference fringes and the electro-static field is important for two beam coupling, one of the figures of merit for the photorefractive effect as applied to optical phase conjugation. Two beam coupling is the coupling of energy from one of the incident (interfering) beams which writes the index grating to the other as they propagate through this grating they have written.

Two theoretical expressions for two beam coupling were developed. The first is an extension of Feinberg's Hopping Model. The second assumes an index grating exists and solves the wave equation for light propagating through its grating. Although each expression is uniquely developed, they both indicate that if no spatial phase shift exists between the interference fringes and the electro-static field, no beam coupling will occur.

Two other figures of merit for the photorefractive effect as applied to optical phase conjugation are diffraction efficiency and phase conjugate reflectivity. Two theoretical expressions for each of these figures of merit were also developed. Diffraction efficiency is the amount of power diffracted off a grating at the Bragg angle compared to the amount of power in the wave incident on the grating. Phase conjugate reflectivity is the amount of power in the conjugate wave compared to the amount of power in the wave which has been conjugated.

The first expressions for each of these figures of merit were developed from Feinberg's Hopping Model. They showed that these figures were proportional to the square of the magnitude of the electro-static field set up. The second expressions for each assumed an index grating existed and asked for light diffracted off this grating. No clear cut

functional dependencies on the electro-static field could be made on the expressions derived in this way.

When the figures of merit developed by Feinberg were compared to empirical data, they were found to accurately predict the functional dependencies of this data with respect to external electric field applied to the crystal, interference fringe spacing and charge density. However, when Feinberg's expression for two beam coupling was used to predict the direction of the coupling for a particular crystallographic configuration, it proved to be inadequate. Also, when Feinberg's expressions for two beam coupling and diffraction efficiency were used to determine the magnitude of each with respect to various crystallographic orientations of Bismuth Silicate (BSO), they proved to be inaccurate when compared to empirical data.

The conclusion, then, is that the functional dependencies of Feinberg's figures of merit appear to be correct when applied to empirical data. However, if the absolute magnitude of these figures or even relative magnitudes between the different orientations are desired, there are crystallographic orientations for which Feinberg's figures of merit are inaccurate.

By using the expression for two beam coupling developed assuming a sinusoidal index grating existed in the medium, correct predictions for the directionality of the coupling can be made. Predictions for the relative magnitudes of two beam coupling between different crystallographic orientations can also be accurately made using this expression. The intensity gain (or loss) of one beam is a function of the scaled exponential of the magnitude of the index grating while the loss (or gain) of the other is a function of the negative of this exponential. Solutions are made by determining the modulated index with

an index-ellipsoid approach.

The index-ellipsoid approach is also useful in determining the relative diffraction efficiencies between different crystallographic orientations. Feinberg's expression showed the diffraction efficiency to be proportional to the square of the magnitude of the electro-static field (and thus to the square of the magnitude of the modulated refractive index).

Recommendations for Further Research

This thesis is not a complete compilation of all aspects of the photorefractive effect applied to optical phase conjugation. Some questionable areas are listed here.

Experimental Data Versus Theory

Most published papers in optical phase conjugation and other photorefractive phenomena include experimental data points to which the theory is curve fit. Evaluations of the theory derived in this thesis were made compared to this data. Since AFIT can now take photorefractive measurements in house, an attempt should be made at applying the theory to in-house data. Such research should be very insightful in gaining an understanding of the theory.

Self-Pumped Phase Conjugate Mirrors

Since the fundamentals of photorefraction and phase conjugation have been laid out in this thesis, the next logical step seems to be to extend the tutorial to self-pumped phase conjugate mirrors (SPPCMs). SPPCMs greatly broaden the spectrum of PCM applications because they do away with the need for external coherent pump sources. Several papers have been written in the area which are open to interpretation. For a listing of these papers and an overview of self-pumped phase conjugation, refer to Appendix B.

Transient Solutions to the Photorefractive Effect

All the analyses reported in this thesis are steady state solutions. Further research is needed looking into the transient solutions. Because of the nature of the photorefractive effect, it is reasonable to suspect that incident intensity and time might be inversely related in both creating and erasing the diffraction grating. Not only does the theory behind this suspicion require further analysis, but it would be an excellent area in which to make empirical measurements to compare to the theory.

Appendix B presents Feinberg's analysis of photorefractive time decay and some empirical data from other sources.

How Much Does Optical Activity Effect BSO Analyses?

Optical activity is the rotation of the plane of polarization of linearly polarized light as it passes through a medium. The polarization state of light is considered in nearly all the analyses reported in this thesis. Further research is needed to include optical activity in the tracking of polarization as light passes through the crystal and to determine the effect it has on the analyses and derivations, themselves.

Appendix B contains an overview of optical activity.

Can Boundary Conditions be Ignored in Photorefractive Analyses?

In the theory presented in this thesis and in most published papers it appears boundary conditions (i.e. Snell's Law-type diffraction at surfaces) are omitted and assumed to be inconsequential. A superficial analysis of this reveals that in a Figure 9-type geometry, the grating wave vector is given by:

$$\begin{aligned}
\mathbf{k} &= \mathbf{k}_1 - \mathbf{k}_2 \\
&= (2\pi n_1/\lambda) \cos \alpha_1' \cos \theta_1' - 2\pi n_2/\lambda \\
&= [(2\pi n_1/\lambda) \cos \alpha_1' \cos \theta_1' - (2\pi n_2/\lambda) \cos \alpha_2' \cos \theta_2'] \hat{x} \\
&\quad + [(2\pi n_1/\lambda) \cos \alpha_1' \sin \theta_1' - (2\pi n_2/\lambda) \cos \alpha_2' \sin \theta_2'] \hat{y} \\
&\quad - [(2\pi n_1/\lambda) \sin \alpha_1' + (2\pi n_2/\lambda) \sin \theta_2'] \hat{z} \\
&= [(2\pi n_1/\lambda) \cos \alpha_1' \cos \theta_1' - (2\pi n_2/\lambda) \cos \alpha_2' \cos \theta_2'] \hat{x} \\
&\quad + [(2\pi/\lambda) \cos \alpha_1' \sin \theta_1' - (2\pi/\lambda) \cos \alpha_2' \sin \theta_2'] \hat{y} \\
&\quad - (2\pi/\lambda) (\sin \alpha_1' + \sin \alpha_2') \hat{z}
\end{aligned} \tag{240}$$

where

$\alpha_1, \alpha_2, \theta_1, \theta_2$ = Angles of incidence in air

$\alpha_1', \alpha_2', \theta_1', \theta_2'$ = Angles of interference in crystal

$$\alpha_1' = \sin^{-1}[(\sin \alpha_1)/n_1]$$

$$\alpha_2' = \sin^{-1}[(\sin \alpha_2)/n_2]$$

$$\theta_1' = \sin^{-1}[(\sin \theta_1)/n_1]$$

$$\theta_2' = \sin^{-1}[(\sin \theta_2)/n_2]$$

From this rough look at the problem, there is a difference between using the interface angles in the crystal and the angles of incidence outside the crystal. Further research is required to determine the magnitude of this difference or any other problems this difference might lead to.

Appendix A: The Index Ellipsoid

In any crystal, the index of refraction along an axis of the principal coordinate system (PCS) may be used to create an "index ellipsoid" as follows:

$$\frac{x^2}{n_x^2} + \frac{y^2}{n_y^2} + \frac{z^2}{n_z^2} = 1 \quad (241)$$

Figure 26 represents equation (241) pictorially. In an isotropic crystal, the three indices are the same so the ellipsoid is a sphere. In a uniaxial crystal two indices are the same and one is different so the axis of the different index is an optic axis. In a biaxial crystal, all three indices are different and the optic axes are off the principal axes.

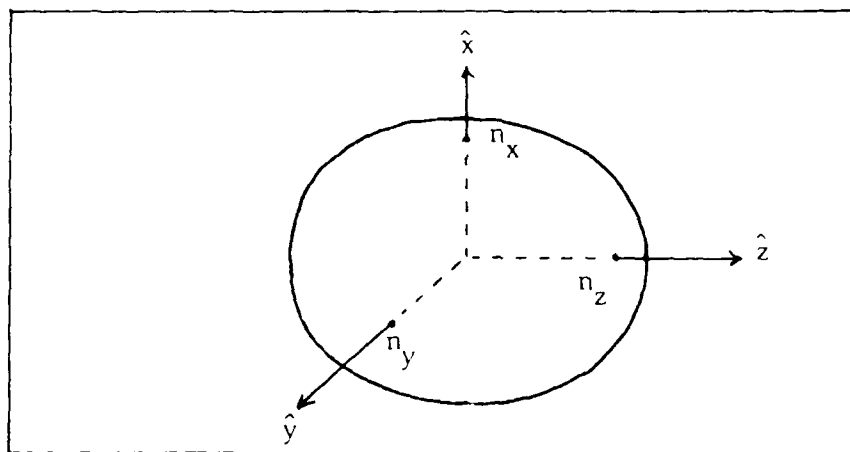


Figure 26. Illustration of the index ellipsoid.

The polarization of light passing through the crystal is broken up into components along the PCS to determine which index each component sees. For a propagation direction, \hat{s} , not along a principal axis, the index ellipsoid must be sliced perpendicular to \hat{s} to determine the indices each polarization component sees (Figure 27).

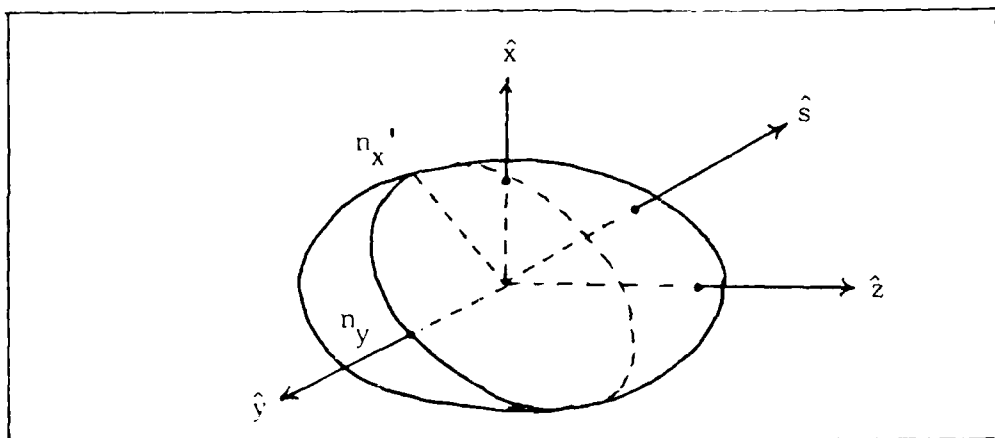


Figure 27. Appropriate indices on index ellipsoid for a propagation direction, \hat{s} .

When an external dc electric field, E , is applied to the crystal, the index ellipsoid is deformed so its representation in the original PCS is:

$$x^2(1/n_x'^2 + \Delta b_1) + y^2(1/n_y'^2 + \Delta b_2) + z^2(1/n_z'^2 + \Delta b_3) + 2 \Delta b_4 yz + 2 \Delta b_5 xz + 2 \Delta b_6 xy = 1 \quad (242)$$

where

Δb_i = i^{th} component of Δb tensor (in contracted form)

$$\Delta b = R \cdot E$$

R = Contracted electro-optic coefficient tensor

The new ellipsoid, of course, also can be written in a form similar to equation (241) in a new coordinate system which is rotated from the original PCS.

To find the indices on axes of the new coordinate system the following determinant is solved for the eigenvalues, :

$$\begin{vmatrix} 1/n_x'^2 + \Delta b_1 - \lambda & \Delta b_6 & \Delta b_5 \\ \Delta b_6 & 1/n_y'^2 + \Delta b_2 - \lambda & \Delta b_4 \\ \Delta b_5 & \Delta b_4 & 1/n_z'^2 + \Delta b_3 - \lambda \end{vmatrix} = 0 \quad (243)$$

where

$$\lambda_i = 1/n_i'^2$$

n_i' = Index in new PCS

The rotation of the coordinate system is found by solving:

$$\begin{bmatrix} 1/n_x^2 + \Delta b_1 - \lambda_i & \Delta b_6 & \Delta b_5 \\ \Delta b_6 & 1/n_y^2 + \Delta b_2 - \lambda_i & \Delta b_4 \\ \Delta b_5 & \Delta b_4 & 1/n_z^2 + \Delta b_3 - \lambda_i \end{bmatrix} \begin{bmatrix} a_{i1} \\ a_{i2} \\ a_{i3} \end{bmatrix} = 0 \quad (244)$$

for a_{ij} where

a_{ij} = Element of rotation matrix

= $\cos \theta_{ij}$

θ_{ij} = Angle between new i^{th} axis and old j^{th} axis.

The following are specific examples of the new indices of refraction given a space-charge field is set up along one of the original principal axes:

BaTiO₃:

$$\begin{pmatrix} 0 & 0 & r_{13} \\ 0 & 0 & r_{13} \\ 0 & 0 & r_{33} \\ 0 & r_{51} & 0 \\ r_{51} & 0 & 0 \\ 0 & 0 & 0 \end{pmatrix} \begin{pmatrix} E_x \\ E_y \\ E_z \end{pmatrix} = \begin{pmatrix} \Delta b_1 \\ \Delta b_2 \\ \Delta b_3 \\ \Delta b_4 \\ \Delta b_5 \\ \Delta b_6 \end{pmatrix} \quad (245)$$

If the grating is set up along \hat{x} , the index ellipsoid in the original PCS is:

$$(x^2 + y^2)/n_o^2 + z^2/n_e^2 + 2r_{51}E_xxz = 1 \quad (246)$$

The rotation is in the $x-z$ plane so $n_y' = n_o$ and the eigenvalues are:

$$\lambda = \{1/n_o^2 + 1/n_e^2 \pm [(1/n_o^2 + 1/n_e^2)^2 + 4r_{51}^2E_x^2/(n_o^2n_e^2)]^{1/2}\} / 2 \quad (247)$$

If the grating is along \hat{y} , the index ellipsoid is:

$$(x^2 + y^2)/n_o^2 + z^2/n_e^2 + 2r_{51}E_yyz = 1 \quad (248)$$

Rotation is in the y - z plane so $n_x' = n_o$ and the eigenvalues are the same as equation (247) replacing E_x with E_y . If the grating is along \hat{z} , the index ellipsoid is :

$$x^2(1/n_o^2 + r_{13}E_z) + y^2(1/n_o^2 + r_{13}E_z) + z^2(1/n_e^2 + r_{33}E_z) = 1 \quad (249)$$

The principal axes remain the same with the new indices of refraction being:

$$\begin{aligned} n_x' &= n_y' = n_o/[1 + n_o^2 r_{13}E_z]^{1/2} \\ &\approx n_o - (1/2) n_o^3 r_{13} E_z \\ n_z' &= n_e/[1 + n_e^2 r_{33}E_z]^{1/2} \\ &\approx n_e - (1/2) n_e^3 r_{33} E_z \end{aligned} \quad (250)$$

(Note that this is the form of the index assumed in Chapters IV, V and VI.)

BSO:

$$\begin{pmatrix} 0 & 0 & 0 \\ 0 & 0 & 0 \\ 0 & 0 & 0 \\ r_{41} & 0 & 0 \\ 0 & r_{41} & 0 \\ 0 & 0 & r_{41} \end{pmatrix} \begin{pmatrix} E_x \\ E_y \\ E_z \end{pmatrix} = \begin{pmatrix} \Delta b_1 \\ \Delta b_2 \\ \Delta b_3 \\ \Delta b_4 \\ \Delta b_5 \\ \Delta b_6 \end{pmatrix} \quad (251)$$

If the grating is along \hat{x} , the index ellipsoid is:

$$(x^2 + y^2 + z^2)/n^2 + 2r_{41} E_x yz = 1 \quad (252)$$

Rotation is in the y - z plane so $n_x' = n$, the eigenvalues are:

$$\lambda = 1/n^2 \pm r_{41} E_x \quad (253)$$

and the new indices are:

$$\begin{aligned} n_{y,z}' &= n/[1 \pm n^2 r_{41} E_x]^{1/2} \\ &\approx n \mp (1/2) n^3 r_{51} E_x \end{aligned} \quad (254)$$

(Again, this is the form assumed in Chapters IV, V and VI.)

If the grating is along \hat{y} or \hat{z} , the index ellipsoids are:

$$\begin{aligned}(x^2 + y^2 + z^2)/n^2 + 2 r_{41} E_y xz &= 1 \\ (x^2 + y^2 + z^2)/n^2 + 2 r_{41} E_z xy &= 1\end{aligned}\quad (255)$$

respectively. Rotation is in the x-z and x-y planes, respectively.
 n_y' = n and n_z' = n, respectively. The eigenvalues are the same as equation (253) replacing E_x with E_y or E_z , respectively. New indices are the same as equation (254) replacing E_x with E_y or E_z and n_y' with n_x' or n_z' with n_x' , respectively.

Appendix B: Recommendations for Further Research

Self-Pumped Phase Conjugate Mirrors (SPPCMs)

Papers on the theory and experimentally observed phenomena of SPPCMs include Cronin-Golomb et al. (14:689-691), Feinberg (15:486-488), MacDonald and Feinberg (16:548-553), Gower (21:196,197), Rodriguez et al. (22:1732-11736), Smout et al. (23:77-82), Gunter (24:210-214), and Eason and Smout (25:51-53).

Among the mechanisms of interest in this effect is the self-defocusing of the beam or "beam fanning" (13:46-51) by which part of the beam is redirected as it passes through the crystal (Figure 28-a). The reflection back to the original beam of this redirected part is what sets up the geometry for four wave mixing (Figure 28-b).

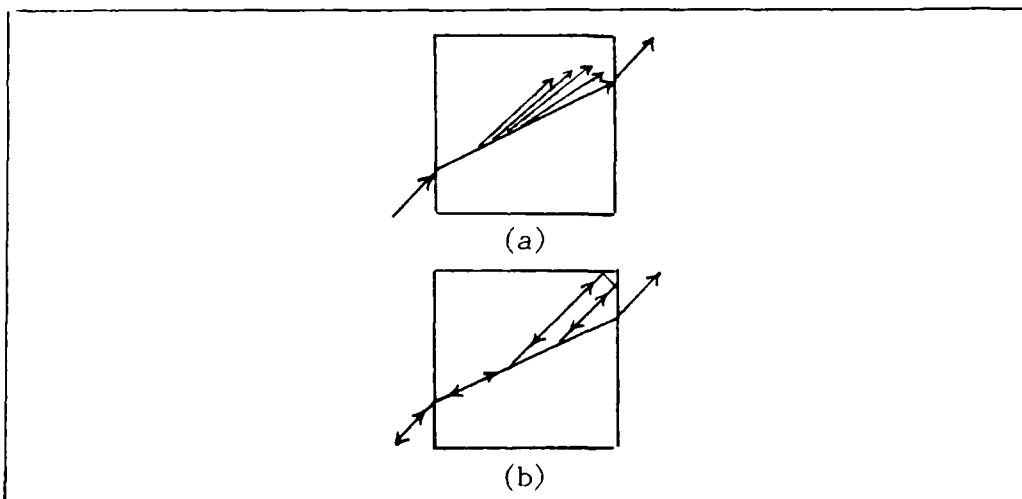


Figure 28. Geometry for self-pumped optical phase conjugation showing (a) beam fanning and (b) four-wave mixing.

Since a major drawback to making an ordinary phase conjugate mirror practical is the required coherence of the probe and pumps, the self-contained geometry of a self-pumped phase conjugate mirror appears to be the solution.

Transient Solutions to the Photorefractive Effect

Feinberg defines the grating erasure rate as follows: If an index grating is written in the crystal by the interference of two beams, then these two writing beams are turned off and a third very weak beam is scattered off the grating while the crystal is illuminated with strong uniform light, a measure of the time decay of the scattered beam is a direct measure of the time decay of the amplitude of the index grating. The modulation index under uniform illumination is:

$$m = 0$$

so the steady state portion of the potential is zero (5:1300).

Since the diffraction efficiency, η , is proportional to $|w|^2$, the decay is proportional to $|w|^2$, as well. From equation (109):

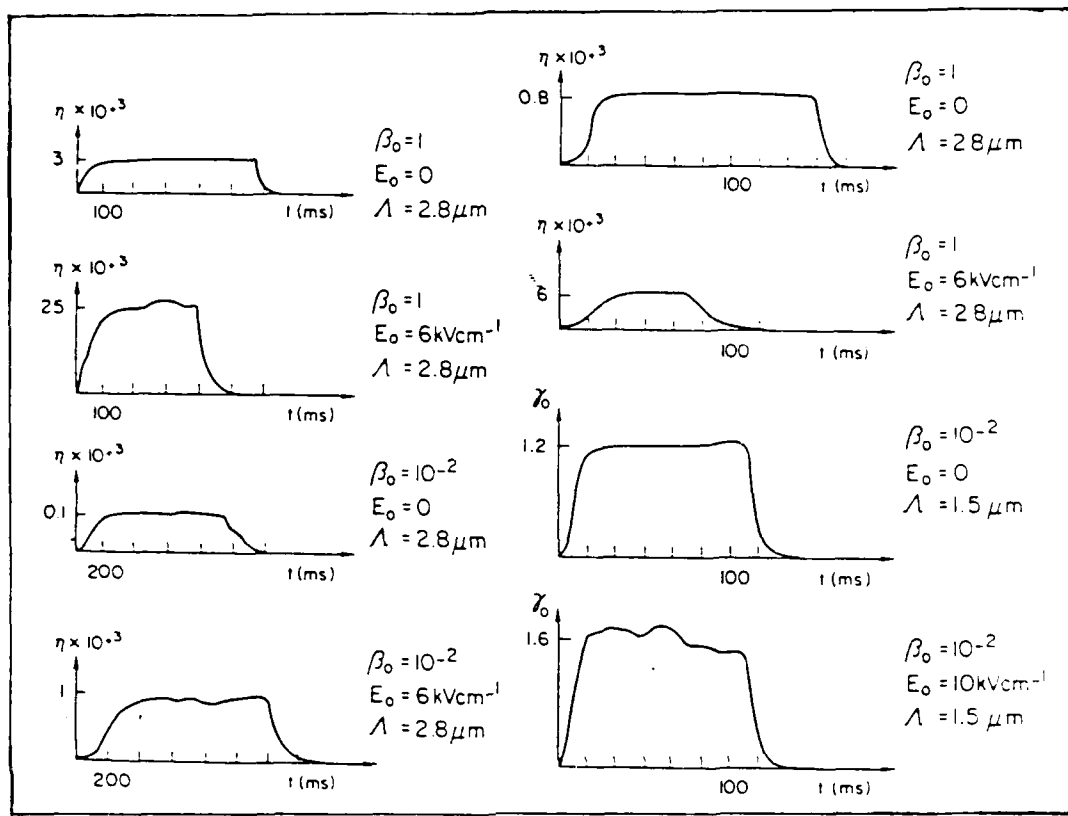
$$|w|^2 \propto \exp[-2\Gamma(\alpha^2 + 1)t] \quad (256)$$

so the decay rate, A_e , is given by:

$$A_e = 2\Gamma(\alpha^2 + 1) \quad (257)$$

(Γ as defined in Chapter IV.) (5:1300)

Gunter presents a set of graphs for diffraction efficiency and intensity gain for two beam coupling versus time for fixed parameters, incident beam intensity ratio (his ρ_0), applied field and fringe spacing (9:262).



(a)

(b)

Figure 29. Time dependence of a.) diffraction efficiency, η , and b.) two beam coupling gain, γ_0 , for BSO (9:262)

How Much Does Optical Activity Effect BSO Analyses?

Optical activity is the rotation of the plane of polarization of linearly polarized light as it passes through a medium. Figure 30 represents this phenomenon. As light propagating in \hat{z} , linearly polarized in \hat{x} , passes through the medium, its polarization vector is rotated until it is linearly polarized in \hat{y} at some length, L (2:94).

Gunter lists the optical activity of BSO to be $45^\circ/\text{mm}$ for 514.5nm wavelength light (9:240). Another existing paper on optical activity is Simon and Bloembergen (26:1104-1114).

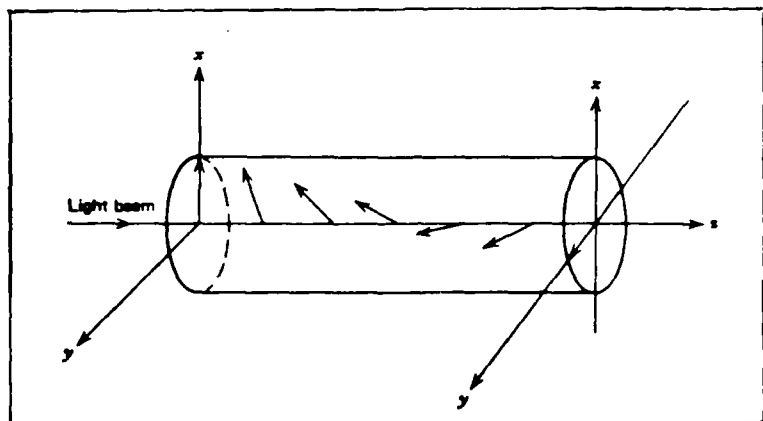


Figure 30. Illustration of optical activity (2:94)

Bibliography

1. Pepper, D.M. "Nonlinear Optical Phase Conjugation," Optical Engineering, 21: 156-181 (March/April 1982).
2. Yariv, A. and P. Yeh Optical Waves in Crystals. New York: Wiley & Sons, 1984.
3. Yariv A. and R.A. Fisher. "Introduction," Optical Phase Conjugation, edited by R.A. Fisher. New York: Academic Press, 1983.
4. Feinberg, J. "Optical Phase Conjugation in Photorefractive Materials," Optical Phase Conjugation, edited by R.A. Fisher. New York: Academic Press, 1983.
5. Feinberg, J. et al. "Photorefractive effects and light-induced charge migration in barium titinate," Journal of Applied Physics, 51: 1297-1305 (March 1980).
6. Skitek, G.G. and S.V. Marshall. Electromagnetic Concepts and Applications. Englewood Cliffs, NJ: Prentice-Hall, 1982.
7. Fischer, B. et al. "Amplified reflection, transmission, and self-oscillation in real-time holography," Optics Letters, 6: 519-521 (November 1981).
8. Valley, G.C. and M.B. Klein. "Optimal properties of photorefractive materials for optical data processing," Optical Engineering, 22: 704-711(November/December 1983).
9. Gunter, P. "Holography, Coherent Light Amplification and Optical Phase Conjugation with Photorefractive Materials," Physics Reports, 93: 199-299 (1982).
10. Kukhtarev, N.V. et al. "Holographic Storage in Electrooptic Crystals. I. Steady State," Ferroelectrics, 22: 949-960 (1979).
11. Kogelnik, H. "Coupled Wave Theory for Thick Hologram Gratings," The Bell System Technical Journal, 48: 2909-2945 (November 1969).
12. Vahey, D.W. "A nonlinear coupled-wave theory of holographic storage in ferroelectric materials," Journal of Applied Physics, 46: 3510-3515 (August 1975).
13. Feinberg, J. "Asymmetric self-defocusing of an optical beam from the photorefractive effect," Journal of the Optical Society of America, 72: 46-51 (January 1982).
14. Cronin-Golomb, M. et al. "Passive (self-pumped) phase conjugate mirror: Theoretical and experimental investigation," Applied Physics Letters, 41: 689-691 (October 1982).

15. Feinberg, J. "Self-pumped continuous-wave phase conjugator using internal reflection," Optics Letters, 7: 486-488 (October 1982)
16. MacDonald, K.R. and J. Feinberg. "Theory of a self-pumped phase conjugator with two coupled interaction regions," Journal of the Optical Society of America, 73: 548-553 (May 1983).
17. White, J.O. and A. Yariv. "Photorefractive Crystals as Optical Devices, Elements, and Processors," SPIE, 464: 7-20 (1984).
18. Cronin-Golomb, M. et al. "Exact solution of a nonlinear model of four-wave mixing and phase conjugation," Optics Letters, 7:313-315 (July 1982).
19. Marrakchi, A. et al. "Diffraction Efficiency and Energy Transfer in Two-Wave Mixing Experiments with $\text{Bi}_{12}\text{SiO}_{20}$ Crystals," Applied Physics, 24:131-138 (1981).
20. Wood, E.A. Crystals and Light (Second Edition). New York: Dover Publications, 1977.
21. Gower, M.C. "Mechanisms for self-pumped phase-conjugate emission from BaTiO_3 crystals," Conference on Lasers and Electro-Optics Technical Digest Series 1987, Vol. 14. 196,197. Washington, DC: Optical Society of America, 1987.
22. Rodriguez, J. et al. "BSKNN as a self-pumped phase conjugator," Applied Optics, 26: 1732-1736 (May 1987).
23. Smout, A.M.C. et al. "Regular Oscillations and Self-Pulsating in Self-Pumped BaTiO_3 ," Optics Communications, 59: 77-82 (August 1982).
24. Gunter, P. et al. "Self-Pulsation and Optical Chaos in Self-Pumped Photorefractive BaTiO_3 ," Optics Communications, 55: 2210-214 (September 1985).
25. Eason, R.W. and A.M.C. Smout. "Bistability and noncommunicative behavior of multiple-beam self-pulsing and self-pumping in BaTiO_3 ," Optics Letters, 12: 51-53 (January 1987).
26. Simon, H.J. and N. Bloembergen. "Second-Harmonic Light Generation in Crystals with Natural Optical Activity," Physical Review, 171: 1104-1114 (July 1968).

VITA

Captain Michael A. Marciniak was born 28 February 1959 in Milwaukee, WI. He graduated from Thomas More HS in Milwaukee in 1977 and attended St. Joseph's College in Rensselaer, IN on a four-year Trustee's Academic Scholarship. After graduating with a dual B.S. degree in Mathematics-Physics, he went on to OTS to be commissioned on 3 December 1981. Captain Marciniak was assigned to the University of Missouri-Columbia in the AFIT undergraduate conversion program where he received the B.S.E.E. degree (*cum laude*) in December 1983. He then served as a Communications and Electro-Optics Engineer at the Air Force Electronic Warfare Center, Kelly AFB, TX from January 1984 to May 1986 before entering the AFIT M.S.E.E. program in Electro-Optics.

Permanent address: PCS East

Kirtland AFB, NM 87116

~~UNCLASSIFIED~~

~~SECURITY CLASSIFICATION OF THIS PAGE~~

REPORT DOCUMENTATION PAGE				Form Approved OMB No. 0704-0188
1a. REPORT SECURITY CLASSIFICATION UNCLASSIFIED		1b. RESTRICTIVE MARKINGS		
2a. SECURITY CLASSIFICATION AUTHORITY		3. DISTRIBUTION/AVAILABILITY OF REPORT Approved for public release; distribution unlimited.		
2b. DECLASSIFICATION/DOWNGRADING SCHEDULE				
4. PERFORMING ORGANIZATION REPORT NUMBER(S) AFIT/GEO/ENP/87D-3		5. MONITORING ORGANIZATION REPORT NUMBER(S)		
6a. NAME OF PERFORMING ORGANIZATION School of Engineering	6b. OFFICE SYMBOL (If applicable) AFIT/ENG	7a. NAME OF MONITORING ORGANIZATION		
6c. ADDRESS (City, State, and ZIP Code) Air Force Institute of Technology Wright-Patterson AFB, OH 45433-6583		7b. ADDRESS (City, State, and ZIP Code)		
8a. NAME OF FUNDING/SPONSORING ORGANIZATION	8b. OFFICE SYMBOL (If applicable)	9. PROCUREMENT INSTRUMENT IDENTIFICATION NUMBER		
8c. ADDRESS (City, State, and ZIP Code)		10. SOURCE OF FUNDING NUMBERS		
		PROGRAM ELEMENT NO.	PROJECT NO.	TASK NO.
				WORK UNIT ACCESSION NO.
11. TITLE (Include Security Classification) See box 19.				
12. PERSONAL AUTHOR(S) Michael A. Marciak, B.S., B.S.E.E., Capt, USAF				
13a. TYPE OF REPORT MS Thesis	13b. TIME COVERED FROM _____ TO _____	14. DATE OF REPORT (Year, Month, Day) 1987 December		15. PAGE COUNT 132
16. SUPPLEMENTARY NOTATION				
17. COSATI CODES		18. SUBJECT TERMS (Continue on reverse if necessary and identify by block number) Nonlinear Optics, Phase Conjugation, Photorefractive		
FIELD	GROUP			
19. ABSTRACT (Continue on reverse if necessary and identify by block number) Title: NONLINEAR OPTICAL PRINCIPLES AND THE PHOTOREFRACTIVE EFFECT APPLIED TO OPTICAL PHASE CONJUGATION Thesis Chairman: Theodore E. Luke Associate Professor of Engineering Physics				
Approved for public release: IAW AFR 190-1 <i>Lynn E. McElver</i> 31 Dec 87 Lynn E. McElver, AFRL/DP/DP/DP/DP Flight Dynamics Laboratory, AFRL/DP Wright-Patterson Air Force Base, OH 45433-6583				
DISTRIBUTION/AVAILABILITY OF ABSTRACT <input checked="" type="checkbox"/> UNCLASSIFIED/UNLIMITED <input type="checkbox"/> SAME AS RPT <input type="checkbox"/> DTIC USERS		21. ABSTRACT SECURITY CLASSIFICATION UNCLASSIFIED		
22a. NAME OF RESPONSIBLE INDIVIDUAL Theodore E. Luke		22b. TELEPHONE (Include Area Code) (513) 255-4498	22c. OFFICE SYMBOL AFIT/ENP	

DISTRIBUTION/AVAILABILITY OF ABSTRACT

UNCLASSIFIED/UNLIMITED SAME AS RPT DTIC USERS

21. ABSTRACT SECURITY CLASSIFICATION
UNCLASSIFIED

22a NAME OF RESPONSIBLE INDIVIDUAL
Theodore E. Luke

22b. TELEPHONE (Include Area Code) 22c.
(513) 255-4498

Approved for public release: 1AW AFR 190-1
Sgt. W. L. Weller 31 Dec 87
LYNN E. MCGLAVER
Director, Defense Science and Professional Development
Defense Science and Professional Development (DSD)
Fort Monmouth, New Jersey 07740-5000 (407) 426-1000
Wesleyan University, Middletown, Connecticut 06457

UNCLASSIFIED

This thesis presents a detailed interpretation of published theory of nonlinear optical phase conjugation by degenerate four wave mixing and by the photorefractive effect. Photorefractive phase conjugation is shown to be a low incident intensity alternative to degenerate four wave mixing (which requires high intensity incident light to achieve the nonlinear polarization of a medium).

The derivations of two models for the photorefractive effect, Feinberg's Hopping Model and Kukhtarev's Solid State Model, are presented. The significance of Kukhtarev's model is his development of criteria for which spatially sinusoidal incident light (interference fringes) produces a spatially sinusoidal electro-static field in the crystal - an assumption casually made in much photorefractive work. Both models culminate in expressions for the magnitude of the space-charge field and the spatial phase shift between the field and the incident interference pattern for small modulation conditions.

Feinberg's model is extended to develop expressions for two-beam coupling, diffraction efficiency and phase conjugate reflectivity. An alternative development for these expressions assumes the electro-static field exists in the crystal and modulates the crystal's refractive index by the linear electro-optic (Pockel's) effect.

The functional dependencies of Feinberg's expressions agree with (published) empirical data. However, specific crystallographic orientations exist for which the absolute magnitude of Feinberg's expressions or even the relative magnitudes between different orientations are inaccurate. Accurate relative magnitude expressions are made by assuming an electro-static field exists in the crystal and using an index-ellipsoid approach to determine refractive indices.

UNCLASSIFIED

